

Neural Field Models: A mathematical overview and unifying framework

Blake J. Cook ^{*†} Andre D. H. Peterson ^{‡†} Wessel Woldman ^{*§}
John R. Terry ^{*§¶}

Abstract

Mathematical modelling of the macroscopic electrical activity of the brain is highly non-trivial and requires a detailed understanding of not only the associated mathematical techniques, but also the underlying physiology and anatomy. Neural field theory is a population-level approach to modelling the non-linear dynamics of large populations of neurons, while maintaining a degree of mathematical tractability. This class of models provides a solid theoretical perspective on fundamental processes of neural tissue such as state transitions between different brain activities as observed during epilepsy or sleep. Various anatomical, physiological, and mathematical assumptions are essential for deriving a minimal set of equations that strike a balance between biophysical realism and mathematical tractability. However, these assumptions are not always made explicit throughout the literature. Even though neural field models (NFMs) first appeared in the literature in the early 1970's, the relationships between them have not been systematically addressed. This may partially be explained by the fact that the inter-dependencies between these models are often implicit and non-trivial. Herein we provide a review of key stages of the history and development of neural field theory and contemporary uses of this branch of mathematical neuroscience. First, the principles of the theory are summarised throughout a discussion of the pioneering models by Wilson and Cowan, Amari and Nunez. Upon thorough review of these models, we then present a unified mathematical framework in which all neural field models can be derived by applying different assumptions. We then use this framework to i) derive contemporary models by Robinson, Jansen and Rit, Wendling, Liley, and Steyn-Ross, and ii) make explicit the many significant inherited assumptions that exist in the current literature. This framework ensures that the validity of these assumptions will be carefully considered when interpreting results derived from NFMs and also in light of further developments in mathematical modelling, neurophysiology and neuroanatomy that enable these assumptions to be updated. We then provide an overview of key application areas of neural field theory and critically examine the limitations inherent in this class of models. Finally, we will discuss several avenues that may be able to address these limitations, including novel methods from stochastic

^{*}Centre for Systems Modelling & Quantitative Biomedicine, Institute for Metabolism and Systems Research, University of Birmingham, B15 2TT, UK

[†]Equal contribution as first author

[‡]Department of Medicine, University of Melbourne, Melbourne, Australia

[§]Equal contribution as last author

[¶]E-mail: J.R.Terry@bham.ac.uk

processes, random neural networks, networked dynamical systems, and ensemble methods that connect the dynamics from the microscale to the macroscale.

Keywords: Neural field theory ; neural mass models ; dynamical systems ; neuroscience ; mathematical modelling ; brain state transitions ; phenomenological models ; brain dynamics ; stochastic field theory ; brain networks ; .

MSC2020 subject classifications: 35A08; 35A24; 35R09; 37G35; 92-08; 92-10; 92B20; 92C20.

Submitted to MNA on March 22, 2021, final version accepted on February 4, 2022.

Supersedes [arXiv:2103.10554v2](https://arxiv.org/abs/2103.10554v2).

1 Overview

The use of mathematics to understand fundamental principles in neuroscience can be traced back to the early 20th century. In 1907, Lapicque [120] introduced what could be termed the first mathematical model of the neuron. Using a set of ODEs for the RC circuit, this approach is an early precursor of many subsequent mathematical studies. Building on advances in experimental methods for isolating neurons *in vitro* and recording electrophysiological activity, the seminal work of Hodgkin and Huxley (1952) [87] introduced a non-linear dynamical systems model to describe the membrane dynamics of a single neuron. Soon thereafter, Beurlle (1956) [12] formulated the first population model of neural tissue. Building from here and inspired by statistical distributions of interacting particles (Reichl, 1999 [170]), the neural field approximation permits a focus on averaged properties of the neuronal ensemble, rather than the effect of each individual neuron on all of the others (Deco et al., 2008 [48]). Effectively, these so-called *neural field models* relate the average pre-synaptic firing rates to the average post-synaptic membrane potentials of neural populations. Over the past several decades, large-scale brain modelling has continued to mature and proliferate, providing theoretical frameworks to study open questions in neurobiology.

One of the primary purposes of this review is to provide a unifying mathematical framework for deriving and explaining neural field models. To achieve this, we first summarise important concepts of neurobiology and give a brief summary of single-neuron models that underpin a “bottom-up” approach to modelling brain dynamics. We then introduce ensemble approaches to modelling brain activity, and the underlying concepts of neural field models. Alongside, an historical summary of the field, we explicitly derive the Wilson-Cowan model, the Amari model, and the Jansen-Rit model, focussing on the assumptions and formalisms used in these “first-order” models. We then consider “second-order” models which stratify the state variables, enabling a more detailed description of the aggregate interaction of multiple neural populations. From a general integral equation description, we use Green’s functions to decouple the spatial and temporal components and derive the cortical model described by Robinson et al. (1997) [178]. Using state-dependent input coefficients on the state variables (i.e. conductance-based synapses), the cortical model of Liley et al. (1999) [124] is derived. Finally replacing the spatial kernel with a point source: reducing the neural field to a neural mass, we demonstrate how the Jansen and Rit (1995) [91] and Wendling et al. (2002) [214] models can be derived. In all cases, significant assumptions are made by these authors which we highlight and discuss their justifications in detail. The assumptions made typically take the form of mathematical approximations and physiological and anatomical simplifications.

Following these historical reviews and unifying derivations, we turn our focus to summarise the background of brain activity measurements using electroencephalography (EEG) and how this is used to inform neural field models. Contemporary applications of neural field theory are then discussed, including studies on the emergence of rhythms in brain activity, sleep cycles, epilepsy and recurrent seizure activity, the action of

anaesthesia on brain rhythms, and the progression of Alzheimer's disease. Upon review of these important applications, we examine the issues with neural field models, specifically the myriad of assumptions on connectivity, the phenomenological nature of these models, and the experimental validity of these theories. We end our review by highlighting areas in which improvements in neural field theory can be made and focus on unaddressed issues between neuroscience and mathematics and the role of neural field theory. Throughout the review, it is assumed that the reader is familiar with differential equations, integral equations, Green's functions, integral transforms, and dynamical systems.

2 Mathematical approaches to modelling emergent brain activity

Mathematical modelling provides an essential method of quantifying the behaviour of complex biological systems, which can be utilised when developing or refining our understanding of the anatomy and physiology of neural systems. This is achieved by proposing and verifying new hypotheses, identifying important mechanisms and parameters, and making predictions based on experimental data. Advancements in accuracy and resolution of experimental measurements of microscale neural activity have led to quantitative mathematical models, such as the Hodgkin-Huxley model, that characterise the signalling processes between neurons from a dynamical systems perspective. Macroscale neural activity however, provides many significant challenges in both measuring and modelling. Small sections of brain tissue typically have a high density of neurons — which themselves are highly complex units, that are coupled together in irregular and non-uniform structures. These challenges require innovative methods for quantifying emergent dynamics of neural populations that reduce the complexity of the system to key parameters, which in turn can be measured using techniques from experimental neuroscience.

From a dynamical systems perspective, there are two main approaches to constructing a mathematical model of the brain: the first is a 'bottom-up approach' where evolution equations are based upon averaged physiological properties of the individual neurons. The second is a 'top-down approach' where evolution equations are defined based upon direct observations of the emergent behaviour of neuronal populations. The sheer number of neurons involved in the generation of macroscopic electrical activity along with the anisotropic and heterogeneous non-local connectivity of neurons makes a 'bottom-up' approach highly non-trivial and largely impractical for modelling brain dynamics from single neuron dynamics. To this end, a 'top-down' approach may be better suited for understanding which key population-level physiological parameters influence macroscopic dynamics. For both these approaches a critical challenge is to relate and bridge the descriptions of neural activity at different spatiotemporal scales. Multiscale neural activity is often temporally separated by several orders of magnitude i.e., milliseconds versus hour timescales). Similarly, for different spatial scales the connection between electro-chemical activities at the micro-metre scale is vastly different to activity at the centimetre scale. The relationship between neural activities at different spatiotemporal scales remains an open topic of research within both theoretical and experimental neuroscience.

In this section we first provide the necessary neurophysiological background for constructing neural field models from microscopic neural activity. A summary of the microscopic dynamics of individual neurons is given along with a discussion of macroscale dynamics of the brain. The issues inherent in a "bottom-up" perspective, which seeks to construct macroscale models by coupling together microscale models of individual neurons is then discussed. We then provide an overview of the alternate "top-down"

modelling approach utilised in neural field modelling. This top-down approach is the primary focus of this review, for which we provide a detailed discussion of the key mathematical machinery involved. In this review we explicitly specify the assumptions made in these models. As with most mathematical models, many assumptions are inherited, and therefore implicit, over many iterations and applications of the model. We have categorised these assumptions into three main types:

- **Mathematical assumption:** Where a substitution of an equation or expression has been made that is believed to be a reasonable qualitative and/or quantitative approximation and/or description of the physical system being described.
- **Physiological assumption:** A simplification of physiological function, usually of neurons and synapses. There are many aspects of the structure-function relationship of brain constituents and neurons that are either unknown or not quantitatively measurable.
- **Anatomical assumption:** A simplification of the anatomical structure of the brain, usually with respect to connectivity. There are many properties of neural connectivity that are not covered by quantitative neuroanatomy, and these are often simplified to a qualitative conjecture or estimate.

2.1 Physiology of the brain

At the microscale, the fundamental cells of the brain are neurons and glia. Both are specialised cells that transmit signals using electrochemical mechanisms. Although glia play a role in neural information processing (Ransom and Sontheimer, 1992 [169], Araque and Navarrete, 2010 [6]), their role is typically less defined. Consequently, the models discussed in this review are primarily centred around describing the activity of neurons and not glia.

Neurons generally receive signals at extensions from their cell body called dendrites and send signals along a filament called the axon (see Figure 1 (a)). Neurons communicate by transmitting signals along axons, referred to as action potentials. These are neural signals where the membrane potential at subsequent points along the axon rapidly rises and falls in a matter of milliseconds. This propagating signal terminates at the axon terminals, where it causes the release of chemical neurotransmitters at the interface with the dendrite, known as the synapse. Additionally, neural communication can also occur at gap-junctions directly between cells via direct electrical signalling, as well as by chemical communication. While all neurons share similar features, the shape and size of neurons can vary significantly. For instance, the number of dendrites and axon terminals can differ considerably, and the length of the axon is generally much longer in peripheral neurons outside of the brain. Moreover, some neurons (such as the neuron depicted in Figure 1 (a)) have insulated axons called “myelination”, which enables faster axonal signal transmission. The myelin is formed by glial cells called oligodendrocytes wrapped around the axon, which insulate and decrease the capacitance across the axonal membrane. Consequently, this increases the conduction velocity and is essential for normal brain function. Myelinated neural tissue is referred to as “white matter” whereas unmyelinated neural tissue is called “grey matter”.

Neurotransmitters activate receptors, which in turn have excitatory or inhibitory effects on the postsynaptic neuron. For example, the key receptors for glutamate all have excitatory effects, whereas for GABA the main receptors result in inhibition. There are many other neurotransmitters, the receptors for which can be both excitatory and inhibitory (e.g. acetylcholine), meaning care should be taken when describing a neurotransmitter as “excitatory” or “inhibitory”. These chemical changes result in a transient change to the postsynaptic membrane potential, termed excitatory postsynaptic

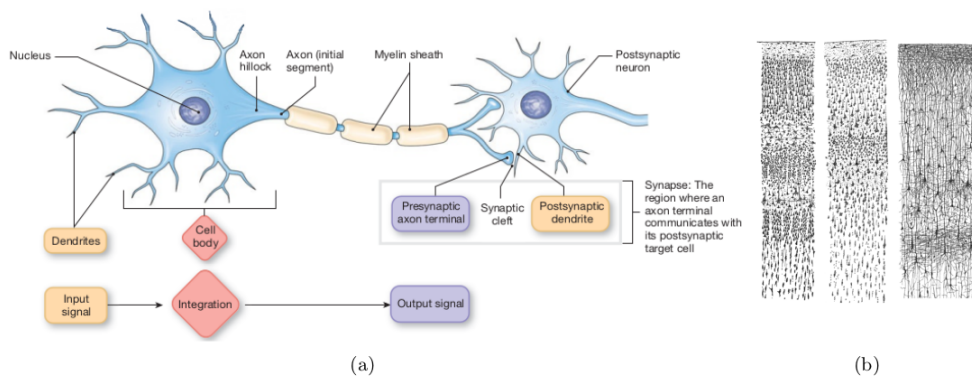


Figure 1: **Neuron and synapse anatomy.** (a) Simplified illustration of neuron anatomy (modified from Silverthorn et al. (2013) [187]). The cellular membrane of neurons maintains a steady state of electrochemical equilibrium at a potential difference around -70 mV. Incoming signals from other neurons perturb the membrane potential at the cell body, until a threshold potential is reached. At this point, the neuron sends a unidirectional self-propagating signal (an action potential) along its axon to the synaptic terminals. These terminals interface with the dendrites and cell bodies of other neurons at junctions called synapses. The anatomy of the synapse is intricate and relies on a number of sub-cellular interactions of neurotransmitters. Neurotransmitters are stored in vesicles at the terminals, which are released into the synaptic junction upon receiving an action potential. The neurotransmitters trigger the movement of ions on the next neuron, depending on which ion channel it activates. Different types of neurotransmitters activate different receptors, which can either excite or inhibit the connecting neuron by increasing or decreasing the membrane potential respectively. (b) Sketches of the lateral arrangement of neuron in the cortex (Ramón y Cajal, 1911 [168]), which form functional units of cortex known as ‘cortical columns’. The activity of these units are described by neural field models, and are thought to be a primary source of the EEG signal due to location and geometric arrangement.

potentials (EPSPs), or inhibitory postsynaptic potentials (IPSPs). These PSPs propagate along the dendrites to the cell body where they are summed and the resulting alteration to the membrane potential of the postsynaptic neuron can lead to the generation of a new action potential and so the process continues. The description above of neurotransmitter kinetics has been vastly simplified, as our definition of microscopic addresses the dynamics of cellular to multi-cellular spatiotemporal scales. Whereas neurotransmitters and all of their numerous associated processes such as extra-cellular dynamics and molecular biochemical pathways constitute entire fields of study within neuroscience and other disciplines such as biophysics.

The vast majority of the volume of the brain, the *cerebrum*, is divided into two hemispheres which can be organised into layers and sections with different physiological structure or class of responsibilities in information processing. Populations of densely interconnected neurons give rise to complex and rich emergent dynamics at the macroscale. Rhythmic oscillations in brain activity are correlated with a variety of functions, which change and learn over time (Zeki, 1993 [223]). Electroencephalography (EEG) is used to measure the aggregated electrical activity in the brain, and as such provides a useful reference point for models of neural activity. It has been demonstrated that the main contributors to the EEG signal are primarily the post synaptic potentials occurring throughout the neuronal population, rather than the action potentials (Buzsáki, 2012 [33]). This is due to the geometry of the axons and dendrites as the apical dendrites form branched structures that orientate vertically to generate an equivalent current dipole that is normal to an EEG electrode (Nunez and Srinivasan, 2006 [157]). Beyond that however, from an electromagnetism perspective, there is a fundamental gap of several orders of magnitude between the local field potentials measure on the microscale and the putative generators of the EEG signal on the macroscale. Because of the lack of data over several orders of magnitude, the complex geometry of the brain and the fact that the microscopic generators are not point sources like electrons but ionic dynamics, it is difficult to apply Maxwell's equations (Gratiy et al., 2017 [80]).

More than half of the surface area of the brain lies within folds and valleys, known as "gyri" and "sulci". On average, the surface area amounts to 2300 cm^2 with a volume of 1200 cm^3 in adult humans (Elias and Schwartz, 1969 [56]). The outer 2–3 mm cerebral tissue is called the "cortex", which can be further subdivided into four sections called "lobes". Cortical tissue is composed of layers of grey matter surrounding layers of white matter. Neurons of the cortex are arranged in specific layers in a somewhat regular column pattern, called "cortical columns", which are illustrate in Figure 1 (b). The cortex can be regarded as the part of brain responsible for cognition, and can be broadly partitioned into regions (or "lobes") according to the types of activities that are processed. The frontal lobe is responsible for higher thought processes, such as behaviour, self-awareness, and problem solving, whereas the occipital lobe at the back of the brain is responsible for visual processing. Between these regions lies the parietal lobe which is primarily involved in sensory processing and motor function. The temporal lobes on the sides of a cortex are mainly utilised in memory processing, and language comprehension.

The base of the brain is where the cerebellum and brainstem are located. The cerebellum has a tightly packed grey matter morphology and has crucial roles in fine motor function and balance. The brainstem connects the brain to the spinal cord, and also contains circuits that are crucial for basic survival functions such as breathing regulation. Deep structures towards the centre of the cerebrum involve structures such as the cingulate cortex, thalamus, hypothalamus, pituitary gland. These structures are essential for relaying information throughout the brain, modulating neurohormones and homeostasis, survival instincts, and processing short-term and long-term memory.

Connectivity in the brain is an ongoing topic of research, most notably with the human connectome project (Van Essen, 2013 [208]). While the brain is a largely heterogeneous structure, some key trends in connectivity on the macroscale have been observed. White matter fibres diffuse out from the thalamus to the cortex, where interestingly there are one hundred times more cortico-thalamic connections than thalamo-cortical connections. A well known principle in neuroscience, often used to simplify models in mathematical neuroscience, is Dale's law (Eccles et al., 1976 [54]). This asserts that a neuron releases the same neurotransmitters at each axon terminal, regardless of the identity of the target cell. Although there are exceptions in reality, this simplification allows neurons to be grouped together into populations by the characteristics of afferent neurotransmission, in its simplest form allows partitioning of neurons into "excitatory" and "inhibitory" populations. In the cortex, 80% of cortical neurons are excitatory whereas the remaining 20% are inhibitory and there is a somewhat regular column pattern in the way neurons are arranged radially. It should be noted that 97% of connections in cortical tissue are to other regions of cortex (Braitenberg and Schüz, 2013 [18]).

Heterogeneous connectivity of neurons in brain tissue remains one of the significant hurdles in experimental and theoretical neuroscience. Arrangements and connections of neurons are unclear from microscopic examination of slices of neural tissue. Neurons in the central nervous system, known as interneurons, feature many more dendrites and axon terminals connecting to many other interneurons in highly non-trivial ways. Often, identifying excitatory and inhibitory neurons is also a difficult task. MRI technologies can be used to investigate bulk connectivities of neurons in neural tissue non-invasively by the diffusion of water along axons, but this is an imperfect imaging process that constitutes its own research sub-domain (Fink and Fink, 2018 [65]).

2.2 Microscopic descriptions of emergent brain dynamics

The complexity of the brain and its multiple spatial and temporal scales of description makes mathematical modelling an attractive tool to aid understanding. At the microscale, the Hodgkin-Huxley model provides a simplified description of the cellular dynamics of a single neuron and describes how a neuron produces an action potential (Hodgkin and Huxley, 1952 [87]). This model was arguably the first great achievement of mathematical neuroscience, recognised through the 1963 Nobel prize in physiology or medicine. It describes the release of an action potential in terms of ion flow across a cellular membrane via four nonlinear ordinary differential equations. Hodgkin and Huxley formulated the mechanisms responsible for the initiation and propagation of an action potential in terms of ionic currents, conductances and membrane potentials. These were based on Kirchoff's laws and R-C circuits using measurements from a giant axon of the squid.

Whilst the Hodgkin-Huxley equations accurately capture the voltage dynamics, they contain a level of detail that is not always necessary, and may in fact hinder progress by convoluting primary dynamical mechanisms. This is particularly the case, when we consider coupling together interacting neurons to form networks. One approach to address this complexity is to reduce the dimensionality of the system by identifying the crucial steady states and stabilities and deriving a simpler dynamical system that has similar dynamics.

An example of such an abstracted approach is seen in the Morris-Lecar model (Morris and Lecar, 1981 [149]), which combines ion gating variables into one state variable and so simplifies the Hodgkin-Huxley equations. Another abstraction of the Hodgkin-Huxley model is the FitzHugh-Nagumo model (FitzHugh, 1961 [66]), which reduces the key dynamics to a two-variable system by generalising the van der Pol oscillator model.

Often the full description of the voltage curve during an action potential is not

necessary to describe the fundamentals of neural dynamics, as it remains reasonably identical in shape and it is the timings of the action potentials that determine the dynamics (Burkitt, 2006 [31], [32]). Hence, further simplifications can be made of which the most simple is the integrate-and-fire (IF) neuron (Dayan and Abbott, 2001 [46], Burkitt, 2006 [31]). This model describes sub-threshold membrane potential dynamics and implements a reset condition at the threshold potential which resets the potential to resting state and represents an action potential spike with a Dirac-delta distribution. Although, there are variations of IF models that represent the action potential, particularly for fast spiking (Izhikevich, 2007 [90]).

From these simplified microscale models, we can straightforwardly create large-scale networks. For example, many spiking models of epilepsy utilise computer simulations of large networks of multi-compartmental Hodgkin-Huxley style neurons. An advantage of this is that they can be informed by *in vitro* studies and so parameters have a direct correspondence to measurable electrophysiological properties. This correspondence can help us understand physiological and pathophysiological brain dynamics by allowing more detailed descriptions of ion channelopathies, such as mutations, channel up/down regulations, glial cell interactions, synaptic changes, and network connectivity. An early pioneer of such an approach was Roger Traub (Traub, 1979 [204], Traub and Wong, 1982 [202]) whose detailed models of both the cortex and the thalamus were amongst the first to reproduce both healthy and abnormal brain dynamics. Critically, these findings were similar to that found in *in vitro* studies (Traub et al., 1989 [200], 1991 [203], 2005 [205]). Building on these early approaches, there are modern-day projects that utilise this simulation-focused “bottom-up” description of the brain: the most highly publicised being the Human Brain Project (Markram, 2012 [132]).

However, there are disadvantages to pursuing this bottom-up approach. For example, there quickly become issues with model complexity, data fitting, and interpretability of results. With 10^{12} neurons in the brain, even an abstracted and simplified spiking model (Giannakopoulos et al., 2001 [78], Larter et al., 1999 [122], Ursino and La Cara, 2006 [206]), will still effectively have the same level of complexity as the brain itself. This requires large scale simulations on a super-computer to be effective. It also challenges the traditional notion of a model: namely that it simplifies the order of complexity of the system being modelled. For a more detailed discussion of the implications of modelling macroscopic brain tissue with ensembles of microscale models, we refer the reader to several review articles including de Garis et al. (2010) [47] and Eliasmith and Trujillo (2014) [57].

2.3 Toward macroscopic descriptions of emergent brain dynamics

An alternative approach is to consider the system from a more “top-down” perspective. A useful metaphor in this regard is that of temperature in a room. We know that temperature arises as the net kinetic energy of atoms within a room. However, it is impractical to calculate temperature by considering interactions between every particle. Instead, we model statistical quantities of particles in the room, leading to much simpler models than can easily be solved.

In a similar manner, rather than considering the behaviour of each individual neuron, neural field models describe the bulk behaviour of an area of cortical tissue *en masse*. When constructing neural field models, neurons are typically segregated into populations with shared statistical factors. As illustrated in Figure 2, the state variables of the system are population-level statistics of large collections of neurons. Following Dale’s Law (introduced earlier), a common characteristic used to partition neurons is the type of synapses they connect to. For most models it is typical to partition neurons into “excitatory” and “inhibitory” populations.

As discussed earlier, these models typically don't consider non-neuronal populations, such as glial cells, even though these are estimated to outnumber neurons around ten-fold (von Bartheld et al., 2016 [211]). This is a significant assumption, since many non-neuronal cells support and actively facilitate connections between neurons. However, including this layer of detail significantly increases the complexity of any neural model, regardless of spatiotemporal scale. Furthermore, the neuronal constituents of these continuum populations are also non-compartmentalised, so we do not consider the full detail of diffusion of neurotransmitters and inputs relative to the neuron cell body using the dynamics of the cable equation.

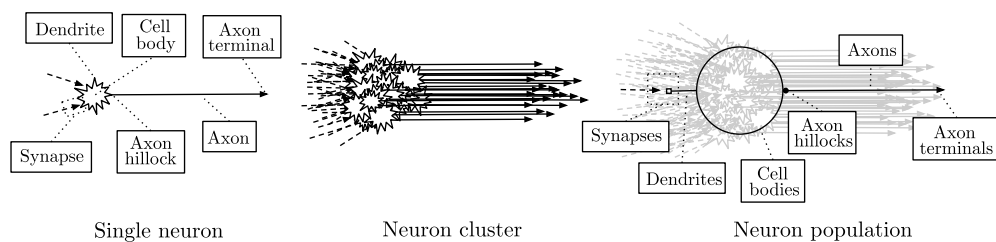


Figure 2: **Diagram of neural mass approximation.** A single neuron description starts on the left, where models such as Hodgkin-Huxley are appropriate to describe quantities such as *membrane potential* and *spike frequency*. Increasing in scale, abstracted neuronal models such as leaky integrate-and-fire are used to model signal transmission amongst interconnected neurons. At larger scales on the right, individually addressing neurons becomes mathematically intractable, so a continuum approximation is typically made. Models at this scale include neural field models and neural mass models, which describe the evolution of aggregate quantities across different populations of neurons. Neurons are grouped together by the type and time-scale of post-synaptic signals they send. Aggregate quantities used in ensemble descriptions of neural dynamics include *mean membrane potential* and *mean spike rate* of sub-populations, which are closely related by a sigmoidal wave-to-pulse transfer function.

Focusing on the statistical quantities of the emergent behaviour results in a simpler theoretical framework. One where the models remain deterministic, and in principle tractable, even if the dynamics of the collective units do not. This provides an approach to define a straightforward neural field model, where the emergent behaviour is defined as the mean of its density. Effectively, this describes the dynamics of the averaged activity across a region of space. Since many techniques used to analyse the brain, such as local field potentials (LFPs), electroencephalography (EEG), or magnetoencephalography (MEG), are observations of population level activity, such models are well suited to understand these data recordings. A crucial advantage of the neural field approach is that the resulting model is considerably less complex than an equivalent microscopic network model. Therefore they are amenable to both forward modelling approaches, such as exact solutions using Green's functions (Coombes et al., 2003 [39]), bifurcation theory (Kuznetsov, 1997 [115]), model inversion techniques such as DCM (Kiebel et al., 2008 [105]), Kalman filtering (Freestone et al., 2013 [73]), (Balson et al., 2014 [9]), as well as machine learning approaches (Ferrat et al., 2018 [64]).

3 A potted history of neural field models

In this section, we will review key aspects of early neural field models. We first define the overall principles and elements of a neural field model, using the Amari

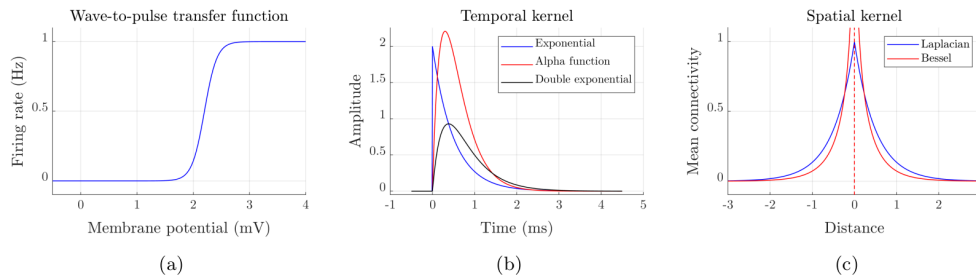


Figure 3: Transfer functions and integral kernels of neural field models. (a) The sigmoidal wave-to-pulse transfer function is responsible for relating the mean membrane potential to the mean firing rate of a neural population. (b) The temporal integral kernel represents how incoming action potentials propagate and decay over time across the neural membrane. An incoming action potential has maximal influence on the neurons membrane potential shortly after it arrives, when neurotransmitters are released at the synaptic junction and interact with the neuron membrane, which perturbs the membrane potential by net ion movement across the neuron membrane. The strength of this potential perturbation depends on the proximity of the synapse to cell body, and decays over time. (c) The spatial kernel assigns weight to neural signals between populations depending on the population types and their spatial proximity, which takes into account the density of connections between populations. The connectivity between populations decays as the spatial distance between two points increases, hence there is a spatial limit on the maximal mean firing rate from one population to another.

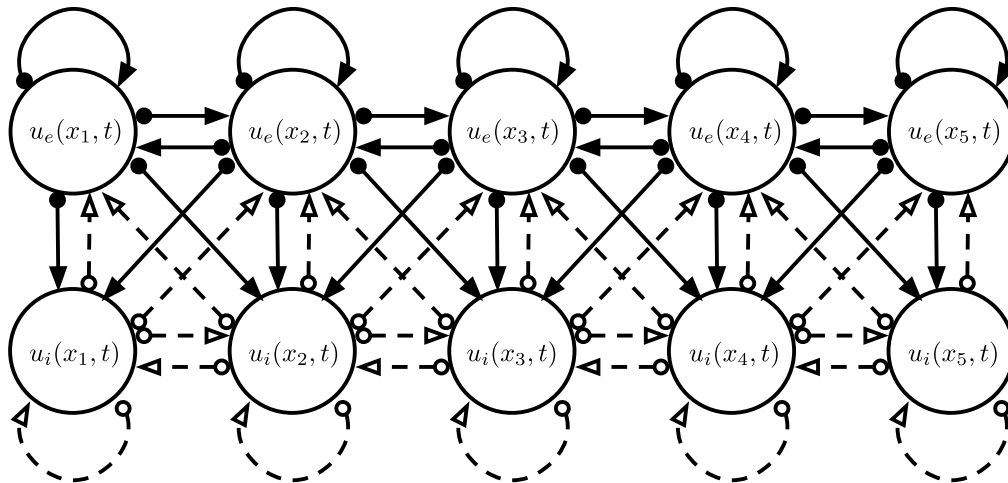


Figure 4: Diagram of basic two population neural field model (adapted from Wilson and Cowan (1973) [218]). This illustration gives a magnified representation of two interconnected neural continuums across one spatial dimension (with only nearest connections shown for brevity). Here we consider an ‘excitatory’ population and an ‘inhibitory’ population, where excitatory connections are represented by solid arrows whereas inhibitory connections are represented by dashed arrows. Neural field models in practice are indexed by a continuous spatial variable, as opposed to the discrete objects represented here. Although long-range connections are not shown for brevity, the strength of connections between neural populations tend to decrease exponentially with distance.

field equations as a scaffold for addressing the main assumptions necessary for the construction of all neural population models. We then provide a brief overview of the history of this class of models from the 1950s to the 1970s before discussing the canonical neural field model by Wilson and Cowan. We then compare this with concurrent formulations of neural field theory by Amari and Nunez and discuss the differences and similarities in mathematical structure. This section sets the scene for a discussion of more recent advances in neural field modelling considered in Section 4.

Before we begin, it is important to note that as neural field modelling approaches have evolved, a variety of names have appeared throughout the literature including ‘neural mass models’, ‘mean field models’, ‘neural population models’. Although these terms are all closely related, they are conceptually different and have been used interchangeably and ambiguously in the literature. The origin of ‘neural mass models’ can be traced back to the work of Walter Freeman and the concept of *mass action*: the observed population-level behaviour of a mass of neurons (Freeman, 1975 [70]). In his seminal work Freeman defined a second-order differential equation to describe the evolution of the population-level response to an external stimulus within the olfactory bulb. Over time, ‘neural mass models’ came to refer to the subset of neural field models constrained to a single point in space that have no spatial dependence. We will continue this discussion in Section 4.3. Since neural field models describe the average behaviour of neural populations, they’re also commonly referred to as ‘mean field models’. However it must be highlighted that this is not the same as utilising the ‘mean-field approximation’ from statistical mechanics (see for example Sompolinsky et al. (1988) [192]), where a network of interacting single neurons is replaced by a Gaussian process describing the average behaviour of a single unit. For more details, we refer the interested reader to Sompolinsky et al. (1988) [192], Vollhardt (2012) [210], Martínez-Cancino and Sotero Diaz (2011) [138], and the many references therein. The connection between this class of models and neural field models will be examined in Section 5.2.2. In this Section our focus is on exploring the origins and principles of the more general class of neural field models.

3.1 Principles of neural field models

Whilst the origin of the modern formulations of neural field models is found in the seminal works of Wilson and Cowan (1972, 1973) [217], [218], the neural field model proposed by Amari (1977) [5] provides a clearer framework for our definitions and the essential assumptions common to all neural field models by construction.

Within the neural field framework, neural interactions occur in a two-dimensional “cortical sheet”. This can be thought of as unfolding the sulci and gyri of the cortex into a flat sheet that is, on average, about 2.6 m^2 (Haberly and Shepherd, 1998 [85]). To mathematically do this, we must take two limits, the first countable and the second uncountable. First we take the thermodynamic limit, where the number of neurons approaches infinity whilst keeping the neuron density constant). Then we apply the continuum limit, where the neurons are treated as true mathematical points and the lattice spacing between the neurons shrinks to zero resulting in a continuum across the sheet.

Mathematical assumption: In neural field models, the cortex is treated spatiotemporally as a continuous two-dimensional sheet, in the sense that radial redundancy exists in the cortical columns and that the cortex is functionally two-dimensional. This is a significant approximation as neurons are actually discrete multi-compartmented entities embedded in a densely connected three-dimensional laminated volume. This assumption is made so that neural tissue can be treated

as an averaged bulk entity (Freeman, 1975 [70]) with approximated spatial and temporal distributions.

Neurons are grouped together in populations based on shared characteristics such as the polarity of signals, timescales of operation, the depth of cortex. The state variables are aggregate quantities of these populations, such as *mean membrane potential* $u_a(x, t)$ where a is a population index, x is a point in the neural field, and t is a point in time. Overall, the mean membrane potential is dictated by the *mean firing rate* of afferent populations. The magnitude of an incoming signal at a neuron depends on which population it arrived from, how far away the afferent neuron is, and how long ago the signal arrived. In turn, the mean membrane potential of a population dictates the mean firing rate of the population, which in turn influences the mean membrane potential of connected populations.

The strength of an incoming signal at a neuron decays soon after the signal is received, which can be represented as a simple temporal integral convolution. We can therefore describe the evolution of the mean membrane potential as

$$u_a(x, t) = \int_{-\infty}^t \psi(t - T) I_a(x, T) dT, \quad (3.1)$$

where the kernel ψ represents the temporal decay on incoming signals, and $I_a(x, t)$ represents the incoming signals received by population a . Contemporary neural field models typically represent these as temporal convolutions to allow for non-linear temporal operators such as those found in conductance-based synapses (Peterson et al., 2018 [162]).

The input term can be represented as a delta spike train corresponding to incoming action potentials with a spatial integral transformation that includes the spatial weighting of signals received by population a ,

$$I_a(x, t) = \sum_b \int_{\Omega} w_{a,b}(x, X) \sum_{m \in \mathbb{Z}} \delta(t - T_b^{(m)}(X)) dX + q_a(x, t), \quad (3.2)$$

where Ω denotes the spatial neural medium, the kernel $w_{a,b}(x, X)$ represents the spatial weighting of signals from population b at position X to population a at position x , $T_b^{(m)}(x)$ is the time of the m 'th action potential spike from population b at the position x , $\delta(t)$ is the Dirac delta distribution, and $q_a(x, t)$ is an external firing rate. The value of $w_{a,b}(x, X)$ can be interpreted as the probability of connection between neurons. In other words, the kernel represents the mean synaptic connectivity from population b at point X to population a at point x . In the vast majority of neural field models, the spatial kernel is assumed to be homogeneous so that $w_{a,b}(x, X) = w_{a,b}(x - X)$ and the corresponding integral transform is a spatial convolution.

Anatomical assumption: For every point in the neuronal medium, each neuron is assumed to be randomly connected, following some spatially homogeneous distribution. Collections of axons connect to nearby neurons, and can connect to neurons of the same population. This is a significant assumption, as a multitude of emergent dynamics of neural tissue arises from the non-trivial and non-local connectivity between constituents, which appears to follow fundamentally non-random trends.

The delta spike train can be replaced with a phenomenologically derived *wave-to-pulse transfer function* (also known as a *firing rate function*). Effectively this converts

the mean membrane potential into a mean firing rate (Freeman, 1992 [72]) if the synaptic response is on a slower timescale than that of the interspike interval and the variance is small (Coombes et al., 2003 [39], Bressloff and Coombes, 2000 [24]). Axonal conduction velocities can be assumed to be infinitely fast at this point in the derivation, however many contemporary models include a finite conduction velocity and a time-dependent component in their definition of $w_{a,b}$. Hence, we can express incoming signals from population b to population a as

$$I_a(x, t) = \sum_b \int_{\Omega} w_{a,b}(x, X) f_b[u_b(X, t - |x - X|/v)] dX + q_a(x, t), \quad (3.3)$$

where v is the axonal conduction velocity, and f_b is the wave-to-pulse transfer function. Traditionally, this is a static nonlinearity such as a sigmoidal function that is continuously differentiable, monotonically increasing, and saturating to a constant for small and large input values. This represents populations of neurons saturating to a maximal firing rate as the mean membrane potential increases. The most common form of this transfer function is the single logistic sigmoid, which is given as

$$f_a(u_a) = \frac{F_a}{1 + \exp[-\lambda_a(u_a - \theta_a)]}, \quad (3.4)$$

where u_a is the membrane potential of population a , F_a is the maximum firing rate of population a , and λ_a/θ_a are the shape/location parameters.

Mathematical assumption: We interpret the sigmoidal function, or in this case the logistic equation, as a close approximation of the cumulative function of a normal distribution (Marreiros et al., 2008 [133]), instead of the usual error function. In this way it has an associated mean and standard deviation of thresholds, that are averaged over a neuronal population. However, this assumes that the thresholding function is that of a McCulloch-Pitts neuron (McCulloch and Pitts, 1943 [143]), which is artificial and over-simplified compared to an actual spiking neuron model. Essentially, the sigmoidal function is a nonlinear function that is continuously differentiable, increasing, and smoothly bounded at both ends. The error function and the logistic equation are examples of sigmoid functions and are found in many natural systems (DeLean et al., 1978 [49]). For further information on its derivation, see the paper by Freeman (1979) [71] which was one of the first papers to try and derive the sigmoid function from experimental data, although it did appear in relation to neural models earlier than this (Freeman, 1972 [67], Wilson and Cowan, 1972 [217], Lopes da Silva et al., 1974 [129], Nunez, 1974 [153]).

In Figure 3 we present illustrations of examples of kernels $\psi(t)$ and $w_{a,b}(x)$, as well as a plot of a wave-to-pulse transfer function. In Figure 3(b), three different temporal kernels are shown. An exponential kernel assumes an instantaneous rise time, for example, where there is no synaptic decay and a decay defined by the membrane time-constant. An alpha function has a finite rise time and a synaptic time-constant that is the same as the membrane time-constant. A double exponential kernel has separate synaptic and membrane time-constants so that the rise and decay can be independent. In Figure 3(c), two different spatial kernels are shown where the Bessel function has a singularity at zero, whereas the Laplacian is finite at zero. Given that the region containing the singularity is immeasurable (zero distance) and largely irrelevant (only the tail of the distribution can be measured), the differences between these two functions are effectively negligible.

Combining the above equations (3.1) and (3.3) and assuming an infinitely fast conduction velocity ($v \rightarrow \infty$) gives us the integral form of a basic neural field model:

$$u_a(x, t) = \int_{-\infty}^t \psi(t - T) \left\{ \sum_b \int_{\Omega} w_{a,b}(x - X) f_b[u_b(X, T)] dX + q_a(x, T) \right\} dT. \quad (3.5)$$

This model represents the classical definition of the Amari equations.

Physiological assumption: The spatiotemporal delay resulting from the finite conduction velocity in Equation (3.3) can be omitted if we assume the conduction velocity is infinitely fast. This can be a suitable assumption for modelling smaller sections of neural tissue. For brevity, we will make this assumption here so as to eliminate the $|x - X|/v$ term in the temporal argument of $u(x, t)$ in the integrand. However, not all neural field models make this assumption.

From this foundation, we are in a better position to understand how neural field models evolved in the following decades, all of which are derived from these same fundamental principles. Referring to this structure also gives a clearer view of concurrent modelling approaches of this era, helping us to understand how this type of modelling was initially conceived between works of key research groups. Before we embark on the discussion of modern neural field modelling, we will revisit some of the early attempts to model neural populations and further highlight the structures and assumptions made. Many of these assumptions continue to be utilised in contemporary neural field models today.

3.2 Origins of neural field theory

The method of studying the average behaviour of a neuronal population can be traced back to Beurle (1956) [12]. Beurle explored the emergent properties of a continuum approximation to a mass of densely connected, uniformly distributed excitable cells, observing plane waves, spherical waves and vortex effects. Subsequently, in the early 1960s Griffith expanded these ideas, proposing a “nonlinear field theory” of neural networks (Griffith, 1963 [81]). Here the concept of a connectivity kernel that related the level of excitation to distance was introduced and the stability of emergent waves was subsequently studied (Griffith, 1965 [83]). Alongside these developments, it was also shown that inhibitory neural action was critical for wave stability (Griffith, 1963 [82]).

What we might now consider to be the beginnings of modern neural field theory, was established through the canonical models of Freeman (1972) [68], Wilson (1972) [217], Wilson and Cowan (1973) [218], Nunez (1974) [153], Lopes da Silva et al. (1974) [129] and Amari (1975 [4], 1977) [5]. Previous approaches only considered a single neuron population, whereas Wilson and Cowan derived the first canonical neural field model in terms of spatially extended masses of excitatory and inhibitory neurons.

Wilson and Cowan start with a description of mean neuronal activities across excitatory and inhibitory populations, and propose expressions for aggregated neural quantities based on concepts from neuronal dynamics. This approach effectively extends the work of Beurle from a single population to multiple populations. A sketch of the physiology considered in this model is given in Figure 4. The state variables used by Wilson and Cowan are *mean neuronal activity* per unit time, where $\hat{A}_e(x, t)$ refers to the activity of the excitatory population and $\hat{A}_i(x, t)$ refers to the activity of the inhibitory population. That is, activity is considered as the proportion of excitatory or inhibitory neurons at (x, t) that are firing action potentials. These variables are related to the

average firing rate: when this is one, the neurons are all firing action potentials at their maximum rate whereas an average firing rate of zero represents typical background activity. Small negative values are permitted and represent a dampening of background activity. Wilson and Cowan state their model in terms of update equations, given by

$$\hat{A}_e(x, t + \tau) = R_e(x, t) S_e[N_e(x, t)], \quad \hat{A}_i(x, t + \tau) = R_i(x, t) S_i[N_i(x, t)], \quad (3.6)$$

where τ represents the synaptic operating delay (time taken for a neuron to fire an action potential after its membrane potential surpasses threshold), $R_a(x, t)$ is the fraction of population a that is primed to fire an action potential (outside the refractory phase), and $S_a(u) = f_a(u) - f_a(0)$ (using f_a from Equation (3.4) with $F_a = 1$) represents a centred wave-to-pulse transfer function. The expression $S_a(N_a(x, t))$ relates mean population input, $N_a(x, t)$, to the fraction of population surpassing threshold excitation and firing action potentials. Wilson and Cowan originally use a centred activation function that passes through the origin and approaches a negative asymptote as the argument decreases below zero, but this is likely due to the choice in definition of the state variables of the system.

Mathematical assumption: This formulation assumes that the primed fraction of the population, $R_a(x, t)$, and the firing fraction of the population $S_a(N_a(x, t))$ are independent. However, in general this is not true (Cowan et al., 2016 [44]), (Smith and Davidson, 1962 [189]). As highlighted by Wilson and Cowan, for finite populations of neurons there will be a correlation between the recency of a neuron firing and its likelihood of firing in the future. However, Wilson and Cowan argue that if the number of neurons in these population is large enough, this correlation will become small, and so independence is considered a reasonable approximation.

The synaptic operating delay τ refers to the period between a neuron’s membrane potential surpassing the threshold potential and the neuron becoming active and initiating an action potential. This quantity is not well described in the 1972 [217] and 1973 [218] papers, but it is effectively a computational timestep for the neural system assumed to have an order of 0.5 ms. The model posed by Beurle (1956) [12] utilised the same terminology, and the work by Wilson and Cowan sought to improve upon these early findings. It should be highlighted here that neural population models at this time were largely conceptual and the data on neuronal activity and synaptic interactions was not well-developed. Significant assumptions about the values of these timescales had to be made in order to begin the study of these particular dynamical systems, which could then be evolved and improved over time.

The proportion of sensitive neurons in the population is complementary to the proportion of neurons that are in the refractory period,

$$R_e(x, t) = 1 - \int_{t-r_e}^t \hat{A}_e(x, T) dT \quad R_i(x, t) = 1 - \int_{t-r_i}^t \hat{A}_i(x, T) dT \quad (3.7)$$

where r_e/r_i are the refractory periods of excitatory/inhibitory neurons. Each spiking input to the population has a magnitude that depends on the connectivity or synaptic strength to the upstream population. Additionally, it is assumed that the populations of neurons sum their net mean inputs and the effect of stimulation decays over time. This can be thought of as the influence of spiking inputs to individual neurons on neuronal activity diminishing as time from the input signal increases. It can be represented as a temporal integral convolution with a kernel denoted by $\alpha(t)$, which is generally taken as a simple exponential.

Physiological assumption It is assumed in the Wilson and Cowan derivations that $\alpha(t) = \hat{\alpha} \exp(-t/\mu)\Theta(t)$ where $\hat{\alpha}$ is the maximum post-synaptic potential amplitude, μ is a time constant of decay and $\Theta(t)$ is the Heaviside step function. It is assumed that the effect of stimulation decays with the same rate across excitatory and inhibitory neurons, so that μ is a population-independent time constant. Future models incorporate this detail into their choice of spatial kernels and setting $\hat{\alpha} = 1$. This alternate method tends to be more common since the magnitude (as well as polarity of signals) tend to be dependent on the afferent population.

In addition to the temporal decay of afferent signals, the initial magnitude of those signals will depend on where they originated from, as we conceptually described in Equation (3.2). Using homogeneous spatial kernels, Wilson and Cowan express the mean population inputs by

$$\begin{aligned} N_e(x, t) &= \int_{-\infty}^t \alpha(t - T) \left\{ [\beta_{e,e} \otimes_x \hat{A}_e](x, t) - [\beta_{e,i} \otimes_x \hat{A}_i](x, t) + P_e(x, t) \right\} dT, \\ N_i(x, t) &= \int_{-\infty}^t \alpha(t - T) \left\{ [\beta_{i,e} \otimes_x \hat{A}_e](x, t) - [\beta_{i,i} \otimes_x \hat{A}_i](x, t) + P_i(x, t) \right\} dT, \end{aligned} \tag{3.8}$$

where $[\beta_{a,b} \otimes_x f](x) = \int_{\Omega} \beta_{a,b}(x - X)f(X) dX$ represents a spatial convolution, and P_e/P_i represent external inputs to the excitatory/inhibitory populations.

Physiological assumption: Connectivity is assumed to be of the form $\beta_{a,b}(x) = \bar{\beta}_{a,b} \exp(-|x|/\sigma_{a,b})$ where $\sigma_{a,b}$ denotes the space constant and $\bar{\beta}_{a,b}$ denotes the mean synaptic weight (Uttley and Matthews, 1955 [207], Sholl, 1956 [186]).

A simpler expression of this system is possible by interchanging the order of temporal and spatial integrals and using the time coarse grained variables

$$A_a(x, t) = \frac{1}{\mu} \int_{-\infty}^t \exp\left(-\frac{t-T}{\mu}\right) \hat{A}_a(x, T) dT \tag{3.9}$$

These new variables provide a first-order simplification of the integro-differential equations.

Physiological assumption: It is assumed here that the membrane time constant is an order of magnitude more significant than the synaptic dynamics. This effectively makes the synapses instantaneous interfaces, which is not the case in reality. Additionally, it is also assumed in the final Wilson and Cowan model that signal propagation along axons is also instantaneous. This may be a suitable simplification on smaller spatial regions, but may be inappropriate for modelling large sections of cortex such as a lobe of the brain.

This change of variables is not without consequence. Wilson and Cowan highlight that such a transformation inevitably removes high frequency variations, but they argue that such variations are not relevant to the implications results. Since the kernel of this integral transformation is $\frac{1}{\mu} \exp(-t/\mu)\Theta(t)$, the Green's function of the differential operator $(1 + \mu \frac{\partial}{\partial t})$. This gives us the relation

$$\hat{A}_a(x, t) = \mu \frac{\partial}{\partial t} A_a(x, t) + A_a(x, t), \tag{3.10}$$

Using the fact that the refractory period of cortical neurons r_a is an order of magnitude lower than the membrane time constant μ (Oshima and Jasper, 1969 [159]), we have $A_e(x, t) \approx A_e(x, t - r)$. We can then integrate both sides of the above relation and apply this approximation to obtain

$$\int_{t-r_a}^t \hat{A}_a(x, T) dT = \mu [A_a(x, t) - A_a(x, t - r)] + \int_{t-r_a}^t A_a(x, T) dT, \quad (3.11)$$

$$\approx r_a A_a(x, t), \quad \implies \quad R_a(x, t) \approx [1 - r_a A_a(x, t)].$$

The derivation by Wilson and Cowan (1973) [218] initially asserts that axonal velocity is finite, but they relax that assumption towards the end of their derivation. In this derivation we will assume that the conduction velocity is infinitely fast so that we may keep our guided derivation simpler. Expanding the left hand side of the Wilson and Cowan Equations (3.6) in a Taylor series gives:

$$\hat{A}_a(x, t + \tau) \approx \hat{A}_a(x, t) + \tau \frac{\partial \hat{A}_a}{\partial t}(x, t), \quad (3.12)$$

where we have omitted the terms of higher order τ^2 , since $\tau \ll 1$. Taking the derivative of \hat{A}_a with respect to t in Equation (3.10) and substituting the result into this expression gives

$$\hat{A}_a(x, t + \tau) \approx A_a(x, t) + (\mu + \tau) \frac{\partial A_a}{\partial t}(x, t) + \tau \mu \frac{\partial^2 A_a}{\partial t^2}(x, t) = \left(1 + \tau \frac{\partial}{\partial t}\right) \left(1 + \mu \frac{\partial}{\partial t}\right) A_a(x, t). \quad (3.13)$$

Here it is assumed that the synaptic operating delay is at least an order of magnitude smaller than the membrane decay constant, enabling a further approximation:

$$\hat{A}_a(x, t + \tau) \approx A_a(x, t) + \mu \frac{\partial A_a}{\partial t}(x, t). \quad (3.14)$$

We can then substitute this result back into Equation 3.6 along with the above results to obtain the system

$$\mu \frac{\partial}{\partial t} A_e(x, t) = -A_e(x, t) + [1 - r_e A_e(x, t)] S_e \{ [w_{e,e} \otimes_x A_e](x, t) - [w_{e,i} \otimes_x A_i](x, t) + Q_e(x, t) \}, \quad (3.15)$$

$$\mu \frac{\partial}{\partial t} A_i(x, t) = -A_i(x, t) + [1 - r_i A_i(x, t)] S_i \{ [w_{i,e} \otimes_x A_e](x, t) - [w_{i,i} \otimes_x A_i](x, t) + Q_i(x, t) \}, \quad (3.16)$$

where $w_{a,b}(x) = \hat{\alpha} \mu \beta_{a,b}(x)$ is a scaled connectivity kernel, and $Q_a(x, t) = \int_{-\infty}^t \alpha(t - T) \hat{Q}_a(x, T) dT$ represents a filtered external input. It should be noted that most neural field models disregard the refractory period at this scale of description, and thus set $r = 0$ implicitly or explicitly as an additional approximation. Disregarding the refractory period, we note this system can also be represented in the more general form:

$$\mu \frac{\partial}{\partial t} A_a(x, t) = -A_a(x, t) + S_a \left\{ \sum_b w_{a,b}(x) \otimes_x A_b(x, t) + Q_a(x, t) \right\}, \quad (3.17)$$

where a, b are generic population indices, μ is the membrane time constant of population a , and $w_{a,b}(x)$ is the connectivity kernel summarising the signed magnitude of post-synaptic potentials.

The Wilson and Cowan model represented a major step forward for the field of macroscale neural modelling, significantly extending the previous models of Beurle and Griffith. Critically, the model proposed by Wilson and Cowan recognised and incorporated the influence on emergent neural dynamics of inhibitory neurons. In contrast, most early neural field models only considered only a single excitatory population. This permanently changed the course of development of models in this field, and directly led to the modern formulations of neural field theory. The dynamical system analyses of resulting fixed points and limit cycles that led to these conclusions and consequent developments are summarised by Zetterberg et al. (1978) [224], Ermentrout Terman (2010) [60], and Neves and Monteiro (2016) [152]. A brief summary of the applications and extensions of the Wilson and Cowan model can be found in the reviews by Kilpatrick (2013) [106] and Chow and Karimipناه (2020) [38].

Following the work of Wilson and Cowan, the neural field models were further developed by other authors. Of note is a publication by Amari who investigated spatiotemporal patterns and information processing in homogeneous neural networks (Amari, 1975 [4]). Amari further developed these approaches in a subsequent publication (Amari, 1977 [5]), that considered an extension from discrete neural networks to a neural field continuum. In contrast to Wilson and Cowan who segregated populations according to whether neurons were excitatory or inhibitory, the neural field model put forth by Amari segregated neurons into populations according to cortical depth. Here, each layer contained both excitatory and inhibitory neurons, whose signals were encoded within the spatial kernels $w_{a,b}$ representing close inhibitory connections and long-range excitatory connections (Amari, 1975 [4]).

Physiological assumption: Amari assumes that each layer of cortical neurons have non-identical time constants. As with the Wilson and Cowan model, it is still assumed that incoming postsynaptic potentials have infinitely fast rise, followed by an exponential decay. This is in fact a generalisation of the work of Wilson and Cowan, which only allowed one time constant for all populations of neurons.

The derivation of the Amari field equations closely follows the principles we discussed in Section 3.1, but instead using population-dependent temporal kernels ψ_a :

$$u_a(x, t) = \int_{-\infty}^t \psi_a(t - T) \left\{ \sum_b \int_{\Omega} w_{a,b}(x - X) f_b[u_b(X, T)] dX + q_a(x, T) \right\} dT, \quad (3.18)$$

where $u_a(x, t)$ is the mean membrane potential of neurons in population a at position x and time t , $\psi_a(t)$ is the temporal kernel of population a , $w_{a,b}(x)$ is the spatially homogeneous spatial kernel that assigns signed weights to incoming signals from population b according to distance, and $q_a(x, t)$ is the external input to population a . Note if we use a linear description of temporal decay of signals, we may utilise Green's functions to invert the convolution and express the Amari model in differential form. As with many other models in this period, it is assumed that spikes are instantaneous and exponentially decay. Hence, Amari utilises the temporal kernel given by $\psi_a(t) = \frac{1}{\mu_a} \exp(-t/\mu_a) \Theta(t)$, where μ_a is the membrane time constant of population a and $\Theta(t)$ is the Heaviside step function, which allows us to express the Amari equations in differential form,

$$\mu_a \frac{\partial}{\partial t} u_a(x, t) = -u_a(x, t) + \sum_b \int_{\Omega} w_{a,b}(x - X) f_b[u_b(X, t)] dX + q_a(x, t). \quad (3.19)$$

This form of the Amari equations appears to resemble the field equations derived by Wilson and Cowan, which we summarised in Equation (3.17) with some key mathematical

differences. The major difference appears to be the ordering of the sigmoidal wave-to-pulse transform and the sum over afferent signals from different populations. Specifically, the Wilson and Cowan model takes the sigmoid of a sum of inputs whereas the Amari model takes the sum of sigmoids of inputs. Another minor difference can be identified in the definition of the wave-to-pulse transformations in either formulation. The Wilson and Cowan model uses a centred sigmoid $S_a(u)$, whereas the Amari equation uses a non-centred sigmoid $f_a(u)$, but this difference can be rectified by a translation mapping given by $S_a(u) = f_a(u) - f_a(0)$. Despite this difference in formulation, both equations give rise to similar dynamics. This is unsurprising since they describe the same physical system from two different perspectives. The Wilson and Cowan model state variables start with a description of “proportion of active neurons at a point”, which can be interpreted as analogous to a mean firing rate of a population. This can be easily visualised by a comparison of the diagrammatic representation of these systems in Figure 5. From a purely mathematical perspective, the Wilson and Cowan model is equivalent to an Amari model with a single membrane time constant $\mu_a = \mu$ subject to the following transformations:

$$u_a(x, t) = \sum_b A_b(x, t) \otimes w_{a,b}(x) + Q_a(x, t), \tag{3.20}$$

$$\mu \frac{\partial}{\partial t} A_a(x, t) + A_a(x, t) = f_a[u_a(x, t)]. \tag{3.21}$$

This substitution and calculation was performed by Miller and Fumarola (2011) [147], but is extended here for spatially-dependent neural fields. By taking the first time derivative of Equation (3.20) we have

$$\begin{aligned} \mu \frac{\partial}{\partial t} (u_a(x, t) - Q_a(x, t)) &= \sum_b \left(\mu \frac{\partial}{\partial t} A_b(x, t) \right) \otimes w_{a,b}(x), \\ &= - \sum_b A_b(x, t) \otimes w_{a,b}(x) + \sum_b S_b[u_b(x, t)] \otimes w_{a,b}(x), \end{aligned} \tag{3.17},$$

$$= -(u_a(x, t) - Q_a(x, t)) + \sum_b S_b[u_b(x, t)] \otimes w_{a,b}(x), \tag{3.20},$$

$$\iff \mu \frac{\partial}{\partial t} u_a(x, t) = -u_a(x, t) + \sum_b f_b[u_b(x, t)] \otimes w_{a,b}(x) + q_a(x, t),$$

where $q_a(x, t) = (\mu \frac{\partial}{\partial t} + 1) Q_a(x, t) + \sum_b f_b(0) \int_{\Omega} w_{a,b}(x - X) dX$. This transformation only works for an Amari model with one membrane time constant instead of multiple population-specific time constants (or if there is only one neural population).

While these models are closely related, the operations follow a different order when applied to their respective state variables. In the Wilson and Cowan model the temporal filter occurs after the sigmoid and before the sum, whereas in the Amari model the temporal filter occurs after the sum and before the sigmoid. We highlight this in Figure 5. Equivalence of these models occurs only if the temporal kernel is population-independent. Under this assumption the operations commute and so are interchangeable. This is due to the nature of the approximations taken by Wilson and Cowan and the original (without time coarse graining) state variables used. However, one can still apply this transformation to obtain an extended Wilson and Cowan model with multiple timescales, but the resulting “activity” state variables will not be identifiable with the original state variables proposed by Wilson and Cowan. Fundamentally, the separation in time scales across populations is a different model that expands beyond the scope of the original Wilson and Cowan equations.

Mathematically, the Wilson and Cowan formulation is arguably more attractive, since linearising a dynamical system over a single sigmoid is less complex than linearising over

a sum of sigmoids. However, this formulation is delicate and requires a large amount of assumptions and conceptual leaps to derive and simplify from first principles as we have seen throughout this Section. Nonetheless, the ideas behind this transformation can be used to transform any neural field model into the single sigmoid form, and we will formalise this within a general mathematical framework in Section 4.2.

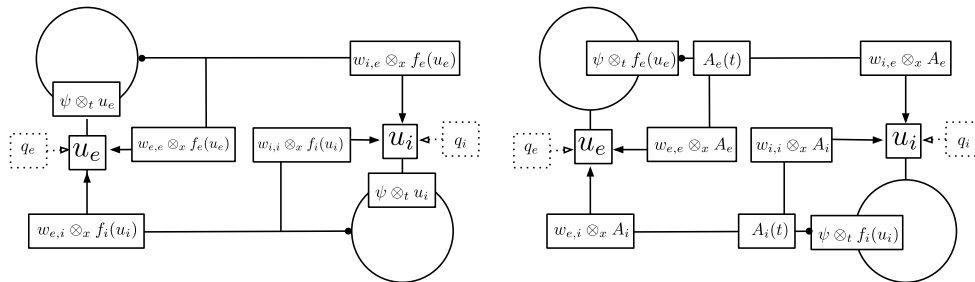


Figure 5: **Comparison of first order neural field by Amari (left) and Wilson and Cowan (right).** The relation between the Wilson-Cowan model and the Amari model is illustrated with annotations of the corresponding state variables A_e, A_i and u_e, u_i . Although the mathematical structure of these models appears different, they describe similar dynamical systems from different perspectives. The differential operator in these models can be represented as a temporal convolution with a kernel ψ using standard methods of integral transforms. Temporal convolution is represented here with \otimes_t and spatial convolution is represented with \otimes_x . Crucially, the Amari formulation considers a sum of sigmoids of inputs whereas the Wilson and Cowan formulation considers a sigmoid of a sum of inputs. These operations do not commute with the temporal kernel ψ unless the kernel is population-independent, hence these formulations are only equivalent when the temporal kernel is population independent.

These early neural field models were an important milestone for the development of mathematical descriptions of large-scale neural activity. Analysing dynamical systems became a common goal amongst a variety of research groups as this methodology became more established throughout the 1970's. However, there were significant limitations of the utility of these models, and some of these limitations have been inherited by modern approaches of neural field theory. In particular, the quantities modelled and parameters used in these constructions were difficult to estimate and fit from methods of data acquisition in experimental neuroscience at the time. This is still a problem that exists today due to limitations in experimental neuroscience, but there are ongoing efforts to improve how we quantify connectivity in neural tissue that can be utilised in new iterations of neural field theory. Synaptic dynamics in particular have more complexity and variability than this, the frameworks put forth by Wilson, Cowan, and Amari can be regarded as *first order neural fields*, as they neglect the variability in the synaptic dynamics and focus only on the overall mean membrane potentials. However, the models proposed by Nunez (1974) [153] (as well as Lopes da Silva et al. (1974) [129] and Freeman (1975) [70]) address this shortcoming in synaptic interactions. Before we discuss modern neural field models, we will review the development of this additional principle through a general overview of the framework by Nunez.

3.3 Synaptic population dynamics

Around the same time as the work of Wilson and Cowan (1972) [217] and Freeman (1972) [68], another distinct approach to modelling neural population dynamics emerged

in the work of Nunez (1974) [153]. The mathematical framework presented by Nunez uses different state variables and finds another balance between biological plausibility and mathematical tractability. The equations appear to be distinct from the Wilson and Cowan equations, as well as the Amari field equations, but as highlighted by Jirsa and Haken (1997) [96], the Nunez brain wave equation is grounded in the same mathematical principles. Instead of connecting the Nunez model to the frameworks of Amari, Wilson, and Cowan, we will instead focus on what made this model distinct in its formulation. Although based in the same principles, this model was constructed on the basis of synaptic interactions, similarly to the models of Freeman (1974) [69] and Lopes da Silva et al. (1974) [129], all of which foreshadow key developments in modern neural field theory.

Instead of modelling multiple populations, the Nunez brain wave equation effectively models one population with both excitatory and inhibitory synapses. This model aims to maintain a close relationship with established biophysics and begins with a decomposition of electroencephalography (EEG) signals in terms of contributions from excitatory/inhibitory post-synaptic potentials and action potentials. We will return to our discussion of EEG in Section 4.4, as there are significant assumptions necessary for this connection to EEG data, but here we will simply consider the conceptual electrical potential of the neural field. Consider a one-dimensional neural field Ω consisting of a single population of cortical neurons. The instantaneous gross potential of the field, Φ , is related to the decomposition

$$\Phi(x, t) \sim \phi \rho A(x, t) + \phi_e \rho_e(x, t) - \phi_i \rho_i(x, t), \tag{3.22}$$

where ρ is the density of cortical cells, ϕ is the local surface potential of a single active cortical cell, A is the fraction of active cortical cells (similar to the state variables in the Wilson and Cowan equations), ϕ_e/ϕ_i is the surface potential of a single excitatory/inhibitory post-synaptic potential, and $\rho_e(x, t)/\rho_i(x, t)$ is the density of the excitatory/inhibitory post-synaptic potentials. The underlying relationship between A and ρ_e/ρ_i is the principle driver of cortical dynamics.

The excitatory/inhibitory post-synaptic potentials ρ_e/ρ_i depend on the aggregated fraction of active cortical cells A , weighted by the mean connectivity. The connectivity in the neural field is described by a spatial kernel within an integral transform, as we have seen for the Amari equations and the Wilson and Cowan equations. The model by Nunez is explicitly intended to model large-scale neural activity, so axonal conduction velocities c are considered. The duration of signal transmission between two points in neural tissue is highly variable, depending on the complex geometry and topology of the relevant neural networks. It is impossible to include this level of detail when modelling at this scale, but the integral kernel can be expanded to incorporate the broad impact of variable conduction velocities. Let $w_a(c, x, X)$ represent the mean connectivity from X to synapse group $a \in \{e, i\}$ at the point x than have an average axonal velocity c . Then the mean excitatory/inhibitory post-synaptic potentials ρ_e/ρ_i can be represented in terms of the fraction of active cortical cells A with

$$\rho_a(x, t) = Q_a(x, t) + \int_0^\infty \int_\Omega w_a(c, x, X) A \left(X, t - \frac{|x - X|}{c} \right) dX dc, \tag{3.23}$$

where $a \in \{e, i\}$ is a synapse index, $Q_a(x, t)$ is an external/sub-cortical synaptic input. With similar justifications as found in the Wilson and Cowan model (Nunez, 1974 [153], 2000 [155], Nunez and Srinivasan 2006 [157]), a typical choice of spatial kernel is given by

$$w_a(c, x, X) = \sum_{n=1}^N \lambda_n^{(a)} f_n^{(a)}(c) \exp(-\lambda_n^{(a)} |x - X|). \tag{3.24}$$

In turn, the aggregated fraction of active neurons A also responds to changes in the excitatory/inhibitory post-synaptic densities ρ_e/ρ_i . The mean membrane potential $u(x, t)$ can be assumed to be represented as a linear sum $u(x, t) = \nu_e \rho_e(x, t) + \nu_i \rho_i(x, t)$, where ν_e/ν_i is the magnitude of excitatory/inhibitory post-synaptic potentials. Using the principle of mass action (Freeman, 1972 [68]), the mean membrane potential is related to the firing rate of the population by a sigmoidal wave-to-pulse transfer function $f(u)$ (Equation (3.4)). Hence, we have the relation $A(x, t) = f(\nu_e \rho_e(x, t) + \nu_i \rho_i(x, t))$ (Jirsa and Haken, 1997 [96]). In the simplest case, this can be expanded about a fixed point of A and this non-linearity can be replaced with a linear relationship, given by $A(x, t) = A_0 + \nu_e \rho_e - \nu_i \rho_i$ (Nunez, 1974 [153], 1989 [154], Jirsa and Haken, 1997 [96]).

To transform these integral equations into partial differential equations, a spatial-temporal Fourier transform can be used. Let $\hat{\rho}_a(x, \omega) = \mathcal{F}\{\rho_a : t \rightarrow \omega\}$ be the temporal Fourier transform of ρ_a . Then from Equation (3.23), we have

$$\hat{\rho}_a(x, \omega) = \hat{Q}_a(x, \omega) + \int_0^\infty \int_\Omega w_a(c, x, X) e^{-i\omega \tau(c, x-X)} \hat{A}(X, \omega) dX dc, \quad (3.25)$$

where $\tau(c, x - X) = |x - X|/c$ is the spatiotemporal delay. Assuming the connectivity is homogeneous, we can write $w_a(c, x, X) = w_a(c, x - X)$. For brevity, we set $W_a(c, x - X, \omega) = w_a(c, x - X) e^{-i\omega \tau(c, x-X)}$. Let $\tilde{\rho}_a(k, \omega) = \mathcal{F}\{\hat{\rho}_a : x \rightarrow k\}$ be the spatial Fourier transform. Combining the above results, we have

$$\tilde{\rho}_a(k, \omega) = \tilde{Q}_a(k, \omega) + \tilde{A}_a(k, \omega) \int_0^\infty \tilde{W}_a(c, k) dc. \quad (3.26)$$

A wave equation can be obtained from this relation by evaluating the transformed connectivity kernel, rearranging this relation, expressing A in terms of ρ_e/ρ_i (with linear approximation or non-linear sigmoidal relation), and inverting the Fourier transforms. Details of further steps in this general derivation, as well as simplifications and approximations, can be found in the works of Nunez (1989) [154], Nunez and Cutillo (1995) [156], Nunez (2000) [155], Nunez and Srinivasan (2006) [157], (2014) [158].

Although the Nunez brain equation only models one cortical population, it resembles a two-population model due to the way it factors the intertwined excitatory and inhibitory synaptic interactions rather than using distinct neural populations. This alternative focus on the synapses rather than the cells was also seen in the models of Freeman (1974) [69], Lopes da Silva et al. (1974) [129], van Rotterdam et al. (1982) [209], and became a dominant concept in the development of modern neural field modelling. Nonetheless, the wave equation derived by Nunez was a significant theoretical development in neural field modelling, and continues to be a source of discussion throughout the literature (Ross et al., 2020 [179]). We will see in practice throughout the next Section how essential this synaptic viewpoint is to the construction of modern neural field models.

4 Modern formulations of neural field modelling

Following the canonical works of Wilson and Cowan, Freeman, Amari, and Nunez in the 1970's, neural field theory continued to evolve as did the mathematical conceptualisation of a neural mass. Neurons are complex multi-compartmental units that transmit an excitatory or inhibitory signal to other neurons if and only if a weighted sum of temporally decaying afferent stimuli exceeds a threshold potential. Each of these constituent units of neural systems exhibit non-local and non-trivial connectivity, and are also susceptible to microscopic stochastic fluctuations. The accumulation of these complexities leads to patterns of complex oscillatory activities - even in relatively small systems - that appear to be crucial for information processing in neural systems. Key results from these early

neural field models demonstrated that a statistical physics approach may be viable, perhaps essential, to explain fundamental modes of function and signal propagation in neural systems. Developments on this front are critical to advancing neuroscience, understanding information processing, and developing novel solutions and therapies to common neurological diseases that exhibit pathological oscillation in brain activity. As this branch of mathematical neuroscience progressed, necessary developments were made in the level of detail of these models, particularly as more neural populations were integrated in this mathematical framework.

This increased granularity and level of detail occurred throughout the resurgence of neural field models in the 1990's (Freeman, 1992 [72], Wright et al., 1994 [221], Wright and Liley, 1995 [222], Nunez and Cutillo, 1995 [156], Jansen and Rit, 1995 [91]), especially when methods to transform the integro-differential equations into partial differential equations were employed (Jirsa and Haken, 1996 [95], 1997 [96], Robinson et al., 1997 [178]). At this point there was a significant increase in the literature as researchers realised that neural field models were a viable way to describe brain activity as measured by the EEG, for example, brain rhythms (Liley et al., 1999 [124], 2002 [125], Nunez and Cutillo, 1995 [156], Robinson et al., 2001 [177], 2003 [176], Rennie et al., 2002 [172]), the effects of anaesthesia (Steyn-Ross, 1999 [195], Bojak and Liley, 2005 [16]), the onset of dementia (Bhattacharya, 2011 [13], Pons et al., 2010 [164], Müller, 2017 [150]), and epilepsy (Lopes da Silva et al., 2003 [130], Breakspear et al., 2006 [19], Blenkinsop et al., 2012 [15], Kramer et al., 2012 [110], Martinet et al., 2017 [137]).

In this section, we will look at central concepts prevalent in all modern neural field (and neural mass) models, where the model output can be interpreted as an integral equation typical of a signal processing problem. The physiological basis for these modern neural field approaches are addressed, and we discuss how this gives rise to differences in mathematical structure between neural field models that describe the same phenomena. Following this, we will give an example derivation of a general multi-population neural field model, utilising the assumptions found in the work of Amari (1977) [5], Robinson et al. (1997) [178], Jirsa and Haken (1997) [96], and Coombes et al. (2003) [39]. We show how the integral form of these equations are reformulated as coupled partial differential equations. The original reduction of the field equation and subsequent derivation of the partial differential wave equation was performed by Jirsa and Haken (1997) [96] and Robinson et al. (1997) [178]. This was recapitulated by Coombes et al. (2003) [39] and is summarised and annotated below for completeness sake, and for future reference. Special attention is paid to the underlying assumptions that lead to the model equations. We will then briefly discuss non-linear and stochastic extensions of the modern neural field modelling framework and conclude with a discussion on the limitations of neural field theory before we show how this framework can be simplified further by considering connectivity at a point only. This eliminates spatial dependence, and provides the common structure to neural mass models.

4.1 A unifying framework for neural fields

Historically, the level of description of neural field models has been at the level of mean membrane potentials (or equivalently the mean firing rate) across neuronal populations. This characterisation using these state variables seems intuitive at first, but it lacks essential detail on the inputs to the mean membrane potential: synaptic transmission. Modelling mean membrane potentials directly often does not allow for the inclusion for different temporal dynamics corresponding to each type of post synaptic potential. Instead, modern neural field models use the *mean post-synaptic potentials* as their state variables to better capture this detail and provide a more realistic model of neuronal dynamics. Neural field models following the publications of Wilson and Cowan

addressed the temporal dynamics of afferent signals in more detail, since the magnitude, sign, and timescale of a received signal is dependent on the particular neurotransmitter used (Zetterberg, 1973 [225], Lopes da Silva et al., 1974 [129], van Rotterdam et al., 1982 [209]). As mentioned in the physiological background in Section 2.1, synapses are remarkably complex interfaces subject to variability in neurotransmitters. This can result in drastically different time-scales and signed magnitudes. Differences can arise from the location of the synapse relative to the cell body, and the kinetics of the neurotransmitter and the ion channels involved, as well as extracellular dynamics.

The representation of neural field models can differ significantly between publications from different authors, sometimes even between publications from the same authors. Throughout the literature, neural field models can be conceptualised as either a temporal differential operator acting on state variables or as a type-II Volterra integral equation (Stone and Goldbart, 2009 [196]). Both forms are equivalent, but have different advantages in practice. For instance, differential operator forms are more useful for the numerical studies of these systems. Theoretically, it is simpler to work with the integral equation formulation, as the temporal integral convolution operator clearly depicts the pulse-to-wave transfer operation, which converts the mean firing rate to a mean post-synaptic potential. All linear differential formulations can be expressed in integral form by using Fourier transforms and Green’s functions. This was demonstrated in the previous section, where we began with an integral description of the Amari field equations in (3.18). and used elementary techniques to translate to a partial differential equation description of the Amari model in (3.19),

$$u_a(x, t) = \int_{-\infty}^t \psi_a(t - T) \left\{ \sum_b \int_{\Omega} w_{a,b}(x - X) f_b[u_b(X, T)] dX + q_a(x, T) \right\} dT,$$

$$\iff \mu_a \frac{\partial}{\partial t} u_a(x, t) = -u_a(x, t) + \sum_b \int_{\Omega} w_{a,b}(x - X) f_b[u_b(X, t)] dX + q_a(x, t),$$

where $\psi_a(t) = \frac{1}{\mu_a} e^{-\frac{t}{\mu_a}} \Theta(t)$ is referred to as the temporal kernel (and $\Theta(t)$ is the Heaviside step function). This formulation allows for a clearer interpretation of neural fields as a signal processing problem, where the temporal kernel represents post-synaptic processing. The temporal kernel can be any suitable function that is zero for all negative t , has a sharp rise to maximum, and decays to zero as t increases.

The Amari field equations were a crucial extension of the model by Wilson and Cowan, allowing for population-specific timescales. This permitted the inclusion of more realistic population interactions, as different membrane timescales can account for different trends in synapse locations and/or different neurotransmitter dynamics across different populations. Neural field models following the work of Amari expanded on this concept, and further generalised the input to the field equations to allow for the inclusion of more detailed interactions at the synapse junctions between populations. We can illustrate this critical expansion by extending the Amari field equations directly.

Consider a neural field across a one dimensional spatial domain Ω composed of N generic neural populations and let $u_a(x, t)$ denote the mean membrane potential of population a at the point $x \in \Omega$ at time t . The mean membrane potential is determined by the mean post-synaptic potential $V_{a,b}(x, t)$ where b is a population that connects to population a . The current mean membrane potentials will influence the conductance, hence we can summarise the magnitude and polarity of the post-synaptic potentials with state-dependent constants $\nu_{a,b}(u_b(x, t))$. This weighted sum of post synaptic potentials (as well as any external input) will be temporally filtered, since the strength of a signal decays rapidly. We can mathematically express this relation between $u_a(x, t)$ and $V_{a,b}(x, t)$

as

$$u_a(x, t) = \int_{-\infty}^t \eta_a(t - T) \left\{ \sum_b \nu_{a,b}(u_b(x, T)) V_{a,b}(x, T) + u_a^0(x, T) \right\} dT, \quad (4.1)$$

where $\eta_a(t)$ represents the synaptic kernel of population a . We note here that some models (such as the cortical model from Liley et al. (1999) [124]) include an external input term within the braces in the integral, but the formulation of external inputs differs between publications so we will omit these terms for now. More elaborate neural field models, such as those seen in the work of Liley et al. (1999) [124] and Steyn-Ross et al. (1999) [195], include more realistic conductance-based synaptic dynamics (Peterson et al., 2018 [162]) at the expense of introducing further non-linearity to the model equations. However, most neural field models in practice tend to use the simplest mapping from mean post-synaptic potentials to mean membrane potentials by assuming synapses act instantaneously and that synaptic weights are state-independent. That is, most authors set $\eta_a(t) = \delta(t)$ where δ denotes the Dirac delta distribution, and set $\nu_{a,b}(u_b)$ to be a constant value $\nu_{a,b}$ for each a and b . This gives the mapping

$$u_a(x, t) = \sum_b \nu_{a,b} V_{a,b}(x, t) + u_a^0(x, t). \quad (4.2)$$

Each of these post-synaptic potentials can be expressed as a spiking input that is temporally weighted, which is represented by a spatial convolution with a connectivity kernel,

$$V_{a,b}(x, t) = \int_{-\infty}^t \psi_{a,b}(t - T) \phi_{a,b}(x, T) dT. \quad (4.3)$$

where $\phi_{a,b}(x, t)$ denotes the mean pulse density at the synapses of population a from the population b . For most neural field models, the external input to the system is added on the post-synaptic potential level, rather than the mean membrane potential level. This can be achieved by splitting the membrane external input $u_a^0(x, t) = \sum_b \nu_{a,b} V_{a,b}^0(x, t)$ and rewriting equations (4.2) and (4.3) as

$$u_a(x, t) = \sum_b \nu_{a,b} V_{a,b}(x, t), \quad (4.4)$$

$$V_{a,b}(x, t) = \int_{-\infty}^t \psi_{a,b}(t - T) \phi_{a,b}(x, T) dT + V_{a,b}^0(x, t). \quad (4.5)$$

The temporal decay and magnitude of post-synaptic potentials will depend on which population they originate from. Using the same principles as for the Amari equation, this can be expressed in the form of a temporal convolution describing the rise and fall of an incoming synaptic transmission.

$$\phi_{a,b}(x, t) = \int_{\Omega} w_{a,b}(x - X) f_b[u_b(X, t)] dX \quad (4.6)$$

The average firing rate is related to the average membrane potential using the same non-linear sigmoidal transfer function f_b employed in early neural field models, as we saw in the previous section. The logistic function is a common choice of sigmoid across this period of neural field models as well. A parameterisation of this used by Robinson et al. (2001) [177] is

$$f_a[u_a(x, t)] = \frac{F_a}{1 + \exp[-(u_a(x, t) - \theta)/\sigma']}, \quad (4.7)$$

where F_a is the maximum firing rate of neurons in population a , and $\sigma' = \sigma\sqrt{3}/\pi$ so that θ and σ are the mean and standard deviation of a distribution of threshold values over

the neuronal population. The normalisation of σ tends to be done so that the derivative of the sigmoid approximates a Gaussian (Rennie et al., 1999 [171]). The voltage scale used here is with respect to the resting potential of the population, which is approximately the same as the reset voltage after firing in a single neuron (Koch, 2004 [108]). In a single neuron, this is approximately -70 mV, and the threshold would be approximately -55mV (Destexhe, 1997 [50], Meffin et al., 2004 [145]). Therefore the threshold relative to resting potential is a difference of 15mV, of which Robinson et al. (2004) [175] uses a value of $\theta = 13.3$ mV. Common parameter values seen in the work of Robinson et al. include $F_a = 340$ Hz and $\sigma = 3.8$ mV.

Combining equations (4.4), (4.5), and (4.6) results in the expression

$$u_a(x, t) = \sum_b \nu_{a,b} \left\{ \int_{-\infty}^t \psi_{a,b}(t-T) \left[\int_{\Omega} w_{a,b}(x-X) f_b \left(\sum_c \nu_{b,c} V_{b,c}(X, T) \right) dX \right] dT + V_{a,b}^0(x, t) \right\}. \quad (4.8)$$

Using the mean membrane potential in analysis of these models can be cumbersome in this more detailed framework, so typically the dynamics of the post-synaptic potentials are analysed before linearly combining the results to give the mean membrane potential. Upon interchanging the order of spatial and temporal convolutions, a general framework for modern second-order neural field models is given by

$$u_a(x, t) = \sum_b \nu_{a,b} \int_{-\infty}^t \psi_{a,b}(t-T) \left[\int_{\Omega} w_{a,b}(x-X) f_b(u_b(X, T)) dX \right] dT + u_a^0(x, t), \quad (4.9)$$

$$V_{a,b}(x, t) = \int_{-\infty}^t \psi_{a,b}(t-T) \left[\int_{\Omega} w_{a,b}(x-X) f_b \left(\sum_c \nu_{b,c} V_{b,c}(X, T) \right) dX \right] dT + V_{a,b}^0(x, t), \quad (4.10)$$

where $\int_{-\infty}^t \psi_{a,b}(t-T) q_{a,b}(x, T) dT = V_{a,b}^0(x, t)$ and $u_a^0(x, t) = \sum_b \nu_{a,b} V_{a,b}^0(x, t)$ are external inputs. The generalised parameters derived throughout this Section are summarised in Table 1. An illustration of the advantages that come with additional complexity of these NFM models is given in Figure 6

4.2 Derivation of modern neural field models

Although they are rarely explicitly derived, most neural field models in the literature can be manipulated and rearranged to resemble Equations (4.9) and (4.10), revealing common underlying structures that differ only in their choices of spatiotemporal kernels, populations and connectivity structures, and assumptions made. This common mathematical framework allows for a more direct comparison of neural field models and explicit signposting and discussion of their underpinning assumptions. To illustrate this, we consider a common neural field model of cortical tissue by Robinson et al. (1997) [178]. This models the evolution of the mean membrane potential via the interactions of mean post-synaptic potentials. Here we will derive the cortical model and show how the integral equation formulation is transformed into a set of partial differential equations, which can then be expressed as a system of ordinary differential equations (or stochastic differential equations, depending on the nature of external inputs).

The cortical neural field model from Robinson et al. (1997) [178] contains two neuronal populations, an excitatory (e) population and an inhibitory (i) population, in similar fashion to the Wilson and Cowan model. This can be interpreted as modelling the most prevalent types of neurons in the cortex, which secrete the excitatory neurotransmitter AMPA and the inhibitory neurotransmitter GABA-A. A key simplification is made to the general neural field model in Equation (4.9) where the kinetics and electrodynamic response of these neurotransmitters, and hence the synaptic kernel of both populations, is assumed to be the same.

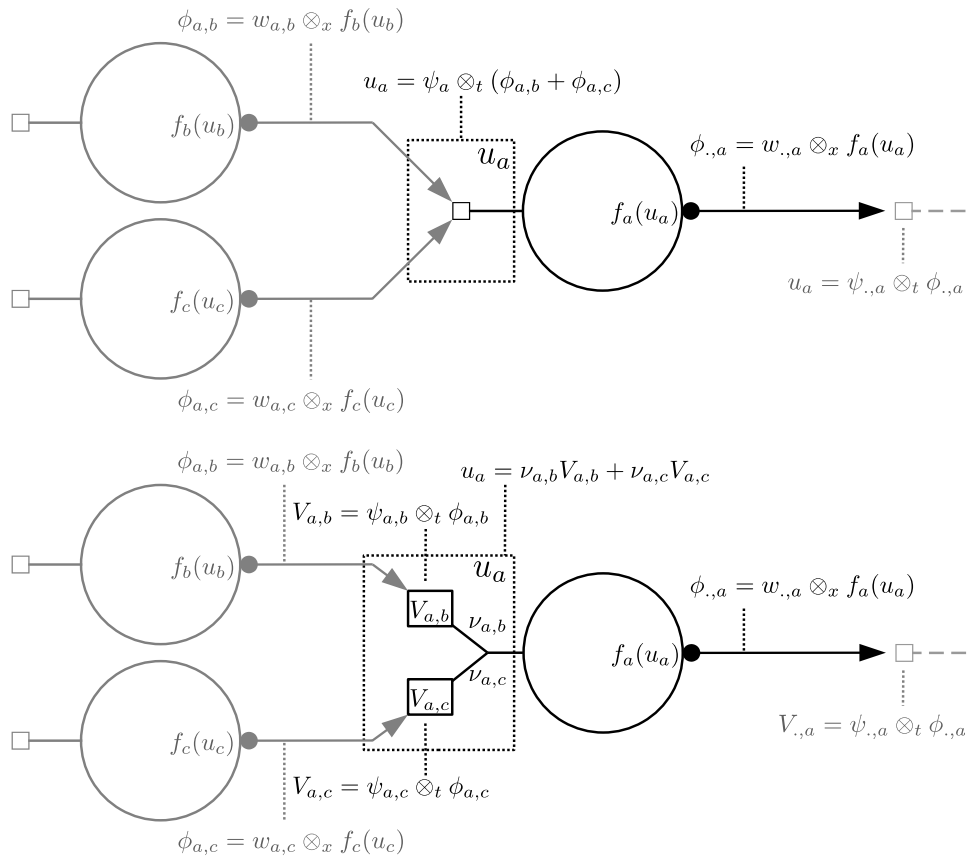


Figure 6: **Comparison of 1st order NFM (top) to 2nd order NFM (bottom).** We illustrate this difference using a generic junction in a neural field model with three populations where population b and c connect to population a . A key development in modern Neural Field Models is the stratification of mean membrane potential state variables u_a into a set of mean post-synaptic potential state variables $V_{a,b}, V_{a,c}$ with weights $\nu_{a,b}, \nu_{a,c}$. This allows for the inclusion of specific hypotheses and assumptions about the differences in temporal dynamics of synaptic transmission.

| Quantity | Physical interpretation |
|--------------------|--|
| 1st order: | $u_a(x, t) = \int_{-\infty}^t \psi_a(t - T) \{ \sum_b \phi_{a,b}(x, T) + q_a(x, T) \} dT,$ $\phi_{a,b}(x, t) = \int_{\Omega} w_{a,b}(x - X) f_b[u_b(X, t)] dX,$ |
| $u_a(x, t)$ | Mean membrane potential of neuronal population a at position x and time t |
| $\psi_a(t)$ | Membrane Temporal kernel of population a |
| $w_{a,b}(x)$ | Spatial kernel of connections from population b to population a at position x |
| $\phi_{a,b}(x, t)$ | Pulse density of action potentials from population b to population a at position x and time t |
| $q_a(x, t)$ | External input to population a |
| $T_a^{(m)}(x)$ | Time of m 'th action potential from population a at position x |
| $f_a(u)$ | Wave-to-pulse transfer function for population a |
| 2nd order: | $u_a(x, t) = \sum_b \nu_{a,b} V_{a,b}(x, t),$ $V_{a,b}(x, t) = \int_{-\infty}^t \psi_{a,b}(t - T) \{ \phi_{a,b}(x, T) + q_{a,b}(x, T) \} dT,$ $\phi_{a,b}(x, t) = \int_{\Omega} w_{a,b}(x - X) f_b[u_b(X, t)] dX,$ |
| $V_{a,b}$ | Mean post-synaptic potential at population a from population b |
| $\nu_{a,b}$ | Magnitude and polarity of post-synaptic potentials at population a from population b |
| $\eta_a(t)$ | Synaptic temporal kernel of population a |
| $\psi_{a,b}(t)$ | Membrane temporal kernel of transmissions from population b to population a |
| $q_a(x, t)$ | External input to population a from population b |

Table 1: **Table of quantities used in general neural field models.** Physical interpretations of quantities are provided for the notation used throughout discussions and derivations of the first order neural field models in Section 3 and the second order neural field models discussed in Section 4.

Physiological assumption: We assume that the shape of the synaptic filtering is the same for both excitatory and inhibitory inputs i.e. both AMPA and GABA-A receptors. Their responses are in fact very close with GABA-A having only a slightly higher rise time than AMPA, which is itself very small (Dayan and Abbott, 2001 [46]). This has the consequence that the synaptic τ and membrane time constants μ are the same for both inhibitory and excitatory populations.

This gives us a single temporal kernel in our integral equation $\psi_{a,b}(t) = \psi(t)$ for all a, b in e, i . This allows us to push the sum over afferent populations into the temporal integral, so we have

$$u_a(x, t) = \int_{-\infty}^t \psi(t-T) \left[\sum_b \nu_{a,b} \int_{\Omega} w_b(x-X) f \left(u_b \left(X, T - \frac{|x-X|}{v} \right) \right) dX + q_a(x, T) \right] dT, \tag{4.11}$$

where we have combined $\sum_b \nu_{a,b} q_{a,b}(x, t) = q_a(x, t)$ for brevity. It should be noted here that we only consider a neural field with one spatial dimension throughout this derivation, and can be readily extended to two dimensions.

The external input is conceptualised as an “external” population (s), but for our purposes this is notational. The significance of this term will not largely be discussed here, as the form tends to depend on the model and application. The notation used throughout the literature is $q_a(x, t) = \nu_{a,s} \phi_s(x, t)$, where $\nu_{a,s}$ is a scalar synaptic weighting and ϕ_s is the firing rate of the external population.

The spatial connectivity, in addition to assuming random connectivity in the thermodynamic limit, is also formulated such that neurons of either population indiscriminately synapse onto other populations. That is, the spatial weighting on the incoming firing rate from surrounding populations only depends on the spatial density of afferent neurons. This allows us to make an additional notational simplification on the synaptic kernel $w_{a,b}(x) = w_b(x)$. In this sense, the spatial kernels dictate the spatial density of neurons rather than the spatial density of synapses. In addition to this, the same sigmoidal potential-to-rate transfer function is used for both populations, making the notational simplification $f_b(u_b) = f(u_b)$. When considering finite conduction velocities, spatiotemporal delays are incorporated into the model as

$$u_a(x, t) = \int_{-\infty}^t \psi(t-T) \left[\sum_b \nu_{a,b} \int_{\Omega} w_b(x-X) f \left(u_b \left(X, T - \frac{|x-X|}{v} \right) \right) dX + \nu_{a,s} \phi_s(x, T) \right] dT. \tag{4.12}$$

where we assume a constant axonal propagation velocity v (Coombes et al., 2003 [39]).

Physiological assumptions: The axonal conduction velocity is assumed to be a constant and identical for all populations on the same spatial scale. Axonal velocities are different for different spatial scales depending on whether the axons are myelinated or not, and are proportional to the thickness or the diameter of the axon (Lohmann and Rörig, 1994 [127]). Experimental values also show that there is a distribution of axonal conduction velocities between populations on the same scale (Bojak and Liley, 2010 [17]) and that these act as a linear filter (Roberts and Robinson, 2008 [174]). This distribution is neglected in this model for the sake of simplicity and the conduction velocity will be constant unless otherwise explicitly stated.

This equation now serves as the starting point of the derivation of the wave equation (Jirsa and Haken, 1997 [96]). The neural field (in terms of the firing rate) is a convolution of the spatial kernel with the spatiotemporally delayed sigmoid

$$\phi_b(x, t) = \int_{\Omega} w_b(x - X) f \left[u_b \left(X, t - \frac{|x - X|}{v} \right) \right] dX, \quad (4.13)$$

and the membrane potential is a convolution of the synaptic (temporal) kernel with the neural field

$$u_a(x, t) = \int_{-\infty}^t \psi(t - T) \sum_b \nu_{a,b} \phi_b(x, T) dT. \quad (4.14)$$

Green's functions and Fourier transforms are now used to reduce the canonical neural field equation (4.9) into coupled partial differential equations (Jirsa and Haken, 1997 [96], Coombes et al., 2003 [39]) by decoupling the spatial and temporal components.

According to the theory of Green's functions, we have

$$\mathbf{D}_t \{u_a(x, t)\} = \sum_b \nu_{a,b} \phi_b(x, t), \quad \mathbf{D}_t \{\psi(t)\} = \delta(t), \quad (4.15)$$

$$\mathbf{D}_x \{\phi_b(x, t)\} = f \left[u_b \left(X, t - \frac{|x - X|}{v} \right) \right], \quad \mathbf{D}_x \{w_b(x)\} = \delta(x), \quad (4.16)$$

where the differential operators over time \mathbf{D}_t and space \mathbf{D}_x are dependent on the exact forms of $\psi(t)$ and $w_b(x)$, respectively. In order to deal with the spatiotemporal delay, the neural field is redefined so that the delay is absorbed into the spatial kernel with a delta distribution where

$$\phi_b(x, t) = \int_{\Omega} \int_{-\infty}^t G_b(x - X, t - T) f [u_b(X, T)] dT dX, \quad (4.17)$$

where $G_b(x, t) = \delta(t - |x|/v)w_b(x)$ so that

$$\mathbf{D}_t \{u_a(x, t)\} = \sum_b \nu_{a,b} \phi_b(x, t), \quad \mathbf{D}_t \{\psi(t)\} = \delta(t), \quad (4.18)$$

$$\mathbf{D}_x \{\phi_b(x, t)\} = f [u_b(x, t)], \quad \mathbf{D}_x \{\delta(t - |x|/v)w_b(x)\} = \delta(x). \quad (4.19)$$

To express this neural field in terms of coupled partial differential equations (PDEs), we need to derive the operators \mathbf{D}_x and \mathbf{D}_t that correspond to the choice of temporal kernel $\psi(t)$ and spatial kernels $w_b(x)$ we make. In what follows, we will derive the operator \mathbf{D}_x using Fourier transforms to deal with the spatial time delay. After deriving the spatial PDE, we will then derive the temporal differential operator \mathbf{D}_t from experimental principles and show how this is equivalent to using a double-exponential temporal kernel.

Finding the partial differential equation associated with the spatial differential operator \mathbf{D}_x is a matter of determining a realistic connectivity kernel $w_b(x)$ for each population and then taking spatiotemporal Fourier transform. Most neural field models tend to use the Laplacian distribution, $w_b(x) = \exp(-|x|/r_b)/2r_b$ where r_b is the axonal range of population b . The Robinson neural field model uses a different kernel instead, given by $w_b(x) = K_0(x/r_b)/2\pi r_b^2$ where K_0 is a Bessel function of the second kind. This has a similar decay rate to the Laplacian distribution, but this function is singular at the origin, implying infinite connectivity between neuronal populations at a point. From a modelling perspective, the difference in kernels, whether they have a singularity or not, does not significantly change the model. This is because the region containing the singularity is immeasurable and largely irrelevant to the millimetric scale at which a

neural field model describes. After choosing the Bessel spatial kernel, equation (4.19) further simplifies to the resulting PDE,

$$\left[\left(1 + \frac{1}{\gamma_b} \frac{\partial}{\partial t} \right)^2 - r_b^2 \nabla^2 \right] \phi_b(x, t) = f(u_b(x, t)), \quad (4.20)$$

where $\gamma_b = v/r_b$ as a temporal dampening term.

To obtain the corresponding temporal PDE, we can derive the temporal differential operator \mathbf{D}_t (and the analogous integral kernel) from biophysical principles. We start from canonical R-C circuit equations, inspired by simplified spiking models such as integrate-and-fire neurons with current based synapses (Burkitt, 2006 [32]). In this case there is no spiking mechanism and the state variables are treated as population averages with rate based inputs. The membrane is described as a leaky capacitor with $C_a u_a(x, t) = q_a(x, t)$ where C_a is the capacitance — assumed to be constant for a given population — and $q_a(x, t)$ is the charge at population a at position x at time t . Taking the derivative of this gives us the current which can be separated into the leak and synaptic currents

$$\begin{aligned} C_a \frac{\partial}{\partial t} u_a(x, t) &= I_a^{\text{leak}}(x, t) + I_a^{\text{syn}}(x, t), \\ \implies \frac{\partial}{\partial t} u_a(x, t) &= -\frac{1}{\mu} u_a(x, t) + \frac{1}{C_a} \sum_b N_{a,b} I_{a,b}(x, t), \end{aligned} \quad (4.21)$$

where the membrane potential leaks over the membrane time constant μ (which we had previously assumed is the same for all populations) and the synaptic current is the linear sum of all the incoming currents $I_{a,b}(x, t)$, with coefficients $N_{a,b}$ that quantify the number of connections from population b to population a .

Physiological assumption: We approximate the synaptic and dendritic filtering of the post-synaptic current $I_{a,b}(t)$ as exponentially decaying from a maximal current, over a synaptic time constant. This is a reasonably good fit to experimental data as can be seen in previous modelling work by Destexhe et al. (1994) [51].

Continuing the derivation, the form of the decaying exponential for the post-synaptic current is defined as

$$\frac{\partial}{\partial t} I_{a,b}(x, t) = -\frac{1}{\tau} I_{a,b}(x, t) + A_b \phi_b(x, t). \quad (4.22)$$

where A_b is the maximal current amplitude and τ is the synaptic time-constant. Differentiating Eq.(4.21) with respect to time and substituting Eq.(4.22) gives

$$\frac{\partial^2 u_a}{\partial t^2} = \frac{-1}{\mu} \frac{\partial u_a}{\partial t} - \frac{1}{C_a \tau} \sum_b N_{a,b} I_{a,b}(x, t) + \frac{1}{C_a} \sum_b N_{a,b} A_b \phi_b(x, t). \quad (4.23)$$

Then back-substituting Eq.(4.21) into the second term on the right hand side of the above equation gives

$$\frac{\partial^2 u_a}{\partial t^2} = -\frac{1}{\mu} \frac{\partial u_a}{\partial t} - \frac{1}{\tau} \left[\frac{\partial u_a}{\partial t} + \frac{u_a(x, t)}{\mu} \right] + \frac{1}{C_a} \sum_b N_{a,b} A_b \phi_b(x, t), \quad (4.24)$$

which, after collecting terms and multiplying through by $\tau\mu$, becomes

$$\left[\tau\mu \frac{\partial^2}{\partial t^2} + (\tau + \mu) \frac{\partial}{\partial t} + 1 \right] u_a(x, t) = \sum_b \nu_{a,b} \phi_b(x, t), \quad \nu_{a,b} = N_{a,b} s_b, \quad s_{a,b} = \frac{A_b \tau \mu}{C_a}. \quad (4.25)$$

A more through discussion of this derivation for single neuron models can be found in works by Gerstner and Kistler (2002) [77], Ermentrout and Terman (2010) [60]. More complex descriptions of synaptic dynamics, such as non-linear conductance-based synapses, can be utilised instead which is seen in the work of Liley et al. (1997) [123], Pinotsis et al. (2013) [163], and Peterson et al. (2018) [162]. We will comment on these non-linear extensions later. For this derivation, we will consider only linear synaptic kernels so that we may derive the differential operator using Green's functions, which gives rise to the following partial differential equation

$$\left(\tau \frac{\partial}{\partial t} + 1\right) \left(\mu \frac{\partial}{\partial t} + 1\right) u_a(x, t) = \sum_b \nu_{a,b} \phi_b(x, t), \quad (4.26)$$

which corresponds to the double exponential synaptic kernel,

$$\psi(t) = \frac{1}{\tau - \mu} [e^{-t/\tau} - e^{-t/\mu}] \Theta(t), \quad (4.27)$$

where μ and τ are the membrane and synaptic time constants, respectively.

The basic form of the Robinson model utilises three populations: excitatory cortical neurons (e), inhibitory cortical neurons (i), and external non-specific neurons (s). At this point, the Robinson model begins to deviate from other neural field models by making a major anatomical assumption that effectively combines the cortical populations. A diagrammatic comparison contrasting the Robinson model with typical neural field models can be found in Figure 7.

Anatomical assumption: The local connectivity approximation Rennie et al. (1999) [171] is used i.e. that the intra-cortical connectivities are proportional to the density of neurons, as well as the average number of synapses involved. That is, there is a symmetry between the type of post-synaptic neurons that a pre-synaptic neuron will synapse onto. For example, if $N_{a,b}$ is the connectivity from a population of neurons b , to a population a , then $N_{e,b} = N_{i,b}$. That is, there are approximately the same proportion of connections from population b , to both the excitatory e , and inhibitory i , populations. This approximation is also made with regards to the synaptic response $s_{a,b}$ where $s_{e,b} = s_{i,b}$. Since the synaptic constant for each population interface is given by the product $\nu_{a,b} = N_{a,b} s_{a,b}$, we have $\nu_{e,b} = \nu_{i,b}$ for all populations b . Please refer to Rennie et al. (1999) [171] for further details of this approximation. We also assume that the sigmoidal functions used for both populations are identical.

The main consequence of this approximation is that the membrane potential for both excitatory neurons and inhibitory neurons are equivalent. Upon expansion of the input equation Eq. (4.26),

$$\left(\tau \frac{\partial}{\partial t} + 1\right) \left(\mu \frac{\partial}{\partial t} + 1\right) u_a(x, t) = \sum_b \nu_{a,b} \phi_b(x, t), \quad (4.28)$$

to both excitatory and inhibitory populations $a \in \{e, i\}$ with an external input ϕ_s , and $b \in \{e, i, s\}$, we have

$$\left(\tau \frac{\partial}{\partial t} + 1\right) \left(\mu \frac{\partial}{\partial t} + 1\right) u_e(x, t) = \nu_{e,e} \phi_e(x, t) + \nu_{e,i} \phi_i(x, t) + \nu_{e,s} \phi_s(x, t), \quad (4.29)$$

$$\left(\tau \frac{\partial}{\partial t} + 1\right) \left(\mu \frac{\partial}{\partial t} + 1\right) u_i(x, t) = \nu_{i,e} \phi_e(x, t) + \nu_{i,i} \phi_i(x, t) + \nu_{i,s} \phi_s(x, t). \quad (4.30)$$

When we apply the local connectivity approximation to these equations where $\nu_{e,b} = \nu_{i,b}$, it is clear that Eq. (4.30) becomes redundant as it is identical to Eq. (4.29). For simplicity, we set $u_i = u_e$ and $\nu_{a,b}$ becomes ν_b , as there is only one afferent neural population.

Physiological assumption: As a consequence of both populations having the same time constants and the local connectivity approximation, inhibitory neurons are assumed to have exactly the same characteristics as excitatory neurons, which is obviously not true for biological neurons.

Even though there is only effectively one type of neuron, we can still distinguish between populations as well as an external input. This is due to the different synaptic products $\nu_b = N_b s_b$ of the different populations and the different axonal dampening coefficients γ_b . Although it is possible to treat the populations individually, this effectively doubles the number of parameters and dimensionality of state space of the model. Analytical and computational studies with spiking models have shown that when the populations are treated differently, the results of a stability analysis are not substantially different (Brunel, 2000 [27], Meffin et al., 2004 [145]).

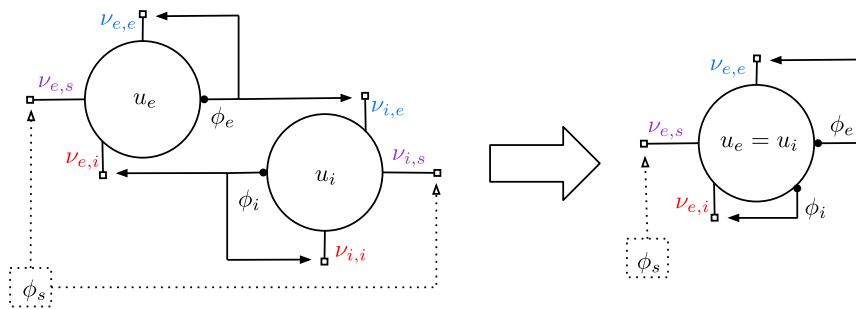


Figure 7: **Diagram of simplification in the Robinson cortical NFM.** This diagram shows the simplification made by equating the synaptic coefficients $\nu_{e,b} = \nu_{i,b}$ (highlighted by matching colours), which effectively combines the cortical excitatory and inhibitory populations into one cortical population with two self-connections. External inputs are represented by dotted arrows.

Mathematical assumption: As is commonly done in the literature, we will only examine the spatially invariant case of the dampened wave equation i.e. the global spatial modes.

To investigate the spatially uniform activity, the spatially inhomogeneous term in the wave equation Eq. (4.20) is set to zero $r_b^2 \nabla^2 \phi_b(x, t) = 0$. To make this a neural mass model, we would set the axonal range to zero $r_b = 0$. However, setting $\nabla^2 \phi_b(x, t) = 0$ allows us to solve for the spatially uniform solutions of the neural field model. This removes the spatial variation while still preserving the axonal range, conduction velocity and intra-cortical connectivities. The damped wave equation now becomes

$$\left(\frac{1}{\gamma_a} \frac{\partial}{\partial t} + 1 \right)^2 \phi_a(x, t) = f(u_a(x, t)), \tag{4.31}$$

where we have removed the spatially dependent term. Since solutions to these equations are spatially homogeneous, we may drop the x -dependence and treat this as though it were a neural mass model. Even though the model is assumed to be spatially isotropic and homogeneous, there is still some spatial structure contained in the temporal dampening term $\gamma_b = v/r_b$, which contains information about the spatiotemporal delay. This makes the category of the model somewhat ambiguous. Technically it is not a neural field model as the field is spatially invariant, but it layers on top of one by including only the spatially uniform solutions. Yet it could also be described as an atypical neural mass model with spatiotemporal delays, so it is somewhere in between both categories. In the literature it is described as a neural field model with only global spatial modes.

Previously, this cortical neural field model has been used to describe the whole cortex (Robinson et al., 1997 [178], Rennie et al., 1999 [171]) and extended to a thalamo-cortical model (Rennie et al., 2002 [172], Robinson et al., 2004 [175], Breakspear et al., 2006 [19]). In both instances, the axonal range r_a is different for both the excitatory, r_e , and the inhibitory, r_i , neurons. By taking the “local inhibition approximation” (Rennie et al., 1999 [171]) it is assumed that all long range connections are purely excitatory, hence we can use $r_i \ll r_e \implies \gamma_i \gg \gamma_e$. So as $r_i \rightarrow 0$, $\gamma_i \rightarrow \infty$, which means that if separate wave equations are written for both the excitatory γ_e, ϕ_e , and inhibitory γ_i, ϕ_i components, the inhibitory wave equation

$$\left(\frac{1}{\gamma_i} \frac{\partial}{\partial t} + 1\right)^2 \phi_i(t) = f(u_i(t)) = f(u_e(t)) \tag{4.32}$$

becomes $\phi_i(t) = f(u_e(t))$. Therefore the inhibitory firing rate is governed by the sigmoidal function of the membrane potential. Another consequence of this assumption is that the long range excitatory to inhibitory connections are not included.

Anatomical assumption: In this model, since there are not distinct excitatory and inhibitory cortical populations, there are no local inhibitory-inhibitory connections. These are hypothesised in other neural models to play a significant role in brain dynamics such as alpha rhythmogenesis (Liley et al., 1999 [124]), and epilepsy (Wendling et al., 2002 [214]). Further, long-range excitatory-inhibitory connections have also not been included i.e. afferent connections from pyramidal neurons synapsing on inhibitory interneurons. These would also significantly affect overall cortical dynamics.

This gives us the full cortical neural field model proposed by Robinson et al. (1997) [178],

$$\begin{aligned} \left(\frac{1}{\gamma_e} \frac{\partial}{\partial t} + 1\right)^2 \phi_e(t) &= f(u_e(t)), \\ \left(\mu \frac{\partial}{\partial t} + 1\right) \left(\tau \frac{\partial}{\partial t} + 1\right) u_e(t) &= \nu_{e,e} \phi_e(t) + \nu_{e,i} f(u_e(t)) + \nu_{e,s} \phi_s(t), \end{aligned} \tag{4.33}$$

which, when rearranged and put into a coupled ordinary differential equation (ODE) form, are usually expressed in the literature as

$$\begin{aligned} \ddot{\phi}_e(t) &= \gamma_e^2 [f(u_e(t)) - \phi_e(t)] - 2\gamma_e \dot{\phi}_e(t), \\ \ddot{u}_e(t) &= \alpha \beta [\nu_{e,e} \phi_e(t) + \nu_{e,i} f(u_e(t)) + \nu_{e,s} \phi_s(t) - u_e(t)] - (\alpha + \beta) \dot{u}_e(t), \end{aligned} \tag{4.34}$$

where $\alpha = \mu^{-1}$ and $\beta = \tau^{-1}$.

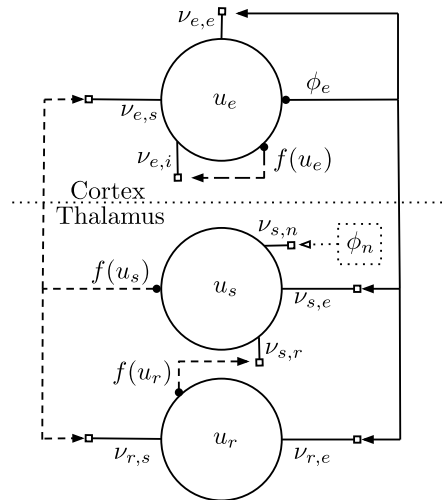


Figure 8: **Illustration of Robinson cortico-thalamic NFM.** External inputs are represented by dotted arrows and connections that utilise the limiting axonal range assumption $r_a \rightarrow 0$ are shown in dashed lines. Connections that cross the cortex-thalamus boundary incur a time delay of $t_0/2$.

This cortical model by Robinson et al. was extended to include thalamic populations. Recent publications generally analyse the full thalamo-cortical model, which includes a time delay between cortical and thalamic populations, but overall uses the same principles as discussed in this section so far. In a sense, we can interpret this thalamic extension as an expansion of the non-specific external population term $\nu_{e,s}\phi_s(t)$ in the cortical model. In addition to the cortical neurons, composed of excitatory (e) and inhibitory (i) sub-populations, Robinson et al. also consider populations from the specific thalamic nucleus (s), the reticular thalamic nucleus (r), and a new input term arising from non-specific subcortical neurons (n). The equations for the thalamo-cortical neural field model are given by

$$\begin{aligned}
 & \left(\frac{1}{\gamma} \frac{\partial}{\partial t} + 1\right)^2 \phi_e(t) = f(u_e(t)), \\
 & \left(\mu \frac{\partial}{\partial t} + 1\right) \left(\tau \frac{\partial}{\partial t} + 1\right) u_e(t) = \nu_{e,e}\phi_e(t) + \nu_{e,i}f(u_e(t)) + \nu_{e,s}f\left(u_s\left(t - \frac{t_0}{2}\right)\right), \\
 & \left(\mu \frac{\partial}{\partial t} + 1\right) \left(\tau \frac{\partial}{\partial t} + 1\right) u_s(t) = \nu_{s,e}\phi_e\left(t - \frac{t_0}{2}\right) + \nu_{s,r}f(u_r(t)) + \nu_{s,n}\phi_n(t), \\
 & \left(\mu \frac{\partial}{\partial t} + 1\right) \left(\tau \frac{\partial}{\partial t} + 1\right) u_r(t) = \nu_{r,e}\phi_e\left(t - \frac{t_0}{2}\right) + \nu_{r,s}f(u_s(t)),
 \end{aligned} \tag{4.35}$$

which, when simplified and expressed in ODEs,

$$\begin{aligned}
 \ddot{\phi}_e(t) &= \gamma^2 [f(u(t)) - \phi(t)] - 2\gamma \dot{\phi}(t), \\
 \ddot{u}_e(t) &= \alpha\beta \left[\nu_{e,e}\phi_e(t) + \nu_{e,i}f(u_e(t)) + \nu_{e,s}f\left(u_s\left(t - \frac{t_0}{2}\right)\right) - u_e(t) \right] - (\alpha + \beta) \dot{u}_e(t), \\
 \ddot{u}_s(t) &= \alpha\beta \left[\nu_{s,e}\phi_e\left(t - \frac{t_0}{2}\right) + \nu_{s,r}f(u_r(t)) + \nu_{s,n}\phi_n(t) - u_s(t) \right] - (\alpha + \beta) \dot{u}_s(t), \\
 \ddot{u}_r(t) &= \alpha\beta \left[\nu_{r,e}\phi_e\left(t - \frac{t_0}{2}\right) + \nu_{r,s}f(u_s(t)) - u_r(t) \right] - (\alpha + \beta) \dot{u}_r(t),
 \end{aligned}
 \tag{4.36}$$

where $\alpha = \mu^{-1}$ and $\beta = \tau^{-1}$, and t_0 is the time delay of the full thalamo-cortical loop (hence $t_0/2$ represents the unidirectional delay from a thalamic population to a cortical population or vice versa). An illustration of the full thalamo-cortical neural field model is given in Figure 8.

Building off of the prior derivation and assumptions, the cortical model by Robinson has lower dimensionality in state space and parameter space in comparison to other neural field models. This allows extensions of the model to include more sophisticated anatomical and physiological factors that are generally not possible in other neural field frameworks. The neural field model proposed by Robinson and colleagues has undergone a variety of modifications since its first appearance in the literature in 1997, and has inspired other authors to make their own simplifications and extensions Marten et al. (2009) [134]. Another canonical neural field that is contemporaneous of the Robinson model is by Liley et al. (1999) [124]. This NFM was the first model to extend neural field models to include more physiologically realistic conductance-based synaptic dynamics as we discussed in Equation (4.1),

$$u_a(x, t) = \int_{-\infty}^t \eta_a(t - T) \left\{ \sum_b \nu_{a,b}(u_b(x, T)) V_{a,b}(x, T) + u_a^0(x, T) \right\} dT. \tag{4.37}$$

That is, the nonlinear mapping from mean postsynaptic activities $V_{a,b}$ to mean membrane potential u_a is temporally filtered (Ermentrout and Terman, 2010 [60]) and the synaptic weights are state dependent

$$\nu_{a,b}(u_b) = \frac{u_a^{\text{rev}} - u_b}{|u_a^{\text{rev}} - u_a^{\text{rest}}|}, \tag{4.38}$$

where u_a^{rev} is the reversal potential and u_a^{rest} is the resting potential. The synaptic kernel considered is a simple exponential, which gives us

$$\begin{aligned}
 \eta_a(t) &= \frac{1}{\tau_a} \exp(-t/\tau_a) \Theta(t), \\
 \implies \left(\frac{1}{\tau_a} \frac{\partial}{\partial t} + 1 \right) u_a(x, t) &= \sum_b \frac{u_b^{\text{rev}} - u_a}{|u_b^{\text{rev}} - u_a^{\text{rest}}|} V_{a,b}(x, t) + u_a^0(x, t).
 \end{aligned}
 \tag{4.39}$$

From Eq.(4.39), we can see that because conductance-based synapses are linear in both u_a and $V_{a,b}$, they are bilinear, which introduces another nonlinearity into the equations. Eq.(4.39) cannot be written as a linear operator because the sum is nonlinear. This makes this model fundamentally different to the other models described in this paper. The Robinson model has been derived with conductance-based synapses and its dynamics directly compared to linear current-based synapses (Peterson et al., 2018 [162]). Although, this is more biologically realistic, it introduces another layer of complexity and makes the analysis more difficult. Unlike the model by Robinson et al.

(1997) [178], the Liley model also includes long-range excitatory to inhibitory connections and different PSP's for excitatory and inhibitory populations.

Physiological assumption: In this relatively simple formulation of conductance-based synapses, it is assumed that the reversal potentials are static parameters. More accurate models also include additional extra-cellular dynamics where the reversal potentials are state variables computed from extra- and intra-cellular ionic concentrations (Cressman et al., 2009 [45], Krishnan and Bazhenov, 2011 [111]). Ionic dynamics are known to affect overall brain dynamics, particularly seizures (Ziburkus et al., 2012 [226]).

The Liley model was in turn extended by Steyn-Ross et al. (1999) [195] to a system of stochastic differential equations that includes gap junctions. Gap junctions are electrical synapses that do not have chemical neurotransmitters and are known to affect overall brain dynamics, particularly with respect to neuron coupling and rhythm synchronisation (Larsen, 1983 [121], Evans and Martin, 2002 [61], Traub et al., 1999 [201], Simon et al., 2014 [188]). Further explorations of the dynamics and solutions to these systems forms an entire discipline of mathematical neuroscience in its own right. Many of these concepts are discussed and expanded upon throughout stochastic neural field theory, which we will briefly discuss in Section 5.2.1.

4.3 Reduction to neural mass models

It is not always desirable to consider significant spatial extent within a neural field model. For smaller spatial scales that are relatively isotropic and homogeneous, having spatial dependence and the incorporation of long-distance spatial connectivity is unnecessary, as this heavily complicates the analysis of neural population models. The earlier work of Wilson and Cowan (1972) [217] initially maintained this smaller scope in a spatially-invariant regime, before extending it to an early neural field model in 1973 (considered in Section 3.2). This earlier 1972 model would come to be known as a “neural mass model” or NMM, which can be considered a special case of a neural field model at a single point in space. This is mathematically equivalent to using delta distribution connectivity kernels $w_{a,b}(x) = c_{a,b}\delta(x)$ for each population. Around the same time, NMMs were further developed and formalised by Lopes da Silva et al. (1974) [129] and Freeman (1975) [70]. NMMs share a concurrent history with neural field models, with many authors publishing significant contributions in both model types. NMMs omit spatial dependence and spatiotemporal time delays but share the same principles of aggregate neural action arising from statistical mechanics. While NMMs still maintain a high degree of mathematical complexity, they provide a simpler realisation of statistical mechanics in neuroscience, and are crucial to understanding the dynamics of neural populations.

Inspired by the work of Katchalsky (1971) [102], Katchalsky et al. (1974) [103], Prigogine and Nicolis (1973) [165] and others, it was Walter Freeman Jr who pioneered what we might term today a “systems approach” to the study of neural masses (Freeman, 1975 [70]) and from where the term “neural mass model” derives. Freeman’s motivation for this approach was essentially to strike a balance between physiological plausibility whilst remaining computationally tractable, such that the output of the model might be directly linked to electrophysiological recordings (LFP data in Freeman’s case). Taking Katchalsky’s extension of Liesegang rings from diffusion-coupled chemical reactions as a basis, Freeman (1975) [70] introduced a topological hierarchy of models styled the *Ki* formalism. The full detail of Freeman’s work is beyond the scope of this section, but

further developments by Freeman led to analysis of neural mass models of the olfactory bulb in the rabbit primary cortex.

Around the same time as Freeman’s formal establishment of neural mass action, an aligned approach to studying the macroscale brain activity was proposed by Lopes da Silva et al. (1974) [129] which they termed the “lumped parameter approach”. To briefly recap this development, Lopes da Silva put forward a computational model of a two-population neural mass model to investigate spontaneous EEG signal generation and alpha-frequency rhythms. To analyse this model within a mathematical framework, they reduced the complexity of the model by deriving a dynamical systems model of aggregate activity within a single cortical column. Utilising the simplest approach, Lopes da Silva and colleagues investigate excitatory thalamocortical relay cells (TRCs) that receive external excitatory pulse density (from neighbouring columns, not explicitly modelled), and inhibitory feedback from local interneurons. External inputs to this system arise from pulse trains from peripheral excitatory neurons in neighbouring columns, and are integrated as another input to the TRC population (typically modelled as a Gaussian process).

The two-population model proposed by Lopes da Silva et al. (1974) [129] was further developed by Zetterberg et al. (1978) [224] by extending it to a three-population model, which during the resurgence of neural field models in the 1990’s, was used by Jansen et al. (1993) [92]. In their 1993 publication, Jansen and Rit propose that the mechanisms guiding the evolution of evoked potentials and spontaneous EEG signal generation are the same. To show this, they constructed a model of pyramidal neurons in cortical columns in the same fashion as done by Lopes da Silva and colleagues. The post-synaptic potentials of the pyramidal population is identified as the EEG signal and also provides input to surrounding interneurons. The model by Lopes da Silva utilises a second population of inhibitory interneurons that provide feedback to the pyramidal neuron population. Jansen and Rit extend this and include a third population of local excitatory interneurons that also provide feedback to the pyramidal neurons. A diagram of the populations in this neural mass model is given in Figure 9. The addition of this third population is motivated by incorporating additional physiological realism of (long-range) excitatory connections. To support the hypothesis of the same governing mechanisms, Jansen and Rit replaced the random input term with transient pulses and reviewed the dynamical model response and found concordance with experimental observations.

Neural mass models can also be well understood within the mathematical framework we derived in Section 4.1. Here we will show how the Jansen and Rit equations can be derived using a general neural field model equation. Since this is a neural mass model, we will immediately make the substitution $w_{a,b}(x) = c_{a,b}\delta(x)$, where $c_{a,b}$ is a connectivity constant and δ is the Dirac delta distribution. This removes spatial dependence entirely, so we may omit the x -ordinate and express our neural mass model as

$$V_{a,b}(t) = \int_{-\infty}^t \psi_{a,b}(t-T) \left[c_{a,b} f \left(\sum_c \nu_{b,c} V_{b,c}(T) \right) + q_{a,b}(T) \right] dT, \quad (4.40)$$

where it is also assumed that each population uses the same potential to rate transfer function $f_b = f$ given by

$$f(u) = \frac{2e_0}{1 + \exp[-r(u - v_0)]}, \quad (4.41)$$

where e_0 determines the maximal firing rate, v_0 is the post-synaptic potential for which 50% of maximal firing rate is achieved, and r is the steepness parameter of the transfer function. A minor deviation is made in this model from the framework we established when the external input is concerned, though this is primarily a notational issue rather than conceptual. Jansen and Rit do not use the mapping $u_a^0 = \sum_b \nu_{a,b} V_{a,b}^0$, instead setting

$u_a^0 = 0$ for all a and considering only external inputs at the post-synaptic potential level. They consider three populations: a pyramidal population (p), an excitatory population (e), and an inhibitory population (i). In the same vein as the model by Lopes da Silva et al., Jansen and Rit impose that the only non-zero connections are from p to e and i , from e to p , and from i to p . This can be seen in Figure 9. The lack of self-connections in this branch of models can be attributed to Lopes da Silva intending to derive the simplest possible model for spontaneous alpha EEG rhythms. Additionally, the temporal filtering of signals is assumed to be specific to the afferent population, giving the notational simplification $\psi_{a,b}(t) = \psi_b(t)$. Furthermore, it is also assumed that the temporal kernel is of the form of an alpha function,

$$\psi_b(t) = \frac{\Gamma_b}{\mu_b} t \exp(-t/\mu_b) \Theta(t), \tag{4.42}$$

where Γ_b is a gain parameter, μ_b denotes the time scale, and Θ is the usual Heaviside function. Different time-scales are implemented for excitatory and inhibitory signals, as there is physiological evidence for different synaptic timescales and gain parameters for common excitatory and inhibitory neurotransmitters. That is, temporal kernels for post-synaptic potentials are set to be

$$\psi_e(t) = \psi_p(t) = \frac{\Gamma_e}{\mu_e} t \exp(-t/\mu_e) \Theta(t), \quad \psi_i(t) = \frac{\Gamma_i}{\mu_i} t \exp(-t/\mu_i) \Theta(t), \tag{4.43}$$

where (Γ_e, μ_e) and (Γ_i, μ_i) are the synaptic gain and time constants of the excitatory and inhibitory synapses, respectively. The physiological manifestation for the difference in excitatory and inhibitory post-synaptic potential amplitudes and timescales arise from the position of afferent synapses relative to the neuron’s cell body. For instance, inhibitory neurons are more likely to synapse near the cell body, producing larger potentials (Martin, 1985 [136]). This is accounted for by taking $\Gamma_e < \Gamma_i$. We can equivalently express this system in terms of temporal differential operators. Using Fourier transforms, it can be shown that the temporal differential operators corresponding to the excitatory and inhibitory synaptic kernels are

$$\mathbf{D}_t^{(e)} = \mathbf{D}_t^{(p)} = \frac{\mu_e}{\Gamma_e} \left[\frac{d^2}{dt^2} + \frac{2}{\mu_e} \frac{d}{dt} + \frac{1}{\mu_e^2} \right], \quad \mathbf{D}_t^{(i)} = \frac{\mu_i}{\Gamma_i} \left[\frac{d^2}{dt^2} + \frac{2}{\mu_i} \frac{d}{dt} + \frac{1}{\mu_i^2} \right], \tag{4.44}$$

Furthermore, we only consider external input to this system via the excitatory to pyramidal synaptic connections, so we will set $q_{a,b}(t) = 0$ for all populations with exception to $q_{p,e}$. Inverting the temporal kernel for each population and applying the connectivity between these populations as proposed by Jansen and Rit gives rise to the following equations,

$$\begin{aligned} \mathbf{D}_t^{(p)} \{V_{e,p}(t)\} &= c_{e,p} f(u_p), & u_p &= \nu_{p,e} V_{p,e}(t) + \nu_{p,i} V_{p,i}(t), \\ \mathbf{D}_t^{(p)} \{V_{i,p}(t)\} &= c_{i,p} f(u_p), & & \\ \mathbf{D}_t^{(e)} \{V_{p,e}(t)\} &= c_{p,e} f(u_e) + q_{p,e}(t), & u_e &= \nu_{e,p} V_{e,p}(t), \\ \mathbf{D}_t^{(i)} \{V_{p,i}(t)\} &= c_{p,i} f(u_i), & u_i &= \nu_{i,p} V_{i,p}(t). \end{aligned} \tag{4.45}$$

Anatomical assumption: It is assumed that the magnitude of inhibitory impulses is larger than than the magnitude of the excitatory impulses. This assumption and subsequent temporal kernels are inherited from van Rotterdam et al. (1982) [209]. The difference in amplitude was justified by considering that inhibitory neurons

typically have axonal terminals that lie closer to the cell body, which results in larger perturbations upon inhibitory synaptic transmission (Kandel and Schwartz, 1985 [101]). Additionally, it is also assumed that excitatory impulses occur on a faster timescale than inhibitory impulses.

Jansen and Rit additionally assume that pyramidal neurons synapse onto both the excitatory and inhibitory populations equally, giving us $c_{e,p} = c_{i,p}$. These constants are set to 1 for simplicity. We can see that this assumption makes the second equation redundant, as we now have $V_{e,p} = V_{i,p} = V_p$. Furthermore, the synaptic coefficients at the pyramidal dendrites are set to $\nu_{p,e} = 1$ and $\nu_{p,i} = -1$. Upon making these substitutions and expanding the operator on the left hand side gives rise to the familiar Jansen and Rit neural mass model seen throughout the literature,

$$\begin{aligned} \ddot{V}_p(t) &= Aa f(V_{p,e}(t) - V_{p,i}(t)) - 2a \dot{V}_p(t) - a^2 V_p(t), \\ \dot{V}_{p,e}(t) &= Aa [c_{p,e} f(\nu_{e,p} V_p(t) + q_{p,e}(t)) - 2a \dot{V}_{p,e}(t) - a^2 V_{p,e}(t), \\ \dot{V}_{p,i}(t) &= Bb c_{p,i} f(\nu_{i,p} \cdot V_p(t)) - 2b \dot{V}_{p,i}(t) - b^2 V_{p,i}(t), \end{aligned} \quad (4.46)$$

where $(A, B) = (\Gamma_e, \Gamma_i)$ and $(a, b) = (\mu_e^{-1}, \mu_i^{-1})$. A follow-up publication by Jansen and Rit in 1995 also investigates a double cortical column model, which effectively couples two copies of the above dynamical system together. However, no substantial differences in model output was found, aside from an extension of time delays that give rise to a slow-wave component in EEG simulation. An extended discussion on the connectivity constants $c_{a,b}$ is given by Jansen and Rit (1995) [91], providing more insight on the physiological and anatomical assumptions used to set the values of these parameters. The typical values taken here replace each connection with a scaled global connectivity parameter C , so the final version of this model sets $c_{p,e} = C, \nu_{e,p} = 0.8C, \nu_{i,p} = 0.25C, c_{i,p} = 0.25C$. The output of this neural mass model is given by the membrane potential of the pyramidal population, $u_p(t) = V_{p,e} - V_{p,i}$, which is considered as the primary component underlying EEG signals.

Physiological assumption: The output of this and the Wendling model assumes that the primary generator of the EEG signal is post-synaptic input to the pyramidal population, given by the sum of the excitatory and inhibitory post-synaptic potentials. This is a common convention when linking neural field models to EEG data, but it is putative and not used across all neural field models. For instance, the models by Liley and Steyn-Ross associate the excitatory post-synaptic potential amplitudes with an EEG signal whereas the models by Robinson et al. use the excitatory population activity. It is typically assumed that an EEG electrode measurement corresponds to the average membrane potential of the excitatory pyramidal population, though it is also argued that inhibitory populations also play a role (Nunez and Srinivasan, 2006 [157]). From an electromagnetic perspective, the primary generators of the EEG are not explicitly known, and the largest microscopic measurements we have are of local field potentials, which are still several orders of magnitude away from what is being measured by the EEG. Hence, from a modelling perspective we cannot currently experimentally validate any assumptions about the primary generators of the EEG. Given, that we have no way of testing any of these assumptions, or if any of the models themselves correctly describe the large scale behaviour of populations of neurons, the choice of model output that corresponds to the EEG is somewhat arbitrary.

The model proposed by Jansen and Rit successfully built on the work Lopes da Silva and colleagues and gave support for leading hypotheses on generation of spontaneous EEG signals and response to evoked potentials. However, this model does not appear to replicate high frequency phenomena, which is problematic for investigations in neuropathology. The temporal kernel can behave similarly as a low-pass filter, which can inadvertently remove high-frequency phenomena. To challenge this, an extension by Wendling et al. (2002) [214], physiologically motivated the addition of another inhibitory population into the framework provided by Jansen and Rit in order to replicate the high-gamma activity seen in EEGs in subjects with epilepsy. The Wendling model utilises the same pyramidal and excitatory populations as Jansen and Rit, but asserts the incorporation of a slow inhibitory population and a fast inhibitory population. The pyramidal population projects to each of the three peripheral populations, which then each feed back into the pyramidal population. In addition to this, the slow inhibitory population is hypothesised to down regulate the fast inhibitory population.

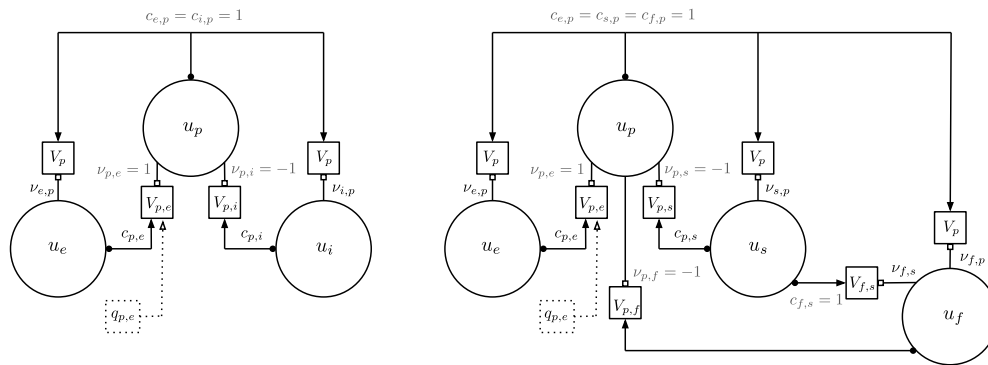


Figure 9: **Diagram of Jansen-Rit (left) and Wendling (right) neural mass models.** The model by Jansen and Rit is an extension of the model by Lopes da Silva, and the model by Wendling is an extension of the model by Jansen and Rit. Each subsequent development adds more structure to the neural mass model and progressively more assumptions about the connectivity and temporal dynamics between neurons in a cortical column, which can be interpreted as a point in a neural field. These proposed models normalise certain connectivity strengths $\nu_{a,b}$ and $c_{a,b}$, and have been annotated in grey.

This extension done by Wendling et al. is motivated by links between different inhibitory currents and the emergence of delta and theta rhythms in EEG (White et al., 2000 [215]) as well as the link between gamma oscillations in EEG arising from the behaviour of inhibitory interneurons (Whittington et al., 2000 [216], Jefferys et al., 1996 [93]). Wendling et al. also refer to the study by Miles et al. (1996) [146], which highlight distinct fast and slow responses to the inhibitory neurotransmitter GABA-A in CA1 pyramidal neurons. Specifically, the neural mass model incorporates an additional level of detail on axonal projections of inhibitory interneurons in cortical columns through the choice of different temporal kernels. The inhibitory synapses that lie at the end of inhibitory interneuron axons can project onto the dendrites of their target neurons, or onto the cell body (soma). Where these synapses project to can greatly influence the way these inhibitory signals are integrated. For instance, a somatic-projecting inhibitory signal will have a larger apparent magnitude and faster timescale relative to a dendritic-projecting inhibitory signal when integrated at the axon hillock of the target neuron due to the spatial origin of these signals. Experimental studies by Dichter (1997) [52] and

Cossart et al. (2001) [41] highlight the importance of this distinction when investigating epilepsy. These aspects can be included by expanding the number of neural populations and corresponding temporal kernels with different parameters.

The Wendling neural mass model can be derived using the modern neural field framework in a similar fashion to the Jansen and Rit neural mass model, using the same delta distribution spatial kernels $w_{a,b}(x) = c_{a,b}\delta(x)$, and alpha function temporal kernels

$$V_{a,b}(t) = \int_{-\infty}^t \psi_b(t-T) \left[c_{a,b} f \left(\sum_c \nu_{b,c} V_{b,c}(T) \right) + q_{a,b}(T) \right] dT, \quad (4.47)$$

$$\psi_b(t) = \frac{\Gamma_b}{\mu_b} t \exp(-t/\mu_b) \Theta(t).$$

Instead, we consider 4 populations: a pyramidal population (p), an excitatory population (e), a slow inhibitory population (s), and a fast inhibitory population (f), with the temporal kernels

$$\begin{aligned} \psi_e(t) &= \psi_p(t) = \frac{\Gamma_e}{\mu_e} t \exp(-t/\mu_e) \Theta(t), \\ \psi_s(t) &= \frac{\Gamma_s}{\mu_s} t \exp(-t/\mu_s) \Theta(t), \\ \psi_f(t) &= \frac{\Gamma_f}{\mu_f} t \exp(-t/\mu_f) \Theta(t). \end{aligned} \quad (4.48)$$

The connectivity between these populations follows the same arrangement as laid out by the Jansen and Rit neural mass model: pyramidal neurons p project onto the peripheral interneuron populations e , s , and f and each of these populations feedback onto the pyramidal population p . Crucially, Wendling et al. also refer to the study by Banks et al. (2000) [10], which suggests that the slow inhibitory population s also projects onto the fast inhibitory population f . The population connectivity is diagrammatically represented in Figure 9. The Wendling model then ‘inherits’ the simplifications made by Jansen and Rit:

- external input is only considered in the excitatory e to pyramidal p connections as before, so we set $q_{a,b}(t) = 0$ for all $(a,b) \neq (p,e)$,
- The connectivity constants projected from the pyramidal population p are set $c_{.,p} = 1$ for simplicity, making separate equations for different pyramidal post-synaptic potentials redundant $V_{.,p}(t) = V_p(t)$,
- The pyramidal synaptic constants are set to $\nu_{p,e} = 1$, $\nu_{p,s} = -1$, and $\nu_{p,f} = -1$,
- The connectivity constant between the inhibitory populations is set to $c_{f,s} = 1$.

From here, the procedure to derive the Wendling model ODEs is identical to the procedure we used for the Jansen and Rit model: we invert the temporal integral operators as linear differential operators and rearrange the equation to obtain

$$\begin{aligned} \ddot{V}_p(t) &= Aa f [V_{p,e}(t) - V_{p,s}(t) - V_{p,f}(t)], \\ \ddot{V}_{p,e}(t) &= Aa \{c_{p,e} f [\nu_{e,p} V_{e,p}(t)] + q_{p,e}(t)\} - 2a \dot{V}_{p,e}(t) - a^2 V_{p,e}(t), \\ \ddot{V}_{p,s}(t) &= Bb c_{p,s} f [\nu_{s,p} V_{s,p}(t)] - 2b \dot{V}_{p,s}(t) - b^2 V_{p,s}(t), \\ \ddot{V}_{p,f}(t) &= Gg c_{p,f} f [\nu_{f,p} V_{f,p}(t) - \nu_{f,s} V_{f,s}(t)] - 2g \dot{V}_{p,f}(t) - g^2 V_{p,f}(t), \\ \ddot{V}_{f,s}(t) &= Bb f [\nu_{s,p} V_{s,p}(t)] - 2b \dot{V}_{f,s}(t) - b^2 V_{f,s}(t), \end{aligned} \quad (4.49)$$

where $(A, B, G) = (\Gamma_e, \Gamma_s, \Gamma_f)$ and $(a, b, g) = (\mu_e^{-1}, \mu_s^{-1}, \mu_f^{-1})$. As with the preceding Jansen and Rit model, the mean membrane potential of the pyramidal population $u_p(t) =$

$V_{p,e}(t) - V_{p,s}(t) - V_{p,f}(t)$ is interpreted as the model output, corresponding to the EEG signal. The connectivity parameters are handled in a similar fashion to the Jansen and Rit model, where the connectivity is set to be proportional to a global coupling parameter C $\nu_{e,p} = C, c_{p,e} = 0.8C, \nu_{s,p} = 0.25C, c_{p,s} = 0.25C, \nu_{f,p} = 0.3C, \nu_{f,s} = -0.1C, c_{p,f} = 0.8C$.

From perturbing the synaptic gain parameters A, B , and G , six primary rhythms are identified by Wendling et al. (2002) [214]. A key conclusion from this model was the impact of dendritic inhibition in epilepsy. That is, the model proposed that a key explanation for the transition from ‘non-seizure’ to ‘seizure’ activity can be explained by the impairment of dendritic inhibition. This neural mass model has thus become the focus of a substantial number of publications in mathematical neuroscience and EEG modelling regarding epilepsy, which we will review in Section 4.4 of this paper.

The neural field models that transpired from the second wave of neural field modelling in the 1990’s continued to refine concepts and systems proposed in canonical publications from Wilson and Cowan, Amari, Freeman, Lopes da Silva, Van Rotterdam, and Nunez. The work of Robinson, Liley, and Steyn-Ross incorporated contemporary findings from neuroscience and proposed new explanations for aggregate neural phenomena across brain regions by using mathematical concepts such as time delays. The models proposed by these authors expanded on the framework used by Amari, and led to new theories on the generation of rhythms in EEG signals and proposed and supported hypothesised mechanisms for seizure generation and spread throughout the cortex. In tandem to this branch of models, spatially invariant neural mass models also saw significant development throughout this period with the work of Jansen, Rit, and Wendling. While these models focused on modelling smaller regions of cortical tissue, they avoid difficulties in justifying spatially homogeneous kernels that have been in use since the canonical field model by Wilson and Cowan. Modelling a single point of cortical tissue as opposed to a continuum allowed for more efficient computation of results and a more concentrated investigation on the aggregate circuitry required in cortical columns required to sustain critical EEG rhythms in response to a random or deterministic input. These theoretical developments were essential steps in realising neural field models as we recognise them today, and provided the roots for contemporary approaches in modelling neural tissue and making clinical inference from mathematical and computational methods.

4.4 Contemporary clinical applications of neural fields

Electroencephalography (EEG) is an essential tool in neuroscience used to monitor and assess aggregate brain activity, and frequently used in clinical neurology for a variety of pathologies. This technique involves using an array of electrodes to detect and record neural activity via fluctuations in the electrical potential on the order of micro-volts (Smith, 2005 [191]). It is one of the oldest modalities in neuroscience with high millisecond temporal resolution at the cost of low spatial resolution. Specific questions where EEG is used include investigations of the origin of common activity patterns in neural tissue, in addition to a variety of clinical applications. EEG plays an important clinical role in the diagnosis, localisation, and management of epilepsy syndromes. Crucially, it can be used to assess emergence of slower rhythms and unprovoked discharges, appearing as “spikes” and “waves” in the signal, which can be indicative of epilepsy (Smith, 2005 [191], St. Louis et al., 2016 [193]). It is also an essential tool in examining brain activity during sleep and transitions in activity during the progression of the sleep cycle to diagnose and treat sleep disorders. Additionally, it is an important tool in monitoring the progression of dementia, assessing severity of tumours and strokes, as well as examining the depth of anaesthesia and coma St. Louis et al. (2016) [193].

Quasiperiodic waves in the EEG are fundamental constituents of the recorded signal and are used to infer neurological conditions. Historically, this has been done using visual inspection of the EEG record, but software tools, such as Persyst (Guillen et al., 2014 [84]), can reveal rhythms through routine Fourier analysis. These brain rhythms are partitioned by frequency ranges and are *not* grouped by function. Certain activities and levels of conscious activity are correlated with different frequency bands, but it should be emphasised that our physiological understanding of the origin of these rhythms is an ongoing topic of research. Slow rhythms include δ waves (1 – 3 Hz) and θ (4 – 7 Hz) waves, which tend to be prevalent in drowsy subjects. Higher frequency ranges are partitioned into α waves (8 – 12 Hz) and β waves (13 – 25 Hz), and γ waves (26 – 100 Hz). The α rhythm is essential feature in every EEG report, as healthy adults at rest with eyes closed tend to display a low-amplitude mixed-frequency background with a dominant α rhythm. Excessive β rhythms are usually caused by drowsiness or sedative drugs. The presence of intermittent slower rhythms in δ and θ bandwidths can also arise from low states of arousal (also common in children and elderly), however they can also be indicative of an epilepsy syndrome or progression of dementia (Medithe and Nelakuditi, 2016 [144], Tatum, 2021 [199], Emmady and Anilkumar, 2021 [58]). Rhythms of higher frequency such as γ waves (26 – 100Hz) and ripples (over 100 Hz) are not common in scalp EEG, but thought to reflect epileptiform discharges. The compositions of rhythms observed on an EEG are unique to each individual, and vary based on a variety of factors such as drowsiness, pharmacology, and neuropathologies.

The activity and rhythms recorded on an EEG are believed to arise from variations in population-level activity in neural tissue, therefore neural field models provide a mathematical framework to identify mechanisms for the emergence of rhythms. Investigations of rhythmogenesis with neural field models appear at least as early as 1974 with the work of Lopes da Silva et al. (1974) [129], which proposed a two population neural mass model alongside a typical neural network simulation. The output of the neural field model used resembles the α -rhythm on an EEG, providing a relatively simple physiological hypothesis for the origin of neurological rhythms as a consequence of neural population arrangements and activity in the cortex. As models of neural fields matured, the questions and investigations of rhythmogenesis became more prevalent. The work by Liley et al. (1997) [123] shows how neural field approaches were refined over the decades and provided progressively more detailed hypotheses between the simulations and the underlying neurophysiology. Rhythms in neural fields are determined by the differences in timescales in difference postsynaptic temporal kernels, but the external input term driving many of these models is also responsible for key aspects of rhythmic output of these models. External inputs to neural field models tend to be simple white noise inputs to an excitatory population, which represents neural activity not explicitly modelled. Although a white noise process is the simplest process to use for this purpose, a study by Freyer et al. (2011) [74] identifies that using a more elaborate stochastic process with state-dependence and feedback produces a more physiologically accurate power spectrum. Pharmacokinetic influence, among other physiological states, are interpreted as different sets of parameter values for neural field models throughout these studies, which provides methods of generating theoretically motivated hypotheses for the prevalence, emergence, and persistence of rhythms. This is an essential step in understanding the dynamics of these types of models, and leads onto crucial questions of stability of rhythms and state transitions, such as regular dynamical changes observed during sleep as well as pathological rhythms of epilepsy. Rhythmogenesis, both endogenous such as sleep or pathological such as seizures is a fundamental part of neuroscience that neural field models can be used to investigate.

Neural field models can also be used to investigate mechanisms of regular activity

state transitions in rhythms that occur during sleep. Despite being widely studied, there is relatively little known about the neurophysiological processes involved during the sleep cycle. Sleep can broadly be partitioned into three stages: Waking stage, the Non Rapid Eye-Movement (NREM) stage, and the Rapid Eye-Movement (REM) stage. The NREM stage comprises approximately 80% of the duration of sleep, and can be distinguished on an EEG by the presence of slow oscillations, increased power in δ frequencies, and distinct bursts of activity such as “spindles” and “K-complexes” (Purves et al., 2001 [166], Nayak and Anilkumar, 2021 [151]). The REM stage, sometimes referred to as paradoxical sleep, is the deepest stage of sleep with little or no arousal in subjects and commonly associated with dreaming. EEG activity recorded during this stage resembles the higher frequency β and γ patterns seen during the waking phase (Purves et al., 2001 [166], Al Sawaf et al., 2021 [3]). During sleep, brain activity alternates between NREM and REM sleep in several cycles before waking, exhibiting discernible state transitions on an EEG (Nayak and Anilkumar, 2021 [151]). Neural field models provide a mathematical route in which these transitions can be modelled and studied in terms of the potential migration of parameters governing mean quantities of neural tissue.

Events that occur during the sleep cycle, such as sleep spindles and K-complexes, provide useful targets for modelling non-linearities and state transitions on EEG. Subjects are typically motionless during sleep, which results in EEG recordings with less extraneous noise compared to an EEG recording during wakefulness. The thalamocortical neural field model summarised in Section 4.2 has also been used to investigate rhythms in sleep. A publication by Abeysuriya et al. (2014) [1] finds a region of parameter space from which the model output resembles sleep spindles. They suggest that these electrophysiological events arise from the thalamic relay nuclei, instead of the reticular nucleus and predict that the power in the harmonic of the spindle scales with the oscillation of the spindle. Alongside this, other investigations by Weigenand et al. (2014) [213] and Costa et al. (2016) [42] derive a two-population cortical neural mass model with conductance-based synapses to investigate transitions between sleep stages. They find a mathematical formulation that replicates patterns and transitions seen on sleep EEGs which is modulated by the neurotransmitter input to the excitatory pyramidal population. Their model was spatially extended to a 4 population cortico-thalamic neural mass model by Costa et al. (2016) [43], which was verified by comparing perturbations in the model to auditory stimulation of subjects during sleep.

Rhythms observed during an EEG recording can be used to inform the depth of sleep and level of consciousness of a subject during a sleep study. This is also a critical component of clinical evaluation when assessing and diagnosing brain death or assessing a comatose state. Additionally, rhythms on EEG can also be used to assess the depth of anaesthesia, which must be carefully monitored before and during a surgery by highly trained professionals. The development of neural field models with non-linear conductance-based temporal dynamics by Liley et al. and Steyn-Ross et al. were highly motivated by this particular application and used to investigate the phase transitions that occur in cortical activity. General anaesthetics, such as isoflurane and benzodiazepines, generally increase the level of inhibition in neural systems. The effects of which can be investigated through bifurcation analysis of a neural field model. Steyn-Ross et al. (1999) [195] investigate the action of modulation of inhibition in a conductance based neural field model with spatial homogeneity and find 3 distinct states that correspond to different EEG morphologies than can be related to the level of anaesthetic action. As inhibition decreases, the models transitions from a “comatose” state, through an “active” state, and eventually reaching a hyperactive “seizure” state, relating to several studies of inhibitory-dominated regimes in microscale neural network models (Brunel,

2000 [27]). Their results predict a rapid transit between comatose states and active states at a critical value of inhibition, and they propose a multistability hypothesis for the switching between these two states. They find concordance between the behaviour of clinical EEGs and model output, where the frequency spectrum peaks before collapsing during the transition from active to comatose. A later publication by Bojak and Liley (2005) [16] alternatively proposes a bifurcation mechanisms, instead of multistability, for the transitions observed during anaesthetic intervention. The competing hypotheses of multistability vs. bifurcation is common to investigations of epilepsy as well, and remains highly contested. In this study, spatial homogeneity is not assumed and they investigate the output of over 70,000 parameter configurations in order to try map the model parameter space to physiologically plausible regions. Investigations of the connection between clinical data and the parameter space are essential to one day utilising these models for directing anaesthetic dosages in clinical practice and further understanding these neurological mechanisms.

Another neurological phenomenon involving state transitions is found in epilepsy, conceptualised as changes between a “seizure” state and a “non-seizure” state. Epilepsy is another extensive sub-class of intermittent brain pathologies which encapsulates a variety of neurological syndromes characterised by recurrent seizures, which can manifest as uncontrolled disturbances to movement, consciousness, perception and/or behaviour. The type of epilepsy is often classified according to the seizures that occur, which in turn indicate which parts of the brain and neural pathways are affected. Epilepsy encompasses a wide variety of different brain disorders that result in recurrent and/or unprovoked seizures. However, like many clinical sciences, there is often much dispute over the terminology and classification of these syndromes that spans decades of discussions across a wide variety of international neurology groups. The pathologies underlying epilepsy are not always clear, but the syndrome appears to be related to abnormalities in brain connectivity. Different people with epilepsy often present different symptoms, levels of severity, and responses to anti-epileptic drugs. Hence, this condition must be treated on an individual case approach instead of a one-size-fits-all strategy, which requires regular consultation with neurologists. Diagnosis of epilepsy from EEG is often a precarious clinical decision making process. A false positive can result in mis-prescription of anti-epilepsy drugs with side effects, in addition to impacts on anxiety and overall mental well-being. On the other hand, a false negative may lead to an untreated epilepsy patient having a seizure without warning during daily activities, which can lead to serious injury or death. Severe cases of epilepsy that cannot be controlled with medication often require highly invasive surgical intervention, which involves mapping of epileptogenic sections of cortex using intracranial EEG and stereotactic EEG. These discussions within the neurological sciences encourages the development of novel approaches to data analysis and mathematical modelling in order to achieve subject-precision treatments and prognosis and to further develop our understanding of state transitions in brain dynamics.

Phase transitions in neural field models have been applied to epilepsy since the 1970s with the works of Kaczmarek (1976) [98] and Kaczmarek and Babloyantz (1977) [99], which identified bifurcation points that give rise to a transition to oscillatory activity in their model. Bifurcation theory continues to be used to explore potential physiological causes behind epileptic state transitions. An illustration of how these concepts are broadly applied is seen in the work of Lopes da Silva (2003) [130], which describes the transition between non-seizure (interictal, steady-state with intrinsic fluctuations) dynamics and seizure (ictal, synchronous oscillations) dynamics via 3 mechanisms acting on a bistability in a neural field model with comparison to data from subjects with photosensitive epilepsies. A study by Breakspear et al. (2006) [19] does a thorough

bifurcation analysis on the cortico-thalamic neural field model by Robinson et al. and identify regions of the parameter space where patterns resembling generalised seizures arise. The choice of bifurcation parameter was motivated by physiological hypotheses, which asserted that the excitatory influence of cortical pyramidal neurons on the specific thalamic nuclei was responsible for seizure activity (McCormick and Contreras, 2001 [142]). Much of the pathological activity seen in the cortico-thalamic neural field model by Robinson et al. arises from the time delay between the cortical populations and the thalamic populations. Marten et al. (2009) [134] investigates physiological rationales for the addition of a time delay and identified the difference in timescales of GABA-A and GABA-B neurotransmitter receptors as the likely explanation. A variety of dynamical characteristics, such as Hopf bifurcations and false bifurcations, were identified in physiologically plausible regions of the model and thus proposes more potential mechanisms for polyspike complexes observed on an epileptiform EEG recording. In a following publication, Marten et al. (2009) [135] convert this system of delayed differential equations to a system of ordinary differential equations by using the 'linear chain trick' (Smith, 2011 [190]), which produces equivalent dynamics to the original cortico-thalamic neural field model.

The neural mass model by Wendling has also been used to study the generation of polyspike events in EEG recordings. A bifurcation analysis by Blenkinsop et al. (2012) [15] connected specific clinical features in EEG recordings to dynamical features present in the Wendling neural mass model. Contemporary results on generalised epilepsies suggest that temporal evolution of seizures may arise from gradual changes in underlying physiological mechanisms, which bifurcation theory is well suited for investigating. A number of Hopf bifurcations, false bifurcations, SNICs and eigenstructure changes are identified in the neural mass model of Wendling et al., which result in the onset of polyspike complexes as observed in EEGs of subjects with epilepsy. These bifurcations are related to specific features of clinical EEG data by comparison with locally stationary segments of patient EEGs. It is imperative to note that a number of different pathways produce the same transitions to epileptic activity, which is critical to be mindful of when interpreting results from neural field modelling for directing clinical strategies for epilepsy and other neurological conditions.

An ongoing research effort in neural field modelling attempts to improve our understanding of macroscale dynamics by investigating connections with data and models on the microscale. For example, a study by Eissa et al. (2017) [55] investigates the connections between different spatial scales upon the onset of seizure activity. As simultaneous recording techniques improve in accuracy and reliability, the mathematical connection between different scale of modelling can be elucidated. The interplay between global and local inhibition is examined as another potential physiological mechanism for seizure onset. Bifurcation analysis of a modified Wilson and Cowan neural field model is used to describe macroscale dynamics, which can then be identified in the data and related to physiological aspects through relevant perturbations in parameter values. Another study by Martinet et al. (2017) [137] uses simultaneous microscale and macroscale recordings in tandem with a Steyn-Ross neural field model to examine mid-seizure dynamics. Guided by data across multiple scales and neural field modelling, they propose candidates for physiological mechanisms that lead to the increased coherence during seizures.

Neural field modelling has played a crucial role in demonstrating consequences from physiological hypotheses on transitions of neural activity states, and continues to further our understanding of brain state dynamics. However, many of the conclusions and results of neural field modelling result in hypothetical and theoretical conclusions that are difficult, if not impossible, to verify due to limitations on experimental neuroscience. Neural field modelling at this stage is showing more promising outcomes by directing

our focus to particular dynamical structures, such as certain bifurcations, that emerge from these mathematical frameworks of mean macroscale neural activity. Results from Kramer et al. (2012) [110] illustrates this by identifying a Hopf bifurcation in a neural field model that presents similar patterns of “slowing” in the mean activity directly before a seizure as observed in the data. Dynamical pathways for seizure onset and offset and biophysically realistic explanations are identified from the neural field model used, and shows concordance between modalities on different spatial scales. This phenomena of “critical slowing” is another ongoing topic of discussion within epilepsy modelling in contemporary literature. There are a variety of publications that develop this hypothesis further, and may provide a method of forecasting critical transitions from recordings of EEG (Maturana et al., 2019 [140]). Overall, identifying bifurcations from data is a promising direction for neural field modelling. Results from Jirsa et al. (2014) [97] utilises an approach of classifying bifurcations by patterns observed in dynamical transitions and uses this as a framework for constructing an oscillatory dynamical system that exhibits the same transitions. Higher order bifurcations are also being analysed and connected to data (Saggio et al., 2017 [182]). Throughout the next Section, we discuss the limitations of neural field modelling and the prospective phenomenological approaches used in the contemporary literature.

5 Discussion and future directions

This review paper on mathematical models of brain dynamics has focused on population-scale models. Throughout we have highlighted a number of critical theoretical developments and the underpinning assumptions necessary to construct neural field models. Compared to traditional bottom-up approaches, neural field modelling uses average quantities of populations of neurons instead of properties of individual neurons. This approach provides an essential balance between biophysical realism and mathematical tractability, however there are some crucial shortcomings and consequences that warranted a more thorough examination. This was addressed through considering the historical context, motivations and derivations of neural field models and explicitly detailing their underpinning mathematical, physiological and anatomical assumptions. Then a general unifying framework was derived from which, in principle, all neural field models (and neural mass models) can be constructed and related back to. Following this, some of the key applications of NFM’s were also explored such as rhythmogenesis, sleep, and epilepsy. We conclude our review with a brief discussion on the limitations of NFM’s and by highlighting some recent research directions that provide more biophysically realistic details whilst maintaining mathematical tractability.

5.1 Limitations of neural field modelling

In order to maintain a balance between biological plausibility and mathematical tractability when constructing models, compromises are inevitably made and it is essential these are carefully considered. Whilst many of these assumptions are straightforward and justifiable, others are more subtle and their validity less clear, especially when they are not currently experimentally verifiable. This ambiguity leads to issues with interpreting results generated by NFM’s. For example, when brain state transitions are linked to connectivity parameters.

A theory should be constructed with ‘a clear physical picture of the process’ being modelled and/or ‘a precise and self-consistent mathematical formalism’ (Dyson, 2004 [53]).

Unfortunately, the current status of NFM’s permits neither of these. Unlike statistical physics, there is not yet a precise and self-consistent mathematical framework that links

the microscopic with the macroscopic. In fact, much of the mathematical toolbox from theoretical physics that is used to deal with complex interacting systems are primarily for closed equilibrium systems. In contrast, like many biological systems, the brain is an open non-equilibrium system with scales that are interdependent and not easily separable.

A primary challenge is the many degrees of freedom that NFM's have, even with the use of averaged and lumped parameters. This is often due to lack of data and an incomplete understanding of the macroscopic structures and processes. The resulting parameter space is often so large and unconstrained that almost any dynamical behaviour can be constructed.

As famously quoted by John Von Neumann:

"With four parameters I can fit an elephant, and with five I can make him wiggle his trunk!" — Dyson (2004, p. 297) [53].

This paints an ambiguous physical picture of what is being modelled, as there is often no direct correspondence between model and experimental parameters. Equations. For example, it is not currently possible to measure the average synaptic connectivity between two neural populations in the cortex. At best the values used in the literature are order of magnitude estimates that are currently unverifiable.

Given the lack of a precise mathematical formalism and/or a clear physiological picture at the macroscopic scale, neural field models could effectively be considered as biologically inspired phenomenological models. As observed throughout the applications outlined in the previous section, the majority of experimental verification is based on a visual comparison to EEG data. This is partly due to the limitations of our understanding of the EEG signal, which is also impacted by the disconnect between activities on different spatial scales. In order for neural field theory to progress from descriptive to predictive, their hypotheses need to be experimentally validated so that the theoretical framework can be successively iterated with experimental results. A fundamental goal for the field then is the generation of testable predictions at the macroscale, similar to those achieved at the neuronal level with the Hodgkin-Huxley equations. Although these equations are phenomenologically derived, they are both descriptive and predictive. This is because the parameters and state variables of the Hodgkin-Huxley model have a one-one correspondence with those measurable in experiments, providing a predictive framework for single neuron dynamics. In order for NFM's to generate novel results that are reproducible and predictive, a concordance between theory and experiment is required.

5.2 Future directions

Neural field theory is a very active area of research with many directions being explored and developed. In this section we present four relatively recent examples: stochastic approaches which extend NFM's to have state-dependent stochastic inputs, random neural networks which studies networked dynamical systems using random matrix theory, abstracted network models which use more abstract models to understand functional neuroimaging data and next-generation field models which develop ensemble solutions that connect the micro and macro-scales.

5.2.1 Stochastic neural field modelling

Stochastic approaches are an active sub-discipline of research within modern neural field modelling. Complex and chaotic variations in cellular and sub-cellular processes and interactions across substantially large populations of neurons are more naturally

modelled by a stochastic process, instead of a detailed deterministic description, which is a theme prevalent across mathematical biology as a whole. The incorporation of stochastic descriptions can capture additional system interactions due to finite size effects and variations in parameters, which often leads to models with more elaborate dynamics at the cost of greater mathematical complexity. In neural field modelling, stochastic extensions significantly change the previously observed behaviour of solutions in neural fields, often changing their stability and the propagation of travelling waves (Bressloff, 2009 [20], 2012 [21]), (Kilpatrick and Ermentrout, 2013 [107]). More details on the principles behind stochastic modelling is found in the works by Bressloff (2014) [22] and Faugeras and Inglis (2015) [62].

Stochastic neural fields arise from two approaches: stochastic extensions of existing neural field frameworks, or population density approaches based on interacting microscale neuron models (Bressloff, 2014 [22]). Extensions typically begin with a simpler neural field framework, such as the Amari field equation (3.5) with one neural population and a first order temporal kernel. In using one population, the deterministic dynamics are constrained to exhibiting only the essential dynamics typical of a neural field while enabling more focus on the impacts of the inclusion of a stochastic term. This approach results in Langevin-type equations of the form

$$U(x, t) = \left(-U(x, t) + \int_{\Omega} w(x - X) f[U(X, t)] dX \right) dt + \sigma(U(x, t)) dW(x, t), \quad (5.1)$$

where $U(x, t)$ represents the mean membrane potential at position $x \in \Omega$ and time t , f is the wave-to-pulse transfer function, w is the homogeneous spatial kernel, σ is a state-dependent diffusion coefficient, and $W(x, t)$ is a canonical Wiener process. Multi-population extensions are also possible (Lima and Buckwar, 2015 [126], Bressloff, 2019 [23]), as well as stochastic delay differential equation perspectives (Buckwar, 2000 [28], Riedler and Buckwar, 2013 [173], Ableidinger et al., 2017 [2]).

Population density approaches to stochastic neural field modelling give a greater focus on the randomness that arises from variation amongst neurons (Buice and Cowan, 2007 [29], Bruice et al., 2010 [30], Bressloff, 2009 [20], Bressloff and Lai, 2011 [25]). There are a variety of formulations of this fashion that incorporate randomness arising from synaptic activity in the form of a point process. With careful analysis, the limiting behaviour can be derived using various methods, which recovers classical neural field equations with additional stochastic terms. The continued development of mathematical methods that prioritise the link between microscale and macroscale activity is essential for resolving issues in neural field modelling. A detailed discussion of stochastic models in neuroscience is beyond the scope of this review given the overall richness and complexity underpinning the mathematical formulation. An advantage of models of this nature comes from a greater reliance on more phenomenological descriptions and thus finding alternate methods of quantifying and modelling neural activity (Sompolinsky et al., 1988 [192], Ostojic, 2014 [160], Mastrogiuseppe and Ostojic, 2017 [139], Ipsen and Peterson, 2020 [89]). In addition, these models can be used to explain phenomena arising from finite-size population effects and the occurrence of large deviations and rare events (Faugeras and Maclaurin, 2014 [63], Kuehn and Riedler, 2014 [112], Bressloff and Newby, 2014 [26], Lang and Stannat, 2017 [119]). Stochastic inputs can be useful for understanding spontaneous state transitions and characteristic changes in time series statistics in systems close to criticality. For example, a study by Freyer et al. (2012) [75] showed that using a multiplicative state-dependent stochastic process results in a more realistic model output closer to the structure of experimental EEG data. Abstractions and stochastic extensions of neural field models can further enhance the focus of these discussions by giving a closer correspondence between experimental data

and mathematical structure, allowing for more data-driven approaches (Kalitzin et al., 2010 [100], Benjamin et al., 2012 [11], Schmidt et al., 2016 [184]).

5.2.2 Random neural network models

In describing the dynamics of large nonlinear networks of neurons, another important mathematical approach is the study of random neural networks (Stern et al., 2014 [194]). Instead of using a continuous spatial kernel to describe the connectivity between neurons, a matrix operator with a discrete topology can be used. This weight matrix connects neural mass models and is mathematically equivalent to a neural field model with a discretised field. This approach treats the dynamics of neural networks as a directed graph dynamical system composed of N first-order neural mass models with instantaneous synapses that are nonlinearly coupled via a random connectivity matrix W . The connectivity weights, which are the elements of W are chosen from identically and independently distributed (IID) random variables such as a normal distribution with mean μ and variance σ . The dynamics of the i -th node is given by

$$\dot{x}_i = -\frac{x_i}{\tau} + \sum_{j=1}^N w_{i,j} \phi(x_j), \quad (5.2)$$

where the state variable x_i represents the average membrane potential of the i -th neural population, τ is the membrane time-constant, $w_{i,j}$ is the synaptic weight from population j to population i and constitutes a single entry in the $N \times N$ connectivity matrix W , and $\phi(x_j)$ is a nonlinear coupling function, similar to a wave-to-pulse transfer function in typical neural field models.

As N becomes large, it is not mathematically tractable (due to nested nonlinear coupling functions) to compute the fixed points and linearise the system around them to quantify the local stability, as is typically performed with dynamical systems. To avoid these complications, random matrix theory (RMT) is used to compute the statistical properties of the eigenspectrum from the statistics of the connectivity matrix via the circular law (Tao et al., 2010 [198]). This analysis establishes an examinable mathematical relationship between the network connectivity structure and phase transitions of the system. This work was originally pioneered in neural networks by Sompolinsky et al. (1988) [192] using dynamical mean-field techniques from spin glass models. However, computations of phase transitions in large nonlinear networked systems can be traced back to the work of May (1972) [141] from theoretical ecology who demonstrated that the larger a system becomes, the more unstable it also becomes, which is known as a May-Wigner transition (Ipsen, 2017 [88]).

In such a networked system of the type shown in Equation (5.2), it was found that the system undergoes a phase transition into a ‘chaotic’ like state with highly fluctuating and complex dynamics (Stern et al., 2014 [194]), where the order parameter is in fact the variance of the connectivity matrix. The microscopic mechanisms underlying this phase transition have also been mathematically examined (Wainrib and Touboul, 2013 [212]) and it was found that there is an explosion from a single or simple set of fixed points to an exponential increase in the number of fixed points. The phase transition can be computed approximately using a Kac-Rice formalism that counts the number of fixed points. However, these results are based on networks with a single randomly connected population drawn from an IID which is not anatomically realistic.

Rajan and Abbott (2006) [167] demonstrated that when a more anatomically realistic connectivity in the form of Dale’s law is added there is a significant change in the nature of the phase transition. Dale’s law states that excitatory (inhibitory) neurons can only give excitatory (inhibitory) signals (Eccles et al., 1976 [54]). This introduces non-random

structure that makes the connectivity matrix entries no longer identically distributed and only partially random, as matrix columns corresponding to the excitatory (inhibitory) elements are positive (negative) entries. The matrix entries for different populations are drawn from different distributions with their own means, variances and proportions with respect to each other e.g. no. of excitatory vs no. of inhibitory. This consequently alters where and how rapidly the phase transition takes place in parameter space. An example “two-population” connectivity matrix is shown in Figure 10 (a). Further, because of the different variances of the populations, the eigenspectrum computed from the circular law is no longer of uniform density (Rajan and Abbott, 2006 [167]), as seen in Figure 10 (b). The non-random connectivity of Dale’s law was also recently incorporated into a Kac-Rice formalism by Ipsen and Peterson (2020) [89] to study the effects it has on the microscopic mechanism of the phase transition. The location of the phase transition critically depended on the different connectivity parameters of the different neural populations. Such a technique enables mathematical investigations to be performed between the network connectivity and network dynamics that would not be possible using standard techniques from classical dynamical systems.

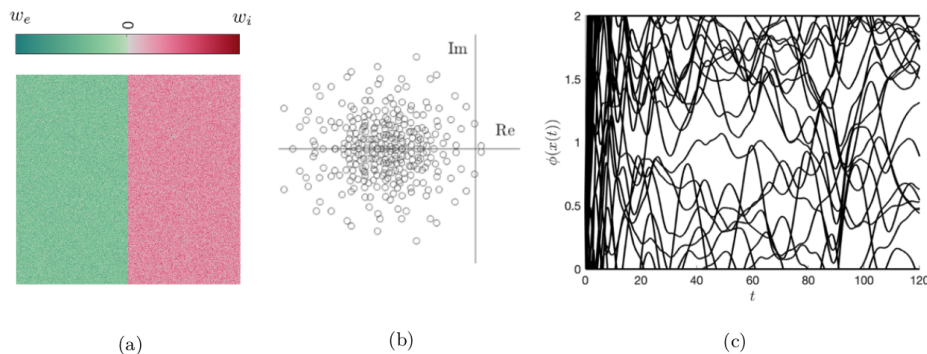


Figure 10: **Instance of a random two-population neural network model.** (a) Heat map of random connectivity matrix. The block structure of the connectivity matrix incorporating Dale’s law with positive excitatory weights w_e and negative inhibitory weights w_i can be seen. (b) Eigenspectrum of connectivity matrix, showing a compact circular support that is non-uniform in density due to Dale’s law (Rajan and Abbott, 2006 [167]) and a pair of unstable eigenvalues. (c) Simulation of networked system. The unstable eigenvalues cause a phase transition as can be seen in simulations, which shows the firing rate activity of individual nodes over time.

Another technique that can be employed in networked dynamical systems that are coupled via heterogeneous matrices is Dynamical Mean-field theory (DMF). In this approach, a many-body deterministic problem is approximated and reduced to a one-body stochastic system. For example, the coupling term in Equation (5.2) is replaced by a stationary Gaussian stochastic process η ,

$$\dot{x}_i = \frac{-x_i}{\tau} + \eta(t). \quad (5.3)$$

The individual trajectories x_i are now stochastic processes, which in the limit of a large network become uncorrelated and statistically equivalent (Ostojic, 2014 [160]), so that the network dynamics can be effectively described by a single process. The first and second order moments of the network activity can be non-trivially computed for certain cases and are strongly dependent on the network parameters. This enables us to

investigate the relationship between the statistics (first two moments) of the activity and the network structure.

5.2.3 Abstracted networked models

Recordings from the brain (e.g. EEG) are effectively a spatially discrete representation of it's activity. Rather than consider spatial kernels that are continuous, more recent approaches have utilised coupled neural mass models to create so-called network dynamic models. Effectively, this is conceptually equivalent to a neural field model with a discretised neural field. Each channel of an EEG measures bulk neuronal activity across centimetres, and neural mass models target the same level of description. Recent developments investigate the coupling of EEG channels by using this approach, providing an illustration of new methods of investigating spatial dependence of neural activity and seizure dynamics (Carvalho et al., 2019 [36], Ersöz et al., 2020 [109]). An example of this in the work of Goodfellow et al. (2016) [79], where intracranial EEG is modelled using a neural field model comprised of coupled neural mass models (each corresponding to an EEG channel). This framework allowed for the inference of a discrete spatial kernel based on measured EEG channel correlations during seizure events, and was used to direct surgical strategies in severe cases of epilepsy. A further development on this work by Lopes et al. (2017) [128] simplifies the neural mass model at each channel to a canonical normal form model containing the SNIC bifurcation responsible for epileptic transitions.

Networked dynamical systems have been prevalent in recent literature outside of neural field theory as well, such is as the works of Kalitzin et al. (2010) [100], Benjamin et al. (2012) [11], Ashwin et al. (2017) [8] and Woldman et al. (2019) [219]. These more abstracted approaches employ a more direct top-down approach and aim to model the properties or features of the data rather than the underlying physical processes, which remains mostly inaccessible given the current state of technology. An example of an abstracted networked dynamical system for neurosurgical planning in cases of severe epilepsy is given in Jirsa et al. (2014) [97], who constructed a coupled oscillator (called the "Epileptor") based on a set of bifurcations that can give rise to the onset and off-set of seizures as recorded in EEG. A saddle-node/homoclinic bifurcation pair is used to describe the majority of seizure-like events based on frequency and amplitude scaling and direct current (DC) shifts upon a state transition. The fast oscillator is based on a system proposed by Hindmarsh et al. (1984) [86] whereas the slow oscillator is based on a system proposed by Roy et al. (2011) [180]. The coupling between these oscillators is mediated by an ultraslow "permittivity" variable, linear inhibitory coupling from the slow to fast subsystem, and low-pass filtered excitatory coupling from the fast to slow subsystem. The equations describing this model are shown below:

$$\begin{aligned}
 \dot{x} &= y - f_1(x, u, z) - z + I_1, & \dot{u} &= -v + u - u^3 + I_2 + 0.002g(x) - 0.3(z - 3.5), \\
 \dot{y} &= 1 - 5x^2 - y, & \dot{v} &= \frac{1}{\tau_2}(-v + f_2(x, u)), \\
 \dot{z} &= \frac{1}{\tau_0}(4(x - x_0) - z), & &
 \end{aligned}
 \tag{5.4}$$

where x and u are driven by independent white noise processes with standard deviation 0.025, $x_0 = -1.6$, $\tau_0 = 2857$, $\tau_2 = 10$, $I_1 = 3.1$, $I_2 = 0.45$, $\gamma = 0.01$, and

$$\begin{aligned}
 f_1(x, u, z) &= \begin{cases} x^3 - 3x^2, & x < 0, \\ x(u - 0.6(z - 4)^2), & x \geq 0, \end{cases} \\
 f_2(x, u) &= \begin{cases} 0, & u < 0.25, \\ 6x(u + \frac{1}{4}), & u \geq 0.25, \end{cases} & g(x) &= \int_{t_0}^t e^{\gamma(t-s)} x(s) ds.
 \end{aligned}
 \tag{5.5}$$

The parameters and construction of the Epileptor is phenomenologically motivated, however the dynamical landscape captures a great deal of detail of state transitions that are observed on EEG (Saggio et al., 2020 [181]). It should be noted that there are ongoing efforts to identify relations between the model parameters and underlying neurophysiology (Chizhov et al., 2018 [37]). The Epileptor is used as a constituent of the networked dynamical system of brain dynamics, called The “Virtual Epilepsy Patient”, by Jirsa et al. (2017) [94]. Each Epileptor node represents a different brain region, and connectivity between nodes in the model is inferred from stereo-EEG data. Despite the lack of identifiable parameters from neuronal activities, the framework presented maintains a close relationship with higher levels of neurological data recording, such as EEG and MEG techniques. A top-down focus may lead to new discoveries in the dynamics of brain state transitions that were previously unidentifiable with classical approaches to mean field modelling.

Another application that utilised abstracted networked dynamical systems is in epilepsy diagnosis and the work of Schmidt et al. (2016) [184] and Woldman et al. (2020) [220], which investigates correlations between EEG channels in resting state as a potential marker for epilepsy using an abstracted multi-level Kuramoto model (Kuramoto, 1975 [114], 1984 [113]). These authors use a multi-level Kuramoto approach in modelling emergent synchronisation from resting state EEG. Consider P populations of oscillators, where each population $p \in \{1, \dots, P\}$ contains N Kuramoto oscillators, each with a natural frequency drawn from a population-specific distribution $g_p(\omega)$. We introduce a $P \times P$ coupling matrix ρ , with entries $\rho_{p,q}$ describing the interactions between populations. These entries may be binary or represent a weighted network. Let C and K_p be the global coupling parameter and the local coupling parameters. The evolution of oscillator $j \in \{1, \dots, N\}$ in population $p \in \{1, \dots, P\}$ is given by,

$$\frac{d\theta_j^p}{dt} = \omega_j^p + \frac{K_p}{N} \sum_{k=1}^N \sin(\theta_k^p - \theta_j^p) + C \sum_{q=1}^P \frac{\rho_{p,q}}{N} \sum_{k=1}^N \sin(\theta_k^q - \theta_j^p). \quad (5.6)$$

In this modular network, synchronisation can emerge locally within a single population as well as across the global network. This was proposed as a model of EEG activity generated by the cortical columns in the study by Schmidt et al. (2014) [183]. The degree of synchrony in the individual nodes is measured using the same order parameters as for the simple Kuramoto model, $r_p e^{i\psi_p} = \frac{1}{N} \sum_{j=1}^N e^{i\theta_j^p}$, and global coupling can be quantified by the absolute mean of these constituent order parameters, $r_g = \left| \frac{1}{P} \sum_{p=1}^P r_p e^{i\psi_p} \right|$. In this context, the non-synchronised incoherent state in the Kuramoto formulation corresponds to healthy background activity observed in EEG, whereas emergent synchronous activity across the network is taken as a proxy for epileptiform activity. As with the Epileptor, this phenomenological framework is based on the oscillatory dynamics observed in high-level descriptions of neural activity rather than emergent properties of large neural networks, unlike the next generation of neural field models. The abstracted nature of these models may provide more accessible options for identifying models to clinical data, rather than explaining physiological mechanisms of neural tissue. For further details on the principles of oscillator models in neuroscience, we refer the reader to the review by Ashwin et al. (2016) [7].

5.2.4 Next-generation neural field modelling

Recently, a “next-generation” approach to neural field modelling has emerged, which is derived from microscopic principles (Coombes and Byrne, 2019 [40]). This recent sub-discipline of mathematical neuroscience re-imagines the principles of neural population

models, deriving macroscale states and parameters from the thermodynamic limit of the well-established quadratic integrate-and-fire model. Using the work of Byrne et al. (2019) [34], we can give a brief overview of the modelling principle used and the derivation of the model, which is based on the work of Luke et al. (2013) [131] and Montbrió et al. (2015) [148]. Consider N neurons equally spaced across a one-dimensional domain Ω . The quadratic integrate-and-fire model is given by

$$\frac{du_i}{dt} = u_i^2 + \eta_i + \sum_m g_m^i(t) [u_m^{\text{rev}} - u_i], \quad (5.7)$$

where u_i represents the membrane potential of neuron i , η_i is a background input to neuron i , u_m^{rev} is the reversal potential of synapse group m , and g_m is the conductance of synapse group m . A Lorentz distribution is chosen for η_i , since this allows exact evaluation of the integrals that follow in this derivation. Note that so far in this model the connectivity between neurons is all to all and the population is purely excitatory. A reset condition is also imposed on each equation, so that the membrane potential u_i is set to a reset potential u_r whenever the u_i reaches a threshold potential u_{th} . Using results from Ermentrout and Kopell (1986) [59], the membrane potential state variables of quadratic integrate-and-fire model can be transformed to phase state variables of the theta model (using $u_i = \tan(\theta_i/2)$), given by

$$\frac{d\theta_i}{dt} = 1 - \cos(\theta_i) + (1 + \cos(\theta_i))\eta_i + \sum_m g_m^i(t) [(1 + \cos(\theta_i))u_m^{\text{rev}} - \sin(\theta_i)], \quad (5.8)$$

Each conductance is influenced by inputs from other neurons, as we have seen in classical neural field modelling,

$$\left(1 + \tau_m \frac{\partial}{\partial t}\right)^2 g_m^i(t) = \frac{2\kappa_m}{N} \sum_{j=1}^N w_m(x_i - x_j) \delta(\theta_j - \pi), \quad (5.9)$$

where τ_m is the synaptic time constant, κ_m is the global coupling strength of synapse m , $w_m(x_i - x_j)$ is the homogeneous spatial kernel that depends on the distance between neuron i and neuron j . Taking the thermodynamic limit of the system of neurons and letting $N \rightarrow \infty$, it can be established that the state of the mean field of a system of coupled oscillators can be described by a probability density function $\rho(x, \eta, \theta, t)$ that obeys the continuity equation (Landau and Lifshitz, 1959 [118], Kuramoto, 1975 [114], 1984 [113], Lancellotti, 2005 [117]), which can be used to derive the partial differential equation,

$$\left(1 + \tau_m \frac{\partial}{\partial t}\right)^2 g_m(t) = \frac{\kappa_m}{\pi} \sum_l \int_{\Omega} \int_0^{2\pi} w_m(x - y) e^{il\theta} \left\{ \int_{-\infty}^{\infty} \rho(y, \eta, \theta, t) d\eta \right\} d\theta dy. \quad (5.10)$$

This system can be simplified by using the Ott-Antonsen ansatz (Ott and Antonsen, 2008 [161]) by restricting the form of ρ to a product of factors $L(\eta)$ and $\sum_n \alpha(x, \eta, t)^n e^{in\theta}$. This can be used to derive a new expression of ρ and another partial differential equation for α . In addition to this, a Kuramoto order parameter is defined for the mean field,

$$z(x, t) = \int_0^{2\pi} \int_{-\infty}^{\infty} \rho(x, \eta, \theta, t) e^{i\theta} d\eta d\theta. \quad (5.11)$$

These results are used to transform Equation (5.10) as

$$\left(1 + \tau_m \frac{\partial}{\partial t}\right)^2 g_m(t) = \kappa_m \int_{\Omega} w_m(x - y) f[z(y, t)] dy, \quad f(z) = \frac{1}{\pi} \frac{1 - |z|^2}{|1 + z|^2}, \quad (5.12)$$

giving us the form of a classical neural field model, where f is a real-valued function that depends on the complex-valued population synchrony measure z , which is analogous to the wave-to-pulse transfer function of classical neural field models. With further computation, a differential equation for z can also be derived, which completes the derivation of the next-gen neural field model.

Here we only give a surface-level overview of the principles and equations involved, an in-depth review can be found in the works of Coombes and Byrne (2019) [40] and Bick et al. (2020) [14]. Although this approach is relatively new, it has already been applied to problems in rhythmogenesis (Byrne et al., 2017 [35], Keeley et al., 2019 [104], Taher et al., 2020 [197], Segneri et al., 2020 [185]), synchronisation of neural activity (Luke et al., 2013 [131]), and propagation of epileptic seizures (Gerster et al., 2021 [76]). Furthermore, this framework can also be extended readily to include neural connectivity via gap junctions (Laing, 2015 [116]) and multiple neural populations (Segneri et al., 2020 [185]), which alters the dynamical landscape significantly.

This new branch of neural field modelling is readily adaptable to many methods of modern statistical mechanics and brings a significant step forward on connecting microscopic dynamics to macroscopic dynamics.

5.3 Concluding remarks

Despite their limitations, neural field models remain the most descriptively accurate models of both normal and abnormal brain dynamics such as those observed in EEG data. They are relatively low dimensional, computationally inexpensive to simulate and can be constructed within an analytical framework. This framework facilitates rigorous mathematical analysis that enables us to carefully map and explain the models behaviour. The parameters of the model, even in the absence of a one to one correspondence with experimental measures, can then be interpreted in a physiologically and anatomically meaningful way. We again reiterate the importance of transparency of the underpinning assumptions needed to construct neural field models, in order to enable careful and meaningful interpretation of the results. This is essential for future developments that aim to address the limitations of neural field theory. Most importantly, the evolution of this type of modelling in parallel with neuroscience experiments and technology means that they are capable of generating testable hypotheses that can be experimentally verified. This gives them the potential to be not only predictive, but to also have significant explanatory power that elucidates some of the unknown mechanisms behind brain function and dysfunction.

References

- [1] Romesh G. Abeysuriya, Chris J. Rennie, and Peter A. Robinson, *Prediction and verification of nonlinear sleep spindle harmonic oscillations*, *Journal of Theoretical Biology* **344** (2014), 70–77.
- [2] Markus Ableidinger, Evelyn Buckwar, and Harald Hinterleitner, *A Stochastic Version of the Jansen and Rit Neural Mass Model: Analysis and Numerics*, *The Journal of Mathematical Neuroscience* **7** (2017), no. 1, 8.
- [3] Abdullah Al Sawaf, Aashrai Gudlavalleti, and Najib Murr, *EEG Basal Cortical Rhythms*, StatPearls, StatPearls Publishing, Treasure Island (FL), (2021).
- [4] Shun-Ichi Amari, *Homogeneous nets of neuron-like elements*, *Biological cybernetics* **17** (1975), no. 4, 211–220.
- [5] Shun-Ichi Amari, *Dynamics of pattern formation in lateral-inhibition type neural fields*, *Biological cybernetics* **27** (1977), no. 2, 77–87.
- [6] Alfonso Araque and Marta Navarrete, *Glial cells in neuronal network function*, *Philosophical Transactions of the Royal Society B: Biological Sciences* **365** (2010), no. 1551, 2375–2381.

- [7] Peter Ashwin, Stephen Coombes, and Rachel Nicks, *Mathematical frameworks for oscillatory network dynamics in neuroscience*, *The Journal of Mathematical Neuroscience* **6** (2016), no. 1, 1–92.
- [8] Peter Ashwin, Jennifer Creaser, and Krasimira Tsaneva-Atanasova, *Fast and slow domino regimes in transient network dynamics*, *Physical Review E* **96** (2017), no. 5, 052309.
- [9] Richard S. Balson, Dean R. Freestone, Mark J. Cook, Anthony N. Burkitt, and David B. Grayden, *Seizure dynamics: A computational model based approach demonstrating variability in seizure mechanisms*, *BMC Neuroscience* **15** (2014), no. 1, P152.
- [10] Matthew I. Banks, John A. White, and Robert A. Pearce, *Interactions between Distinct GABAA Circuits in Hippocampus*, *Neuron* **25** (2000), no. 2, 449–457.
- [11] Oscar Benjamin, Thomas H. B. Fitzgerald, Peter Ashwin, Krasimira Tsaneva-Atanasova, Fahmida Chowdhury, Mark P. Richardson, and John R. Terry, *A phenomenological model of seizure initiation suggests network structure may explain seizure frequency in idiopathic generalised epilepsy*, *The Journal of Mathematical Neuroscience* **2** (2012), no. 1, 1.
- [12] Raymond L. Beurle, *Properties of a mass of cells capable of regenerating pulses*, *Philosophical Transactions of the Royal Society of London. Series B, Biological Sciences* (1956), 55–94.
- [13] Basabdatta Sen Bhattacharya, Damien Coyle, and Liam P. Maguire, *A thalamo-cortico-thalamic neural mass model to study alpha rhythms in Alzheimer's disease*, *Neural Networks* **24** (2011), no. 6, 631–645.
- [14] Christian Bick, Marc Goodfellow, Carlo R. Laing, and Erik A. Martens, *Understanding the dynamics of biological and neural oscillator networks through exact mean-field reductions: A review*, *The Journal of Mathematical Neuroscience* **10** (2020), no. 1, 9.
- [15] Alex Blenkinsop, Antonio Valentin, Mark P. Richardson, and John R. Terry, *The dynamic evolution of focal-onset epilepsies – combining theoretical and clinical observations*, *European Journal of Neuroscience* **36** (2012), no. 2, 2188–2200.
- [16] Ingo Bojak and David T. J. Liley, *Modeling the effects of anesthesia on the electroencephalogram*, *Physical Review E* **71** (2005), no. 4, 041902.
- [17] Ingo Bojak and David T. J. Liley, *Axonal Velocity Distributions in Neural Field Equations*, *PLOS Computational Biology* **6** (2010), no. 1, e1000653.
- [18] Valentino Braitenberg and Almut Schüz, *Cortex: Statistics and Geometry of Neuronal Connectivity*, Springer Science & Business Media, (2013).
- [19] Michael Breakspear, James A. Roberts, John R. Terry, Serafim Rodrigues, Neil Mahant, and Peter A. Robinson, *A Unifying Explanation of Primary Generalized Seizures Through Nonlinear Brain Modeling and Bifurcation Analysis*, *Cerebral Cortex* **16** (2006), no. 9, 1296–1313.
- [20] Paul C. Bressloff, *Stochastic Neural Field Theory and the System-Size Expansion*, *SIAM Journal on Applied Mathematics* **70** (2009), no. 5, 1488–1521.
- [21] Paul C Bressloff, *From invasion to extinction in heterogeneous neural fields*, *The Journal of Mathematical Neuroscience* **2** (2012), no. 1, 6.
- [22] Paul C. Bressloff, *Stochastic Neural Field Theory*, *Neural Fields: Theory and Applications* (Stephen Coombes, Peter beim Graben, Roland Potthast, and James Wright, eds.), Springer, Berlin, Heidelberg, (2014), pp. 235–268.
- [23] Paul C. Bressloff, *Stochastic neural field model of stimulus-dependent variability in cortical neurons*, *PLOS Computational Biology* **15** (2019), no. 3, e1006755.
- [24] Paul C. Bressloff and Stephen Coombes, *Dynamics of Strongly Coupled Spiking Neurons*, *Neural Computation* **12** (2000), no. 1, 91–129.
- [25] Paul C. Bressloff and Yi Ming Lai, *Stochastic synchronization of neuronal populations with intrinsic and extrinsic noise*, *The Journal of Mathematical Neuroscience* **1** (2011), no. 1, 2.
- [26] Paul C. Bressloff and Jay M. Newby, *Path integrals and large deviations in stochastic hybrid systems*, *Physical Review E* **89** (2014), no. 4, 042701.
- [27] Nicolas Brunel, *Dynamics of Sparsely Connected Networks of Excitatory and Inhibitory Spiking Neurons*, *Journal of Computational Neuroscience* **8** (2000), no. 3, 183–208.

- [28] Evelyn Buckwar, *Introduction to the numerical analysis of stochastic delay differential equations*, Journal of Computational and Applied Mathematics **125** (2000), no. 1, 297–307.
- [29] Michael A. Buice and Jack D. Cowan, *Field-theoretic approach to fluctuation effects in neural networks*, Physical Review E **75** (2007), no. 5, 051919.
- [30] Michael A. Buice, Jack D. Cowan, and Carson C. Chow, *Systematic Fluctuation Expansion for Neural Network Activity Equations*, Neural Computation **22** (2010), no. 2, 377–426.
- [31] Anthony N. Burkitt, *A Review of the Integrate-and-fire Neuron Model: I. Homogeneous Synaptic Input*, Biological Cybernetics **95** (2006), no. 1, 1–19.
- [32] Anthony N. Burkitt, *A review of the integrate-and-fire neuron model: II. Inhomogeneous synaptic input and network properties*, Biological Cybernetics **95** (2006), no. 2, 97–112.
- [33] György Buzsáki, Costas A. Anastassiou, and Christof Koch, *The origin of extracellular fields and currents—EEG, ECoG, LFP and spikes*, Nature reviews neuroscience **13** (2012), no. 6, 407.
- [34] Áine Byrne, Daniele Avitabile, and Stephen Coombes, *Next-generation neural field model: The evolution of synchrony within patterns and waves*, Physical Review E **99** (2019), no. 1, 012313.
- [35] Áine Byrne, Matthew J. Brookes, and Stephen Coombes, *A mean field model for movement induced changes in the beta rhythm*, Journal of Computational Neuroscience **43** (2017), no. 2, 143–158.
- [36] Andres Carvallo, Julien Modolo, Pascal Benquet, Stanislas Lagarde, Fabrice Bartolomei, and Fabrice Wendling, *Biophysical Modeling for Brain Tissue Conductivity Estimation Using SEEG Electrodes*, IEEE Transactions on Biomedical Engineering **66** (2019), no. 6, 1695–1704.
- [37] Anton V. Chizhov, Artyom V. Zefirov, Dmitry V. Amakhin, Elena Yu Smirnova, and Aleksey V. Zaitsev, *Minimal model of interictal and ictal discharges “Epileptor-2”*, PLOS Computational Biology **14** (2018), no. 5, e1006186.
- [38] Carson C. Chow and Yahya Karimipناه, *Before and beyond the Wilson–Cowan equations*, Journal of Neurophysiology **123** (2020), no. 5, 1645–1656.
- [39] Stephen Coombes, Gabriel J. Lord, and Markus R. Owen, *Waves and bumps in neuronal networks with axo-dendritic synaptic interactions*, Physica D: Nonlinear Phenomena **178** (2003), no. 3, 219–241.
- [40] Stephen Coombes and Áine Byrne, *Next Generation Neural Mass Models*, Nonlinear Dynamics in Computational Neuroscience (Fernando Corinto and Alessandro Torcini, eds.), PoliTO Springer Series, Springer International Publishing, Cham, (2019), pp. 1–16.
- [41] Rosa Cossart, Céline Dinocourt, June C. Hirsch, Angel Merchan-Perez, Javier De Felipe, Yehezkel Ben-Ari, Monique Esclapez, and Christophe Bernard, *Dendritic but not somatic GABAergic inhibition is decreased in experimental epilepsy*, Nature Neuroscience **4** (2001), no. 1, 52–62.
- [42] Michael Schellenberger Costa, Jan Born, Jens Christian Claussen, and Thomas Martinetz, *Modeling the effect of sleep regulation on a neural mass model*, Journal of Computational Neuroscience **41** (2016), no. 1, 15–28.
- [43] Michael Schellenberger Costa, Arne Weigenand, Hong-Viet V. Ngo, Lisa Marshall, Jan Born, Thomas Martinetz, and Jens Christian Claussen, *A Thalamocortical Neural Mass Model of the EEG during NREM Sleep and Its Response to Auditory Stimulation*, PLOS Computational Biology **12** (2016), no. 9, e1005022.
- [44] Jack D. Cowan, Jeremy Neuman, and Wim van Drongelen, *Wilson–Cowan Equations for Neocortical Dynamics*, The Journal of Mathematical Neuroscience **6** (2016), no. 1, 1.
- [45] John R. Cressman, Ghanim Ullah, Jokubas Ziburkus, Steven J. Schiff, and Ernest Barreto, *The influence of sodium and potassium dynamics on excitability, seizures, and the stability of persistent states: I. Single neuron dynamics*, Journal of Computational Neuroscience **26** (2009), no. 2, 159–170.
- [46] Peter Dayan and Laurence F. Abbott, *Theoretical neuroscience: Computational and mathematical modeling of neural systems*, Computational Neuroscience, Massachusetts Institute of Technology Press, Cambridge, Mass, (2001).

- [47] Hugo de Garis, Chen Shuo, Ben Goertzel, and Lian Ruiting, *A world survey of artificial brain projects, Part I: Large-scale brain simulations*, *Neurocomputing* **74** (2010), no. 1, 3–29.
- [48] Gustavo Deco, Viktor K. Jirsa, Peter A. Robinson, Michael Breakspear, and Karl Friston, *The Dynamic Brain: From Spiking Neurons to Neural Masses and Cortical Fields*, *PLOS Computational Biology* **4** (2008), no. 8, e1000092.
- [49] Andre DeLean, Peter J. Munson, and David Rodbard, *Simultaneous analysis of families of sigmoidal curves: Application to bioassay, radioligand assay, and physiological dose-response curves*, *American Journal of Physiology-Endocrinology and Metabolism* **235** (1978), no. 2, E97.
- [50] Alain Destexhe, *Conductance-Based Integrate-and-Fire Models*, *Neural Computation* **9** (1997), no. 3, 503–514.
- [51] Alain Destexhe, Zachary F. Mainen, and Terrence J. Sejnowski, *Synthesis of models for excitable membranes, synaptic transmission and neuromodulation using a common kinetic formalism*, *Journal of Computational Neuroscience* **1** (1994), no. 3, 195–230.
- [52] Marc A. Dichter, *Basic Mechanisms of Epilepsy: Targets for Therapeutic Intervention*, *Epilepsia* **38** (1997), no. s9, S2–S6.
- [53] Freeman Dyson, *A meeting with Enrico Fermi*, <https://www.nature.com/articles/427297a>, (2004).
- [54] John C. Eccles, Reginald V. Jones, and William D. M. Paton, *From electrical to chemical transmission in the central nervous system: The closing address of the Sir Henry Dale Centennial Symposium Cambridge, 19 September 1975*, *Notes and Records of the Royal Society of London* **30** (1976), no. 2, 219–230.
- [55] Tahra L. Eissa, Koen Dijkstra, Christoph Brune, Ronald G. Emerson, Michel J. A. M. van Putten, Robert R. Goodman, Guy M. McKhann, Catherine A. Schevon, Wim van Drongelen, and Stephan A. van Gils, *Cross-scale effects of neural interactions during human neocortical seizure activity*, *Proceedings of the National Academy of Sciences* **114** (2017), no. 40, 10761–10766.
- [56] Hans Elias and David Schwartz, *Surface Areas of the Cerebral Cortex of Mammals Determined by Stereological Methods*, *Science* **166** (1969), no. 3901, 111–113.
- [57] Chris Eliasmith and Oliver Trujillo, *The use and abuse of large-scale brain models*, *Current Opinion in Neurobiology* **25** (2014), 1–6.
- [58] Prabhu D. Emmady and Arayamparambil C. Anilkumar, *EEG Abnormal Waveforms*, StatPearls, StatPearls Publishing, Treasure Island (FL), (2021).
- [59] G. Bard Ermentrout and Nancy Kopell, *Parabolic Bursting in an Excitable System Coupled with a Slow Oscillation*, *SIAM Journal on Applied Mathematics* **46** (1986), no. 2, 233–253.
- [60] G. Bard Ermentrout and David H. Terman, *Mathematical Foundations of Neuroscience*, *Interdisciplinary Applied Mathematics*, vol. 35, Springer New York, New York, NY, (2010).
- [61] W. Howard Evans and Patricia E. M. Martin, *Gap junctions: Structure and function (Review)*, *Molecular Membrane Biology* **19** (2002), no. 2, 121–136.
- [62] Olivier Faugeras and James Inglis, *Stochastic neural field equations: A rigorous footing*, *Journal of Mathematical Biology* **71** (2015), no. 2, 259–300.
- [63] Olivier Faugeras and James Maclaurin, *Asymptotic description of stochastic neural networks. I. Existence of a large deviation principle*, *Comptes Rendus Mathematique* **352** (2014), no. 10, 841–846.
- [64] Lauric A. Ferrat, Marc Goodfellow, and John R. Terry, *Classifying dynamic transitions in high dimensional neural mass models: A random forest approach*, *PLoS computational biology* **14** (2018), no. 3, e1006009.
- [65] Kathleen R. Tozer Fink and James R. Fink, *4 - Principles of Modern Neuroimaging*, *Principles of Neurological Surgery (Fourth Edition)* (Richard G. Ellenbogen, Laligam N. Sekhar, Neil D. Kitchen, and Harley Brito da Silva, eds.), Philadelphia, January (2018), pp. 62–86.e2.
- [66] Richard FitzHugh, *Impulses and Physiological States in Theoretical Models of Nerve Membrane*, *Biophysical Journal* **1** (1961), no. 6, 445–466.

- [67] Walter J. Freeman, *Linear Analysis of the Dynamics of Neural Masses*, Annual Review of Biophysics and Bioengineering **1** (1972), no. 1, 225–256.
- [68] Walter J. Freeman, *Waves, Pulses, and the Theory of Neural Masses*, Progress in Theoretical Biology, Elsevier, (1972), pp. 87–165.
- [69] Walter J. Freeman, *A Model for Mutual Excitation in a Neuron Population in Olfactory Bulb*, IEEE Transactions on Biomedical Engineering **BME-21** (1974), no. 5, 350–358.
- [70] Walter J. Freeman, *Mass action in the nervous system*, (1975).
- [71] Walter J. Freeman, *Nonlinear gain mediating cortical stimulus-response relations*, Biological Cybernetics **33** (1979), no. 4, 237–247.
- [72] Walter J. Freeman, *Tutorial on neurobiology: From single neurons to brain chaos*, International Journal of Bifurcation and Chaos **2** (1992), no. 03, 451–482.
- [73] Dean R. Freestone, Levin Kuhlmann, M.S. Chong, Dragan Nestic, David B. Grayden, Param Aram, Romain Postoyan, and Mark J. Cook, *Patient-specific neural mass modeling - stochastic and deterministic methods*, Recent Advances in Predicting and Preventing Epileptic Seizures, World Scientific, (2013), pp. 63–82.
- [74] Frank Freyer, James A. Roberts, Robert Becker, Peter A. Robinson, Petra Ritter, and Michael Breakspear, *Biophysical mechanisms of multistability in resting-state cortical rhythms*, Journal of Neuroscience **31** (2011), no. 17, 6353–6361.
- [75] Frank Freyer, James A. Roberts, Petra Ritter, and Michael Breakspear, *A canonical model of multistability and scale-invariance in biological systems*, PLoS Computational Biology **8** (2012), no. 8, e1002634.
- [76] Moritz Gerster, Halgurd Taher, Antonín Škoch, Jaroslav Hlinka, Maxime Guye, Fabrice Bartolomei, Viktor K. Jirsa, Anna Zakharova, and Simona Olmi, *Patient-specific network connectivity combined with a next generation neural mass model to test clinical hypothesis of seizure propagation*, Frontiers in Systems Neuroscience **15** (2021), 675272.
- [77] Wulfram Gerstner and Werner Kistler, *Spiking Neuron Models: An Introduction*, Cambridge University Press. (2002).
- [78] Fotios Giannakopoulos, U. Bihler, Christian Hauptmann, and Heiko J. Luhmann, *Epileptiform activity in a neocortical network: A mathematical model*, Biological Cybernetics **85** (2001), no. 4, 257–268.
- [79] Marc Goodfellow, Christian Rummel, Eugenio Abela, Mark P. Richardson, Kaspar Schindler, and John R. Terry, *Estimation of brain network ictogenicity predicts outcome from epilepsy surgery*, Scientific Reports **6** (2016), 29215.
- [80] Sergey L. Gratiy, Geir Halmes, Daniel Denman, Michael J. Hawrylycz, Christof Koch, Gaute T. Einevoll, and Costas A. Anastassiou, *From Maxwell's equations to the theory of current-source density analysis*, The European Journal of Neuroscience **45** (2017), no. 8, 1013–1023.
- [81] John S. Griffith, *A field theory of neural nets: I. Derivation of field equations*, The bulletin of mathematical biophysics **25** (1963), no. 1, 111–120.
- [82] John S. Griffith, *On the Stability of Brain-Like Structures*, Biophysical Journal **3** (1963), no. 4, 299–308.
- [83] John S. Griffith, *A field theory of neural nets: II. Properties of the field equations*, The Bulletin of Mathematical Biophysics **27** (1965), no. 2, 187.
- [84] Carla Guillen, Wolfram Hesse, and Matthias Brehm, *The PerSyst Monitoring Tool*, Euro-Par 2014: Parallel Processing Workshops (Cham) (Luís Lopes, Julius Žilinskas, Alexandru Costan, Roberto G. Cascella, Gabor Kecskemeti, Emmanuel Jeannot, Mario Cannataro, Laura Ricci, Siegfried Benkner, Salvador Petit, Vittorio Scarano, José Gracia, Sascha Hunold, Stephen L. Scott, Stefan Lankes, Christian Lengauer, Jesús Carretero, Jens Breitbart, and Michael Alexander, eds.), Lecture Notes in Computer Science, Springer International Publishing, (2014), pp. 363–374.
- [85] Lewis B. Haberly and Gordon M. Shepherd, *The synaptic organization of the brain*, Olfactory cortex (1998), 377–416.

- [86] James L. Hindmarsh, R. M. Rose, and Andrew F. Huxley, *A model of neuronal bursting using three coupled first order differential equations*, Proceedings of the Royal Society of London. Series B. Biological Sciences **221** (1984), no. 1222, 87–102.
- [87] Alan L. Hodgkin and Andrew F. Huxley, *A quantitative description of membrane current and its application to conduction and excitation in nerve*, The Journal of Physiology **117** (1952), no. 4, 500–544.
- [88] Jesper R. Ipsen, *May–Wigner transition in large random dynamical systems*, Journal of Statistical Mechanics: Theory and Experiment **2017** (2017), no. 9, 093209.
- [89] Jesper R. Ipsen and Andre D. H. Peterson, *Consequences of Dale’s law on the stability-complexity relationship of random neural networks*, Physical Review E **101** (2020), no. 5, 052412.
- [90] Eugene M. Izhikevich, *Dynamical Systems in Neuroscience - Eugene M. Izhikevich - MIT Press*, (2007).
- [91] Ben H. Jansen and Vincent G. Rit, *Electroencephalogram and visual evoked potential generation in a mathematical model of coupled cortical columns*, Biological cybernetics **73** (1995), no. 4, 357–366.
- [92] Ben H. Jansen, George Zouridakis, and Michael E. Brandt, *A neurophysiologically-based mathematical model of flash visual evoked potentials*, Biological Cybernetics **68** (1993), no. 3, 275–283.
- [93] John G. R. Jefferys, Roger D. Traub, and Miles A. Whittington, *Neuronal networks for induced ‘40 Hz’ rhythms*, Trends in Neurosciences **19** (1996), no. 5, 202–208.
- [94] Viktor K. Jirsa, Timothee Proix, Dionysios Perdikis, Michael M. Woodman, Huifang Wang, Jorge Gonzalez-Martinez, Christophe Bernard, Cristian Bénar, Maxime Guye, Patrick Chauvel, and Fabrice Bartolomei, *The Virtual Epileptic Patient: Individualized whole-brain models of epilepsy spread*, NeuroImage **145** (2017), 377–388.
- [95] Viktor K. Jirsa and Hermann Haken, *Field theory of electromagnetic brain activity*, Physical Review Letters **77** (1996), no. 5, 960.
- [96] Viktor K. Jirsa and Hermann Haken, *A derivation of a macroscopic field theory of the brain from the quasi-microscopic neural dynamics*, Physica D: Nonlinear Phenomena **99** (1997), no. 4, 503–526.
- [97] Viktor K. Jirsa, William C. Stacey, Pascale P. Quilichini, Anton I. Ivanov, and Christophe Bernard, *On the nature of seizure dynamics*, Brain **137** (2014), no. 8, 2210–2230.
- [98] Leonard K. Kaczmarek, *A model of cell firing patterns during epileptic seizures*, Biological Cybernetics **22** (1976), no. 4, 229–234.
- [99] Leonard K. Kaczmarek and Agnessa Babloyantz, *Spatiotemporal patterns in epileptic seizures*, Biological Cybernetics **26** (1977), no. 4, 199–208.
- [100] Stiliyan N. Kalitzin, Demetrios N. Velis, and Fernando H. Lopes da Silva, *Stimulation-based anticipation and control of state transitions in the epileptic brain*, Epilepsy & Behavior **17** (2010), no. 3, 310–323.
- [101] Eric R. Kandel and James H. Schwartz, *Principles of neural science*, Elsevier, (1985).
- [102] Aharon Katchalsky, *Carriers and specificity in membranes. VI. Biological flow structure and their relation to chemiodiffusional coupling*, Neurosciences Research Program Bulletin **9** (1971), no. 3, 397–413.
- [103] Aharon Katchalsky, Vernon Rowland, and Robert Blumenthal, *Dynamic patterns of brain cell assemblies*, Neurosciences Research Program Bulletin **12** (1974), no. 1, 1–87.
- [104] Stephen Keeley, Áine Byrne, André Fenton, and John Rinzel, *Firing rate models for gamma oscillations*, Journal of Neurophysiology **121** (2019), no. 6, 2181–2190.
- [105] Stefan J. Kiebel, Marta I. Garrido, Rosalyn J. Moran, and Karl J. Friston, *Dynamic causal modelling for EEG and MEG*, Cognitive Neurodynamics **2** (2008), no. 2, 121.
- [106] Zachary P. Kilpatrick, *Wilson-Cowan Model*, Encyclopedia of Computational Neuroscience (Dieter Jaeger and Ranu Jung, eds.), Springer New York, New York, NY, (2013), pp. 1–5.
- [107] Zachary P. Kilpatrick and Bard Ermentrout, *Wandering Bumps in Stochastic Neural Fields*, SIAM Journal on Applied Dynamical Systems **12** (2013), no. 1, 61–94.

- [108] Christof Koch, *Biophysics of computation: Information processing in single neurons*, Oxford university press, (2004).
- [109] Elif Köksal Ersöz, Julien Modolo, Fabrice Bartolomei, and Fabrice Wendling, *Neural mass modeling of slow-fast dynamics of seizure initiation and abortion*, PLoS Computational Biology **16** (2020), no. 11, e1008430.
- [110] Mark A. Kramer, Wilson Truccolo, Uri T. Eden, Kyle Q. Lepage, Leigh R. Hochberg, Emad N. Eskandar, Joseph R. Madsen, Jong W. Lee, Atul Maheshwari, Eric Halgren, Catherine J. Chu, and Sydney S. Cash, *Human seizures self-terminate across spatial scales via a critical transition*, Proceedings of the National Academy of Sciences **109** (2012), no. 51, 21116–21121.
- [111] Giri P. Krishnan and Maxim Bazhenov, *Ionic Dynamics Mediate Spontaneous Termination of Seizures and Postictal Depression State*, Journal of Neuroscience **31** (2011), no. 24, 8870–8882.
- [112] Christian Kuehn and Martin G. Riedler, *Large Deviations for Nonlocal Stochastic Neural Fields*, The Journal of Mathematical Neuroscience **4** (2014), no. 1, 1.
- [113] Yoshiki Kuramoto, *Chemical Oscillations, Waves, and Turbulence*, Springer Series in Synergetics, Springer-Verlag, Berlin Heidelberg, (1984).
- [114] Yoshiki Kuramoto, *International symposium on mathematical problems in theoretical physics*, Lecture notes in Physics **30** (1975), 420.
- [115] Yuri A Kuznetsov, *Elements of Applied Bifurcation Theory*, 2nd edition ed., Applied Mathematical Sciences, vol. 112, Springer, (1997).
- [116] Carlo R. Laing, *Exact Neural Fields Incorporating Gap Junctions*, SIAM Journal on Applied Dynamical Systems **14** (2015), no. 4, 1899–1929.
- [117] Carlo Lancellotti, *On the Vlasov Limit for Systems of Nonlinearly Coupled Oscillators without Noise*, Transport Theory and Statistical Physics **34** (2005), no. 7, 523–535.
- [118] Lev D. Landau and Evgenii M. Lifshitz, *Fluid mechanics*, Pergamon Press, (1959).
- [119] Eva Lang and Wilhelm Stannat, *Finite-Size Effects on Traveling Wave Solutions to Neural Field Equations*, The Journal of Mathematical Neuroscience **7** (2017), no. 1, 5.
- [120] Louis Lapique, *Quantitative investigations of electrical nerve excitation treated as polarization. 1907*, Biological Cybernetics **97** (2007), no. 5-6, 341–349.
- [121] William J. Larsen, *Biological implications of gap junction structure, distribution and composition: A review*, Tissue and Cell **15** (1983), no. 5, 645–671.
- [122] Raima Larter, Brent Speelman, and Robert M. Worth, *A coupled ordinary differential equation lattice model for the simulation of epileptic seizures*, Chaos: An Interdisciplinary Journal of Nonlinear Science **9** (1999), no. 3, 795–804.
- [123] David T. J. Liley, *A continuum model of the mammalian alpha rhythm*, Spatiotemporal models in biological and artificial systems. Amsterdam: IOS Press (1997), 89–96.
- [124] David T. J. Liley, David M. Alexander, James J. Wright, and Mathew D. Aldous, *Alpha rhythm emerges from large-scale networks of realistically coupled multicompartmental model cortical neurons*, Network: Computation in Neural Systems **10** (1999), no. 1, 79–92.
- [125] David T. J. Liley, Peter J. Cadusch, and Mathew P. Dafilis, *A spatially continuous mean field theory of electrocortical activity*, Network: Computation in Neural Systems **13** (2002), no. 1, 67–113.
- [126] Pedro M. Lima and Evelyn Buckwar, *Numerical Solution of the Neural Field Equation in the Two-Dimensional Case*, SIAM Journal on Scientific Computing **37** (2015), no. 6, B962–B979.
- [127] Horst Lohmann and Birgit Rörig, *Long-range horizontal connections between supragranular pyramidal cells in the extrastriate visual cortex of the rat*, Journal of Comparative Neurology **344** (1994), no. 4, 543–558.
- [128] Marinho A. Lopes, Mark P. Richardson, Eugenio Abela, Christian Rummel, Kaspar Schindler, Marc Goodfellow, and John R. Terry, *An optimal strategy for epilepsy surgery: Disruption of the rich-club?*, PLoS Computational Biology **13** (2017), no. 8, e1005637.
- [129] Fernando H. Lopes da Silva, A. Hoeks, H. Smits, and L. H. Zetterberg, *Model of brain rhythmic activity*, Kybernetik **15** (1974), no. 1, 27–37.

- [130] Fernando H. Lopes Da Silva, Wouter Blanes, Stiliyan N. Kalitzin, Jaime Parra, Piotr Suffczynski, and Demetrios N. Velis, *Epilepsies as Dynamical Diseases of Brain Systems: Basic Models of the Transition Between Normal and Epileptic Activity*, *Epilepsia* **44** (2003), no. s12, 72–83.
- [131] Tanushree B. Luke, Ernest Barreto, and Paul So, *Complete Classification of the Macroscopic Behavior of a Heterogeneous Network of Theta Neurons*, *Neural Computation* **25** (2013), no. 12, 3207–3234.
- [132] Henry Markram, *The human brain project*, *Scientific American* **306** (2012), no. 6, 50–55.
- [133] André C. Marreiros, Jean Daunizeau, Stefan J. Kiebel, and Karl J. Friston, *Population dynamics: Variance and the sigmoid activation function*, *NeuroImage* **42** (2008), no. 1, 147–157.
- [134] Frank Marten, Serafim Rodrigues, Oscar Benjamin, Mark P. Richardson, and John R Terry, *Onset of polyspike complexes in a mean-field model of human electroencephalography and its application to absence epilepsy*, *Philosophical Transactions of the Royal Society A: Mathematical, Physical and Engineering Sciences* **367** (2009), no. 1891, 1145–1161.
- [135] Frank Marten, Serafim Rodrigues, Piotr Suffczynski, Mark P. Richardson, and John R. Terry, *Derivation and analysis of an ordinary differential equation mean-field model for studying clinically recorded epilepsy dynamics*, *Physical Review E* **79** (2009), no. 2, 021911.
- [136] John H. Martin, *Cortical neurons, the EEG, and the mechanisms of epilepsy*, *Principles of neural science* **48** (1985), 636–647.
- [137] Louis-Emmanuel Martinet, Grant Fiddymont, Joseph R. Madsen, Emad N. Eskandar, Wilson Truccolo, Uri T. Eden, Sydney S. Cash, and Mark A. Kramer, *Human seizures couple across spatial scales through travelling wave dynamics*, *Nature Communications* **8** (2017), no. 1, 14896.
- [138] Ramón Martínez-Cancino and Roberto Carlos Sotero Diaz, *Dynamical Mean Field approximation of a canonical cortical model for studying inter-population synchrony*, *Nature Precedings* (2011), 1–1.
- [139] Francesca Mastrogiuseppe and Srdjan Ostojic, *Intrinsically-generated fluctuating activity in excitatory-inhibitory networks*, *PLOS Computational Biology* **13** (2017), no. 4, e1005498.
- [140] Matias I. Maturana, Christian Meisel, Katrina Dell, Philippa J. Karoly, Wendyl D’Souza, David B. Grayden, Anthony N. Burkitt, Premysl Jiruska, Jan Kudlacek, Jaroslav Hlinka, Mark J. Cook, Levin Kuhlmann, and Dean R. Freestone, *Critical slowing as a biomarker for seizure susceptibility*, *Nature communications* **11**(1) (2020): 1–12.
- [141] Robert M. May, *Will a Large Complex System be Stable?*, *Nature* **238** (1972), no. 5364, 413–414.
- [142] David A. McCormick and Diego Contreras, *On the cellular and network bases of epileptic seizures*, *Annual review of physiology* **63** (2001), no. 1, 815–846.
- [143] Warren S. McCulloch and Walter Pitts, *A logical calculus of the ideas immanent in nervous activity*, *The bulletin of mathematical biophysics* **5** (1943), no. 4, 115–133.
- [144] John W. C. Medithe and Usha R. Nelakuditi, *Study of normal and abnormal EEG*, 2016 3rd International Conference on Advanced Computing and Communication Systems (ICACCS), vol. 01, January (2016), pp. 1–4.
- [145] Hamish Meffin, Anthony N. Burkitt, and David B. Grayden, *An Analytical Model for the ‘Large, Fluctuating Synaptic Conductance State’ Typical of Neocortical Neurons In Vivo*, *Journal of Computational Neuroscience* **16** (2004), no. 2, 159–175.
- [146] Richard Miles, Katalin Tóth, Attila I Gulyás, Norbert Hájos, and Tamas F. Freund, *Differences between Somatic and Dendritic Inhibition in the Hippocampus*, *Neuron* **16** (1996), no. 4, 815–823.
- [147] Kenneth D. Miller and Francesco Fumarola, *Mathematical Equivalence of Two Common Forms of Firing Rate Models of Neural Networks*, *Neural Computation* **24** (2011), no. 1, 25–31.
- [148] Ernest Montbrió, Diego Pazó, and Alex Roxin, *Macroscopic Description for Networks of Spiking Neurons*, *Physical Review X* **5** (2015), no. 2, 021028.

- [149] Catherine Morris and Harold Lecar, *Voltage oscillations in the barnacle giant muscle fiber*, *Biophysical Journal* **35** (1981), no. 1, 193–213.
- [150] Eli J. Müller, Sacha J. van Albada, Jong-won Kim, and Peter A. Robinson, *Unified neural field theory of brain dynamics underlying oscillations in Parkinson’s disease and generalized epilepsies*, *Journal of Theoretical Biology* **428** (2017), 132–146.
- [151] Chetan S. Nayak and Arayamparambil C. Anilkumar, *EEG Normal Sleep*, StatPearls, StatPearls Publishing, (2021).
- [152] Lucas L. Neves and Luiz H. A. Monteiro, *A Linear Analysis of Coupled Wilson-Cowan Neuronal Populations*, *Computational Intelligence and Neuroscience* (2016), 8939218.
- [153] Paul L. Nunez, *The brain wave equation: A model for the EEG*, *Mathematical Biosciences* **21** (1974), no. 3, 279–297.
- [154] Paul L. Nunez, *Generation of human EEG by a combination of long and short range neocortical interactions*, *Brain Topography* **1** (1989), no. 3, 199–215.
- [155] Paul L. Nunez, *Toward a quantitative description of large-scale neocortical dynamic function and EEG*, *Behavioral and Brain Sciences* **23** (2000), no. 3, 371–398.
- [156] Paul L. Nunez and Brian A. Cuttillo, *Neocortical dynamics and human EEG rhythms*, Oxford University Press, USA, (1995).
- [157] Paul L. Nunez, and Ramesh Srinivasan, *Electric Fields of the Brain: The Neurophysics of EEG*, Oxford University Press, (2006).
- [158] Paul L. Nunez and Ramesh Srinivasan, *Neocortical dynamics due to axon propagation delays in cortico-cortical fibers: EEG traveling and standing waves with implications for top-down influences on local networks and white matter disease*, *Brain Research* **1542** (2014), 138–166.
- [159] T. Oshima and Herbert Jasper, *Basic Mechanisms of the Epilepsies*, Basic Mechanisms of the Epilepsies, Boston: Little, Brown, first ed., (1969).
- [160] Srdjan Ostojic, *Two types of asynchronous activity in networks of excitatory and inhibitory spiking neurons*, *Nature Neuroscience* **17** (2014), no. 4, 594–600.
- [161] Edward Ott and Thomas M. Antonsen, *Low dimensional behavior of large systems of globally coupled oscillators*, *Chaos: An Interdisciplinary Journal of Nonlinear Science* **18** (2008), no. 3, 037113.
- [162] Andre D. H. Peterson, Hamish Meffin, Mark J. Cook, David B. Grayden, Iven M. Y. Mareels, and Anthony N. Burkitt, *A homotopic mapping between current-based and conductance-based synapses in a mesoscopic neural model of epilepsy*, arXiv:1510.00427 [cond-mat, physics:physics, q-bio] (2018).
- [163] Dimitris Pinotsis, Marco Leite, and Karl Friston, *On conductance-based neural field models*, *Frontiers in Computational Neuroscience* **7** (2013), 158.
- [164] Antonio J. Pons, Jose L. Cantero, Mercedes Atienza, and Jordi Garcia-Ojalvo, *Relating structural and functional anomalous connectivity in the aging brain via neural mass modeling*, *NeuroImage* **52** (2010), no. 3, 848–861.
- [165] Ilya Prigogine and Grégoire Nicolis, *Fluctuations and the Mechanism of Instabilities*, *From Theoretical Physics to Biology* (1973), 89–109.
- [166] Dale Purves, George J. Augustine, David Fitzpatrick, Lawrence C. Katz, Anthony-Samuel LaMantia, James O. McNamara, and S. Mark Williams, *Stages of Sleep*, *Neuroscience*. 2nd Edition, Sinauer Associates, (2001).
- [167] Kanaka Rajan and Laurence F. Abbott, *Eigenvalue Spectra of Random Matrices for Neural Networks*, *Physical Review Letters* **97** (2006), no. 18, 188104.
- [168] Santiago Ramón y Cajal, *Histologie du système nerveux de l’homme et des vertébrés*, Maloine, Paris **2** (1911), 153–173.
- [169] Bruce R. Ransom and Harald Sontheimer, *The neurophysiology of glial cells*, *Journal of clinical neurophysiology* **9** (1992), no. 2, 224–251.
- [170] Linda E. Reichl, *A modern course in statistical physics*, AAPT, (1999).

- [171] Christoph J. Rennie, Peter A. Robinson, and James J. Wright, *Effects of local feedback on dispersion of electrical waves in the cerebral cortex*, *Physical Review E* **59** (1999), no. 3, 3320–3329.
- [172] Christoph J. Rennie, Peter A. Robinson, and James J. Wright, *Unified neurophysiological model of EEG spectra and evoked potentials*, *Biological Cybernetics* **86** (2002), no. 6, 457–471.
- [173] Martin G. Riedler and Evelyn Buckwar, *Laws of Large Numbers and Langevin Approximations for Stochastic Neural Field Equations*, *The Journal of Mathematical Neuroscience* **3** (2013), no. 1, 1.
- [174] James A. Roberts and Peter A. Robinson, *Modeling distributed axonal delays in mean-field brain dynamics*, *Physical Review E* **78** (2008), no. 5, 051901.
- [175] Peter A. Robinson, Christoph J. Rennie, Donald L. Rowe, and Susie C. O'Connor, *Estimation of multiscale neurophysiological parameters by electroencephalographic means*, *Human Brain Mapping* **23** (2004), no. 1, 53–72.
- [176] Peter A. Robinson, Christoph J. Rennie, Donald L. Rowe, Susie C. O'Connor, James J. Wright, Evian Gordon, and Richard W. Whitehouse, *Neurophysiological modeling of brain dynamics*, *Neuropsychopharmacology* **28** (2003), no. S1, S74.
- [177] Peter A. Robinson, Christoph J. Rennie, James J. Wright, H. Bahramali, Evian Gordon, and Donald L. Rowe, *Prediction of electroencephalographic spectra from neurophysiology*, *Physical Review E* **63** (2001), no. 2, 021903.
- [178] Peter A. Robinson, Christoph J. Rennie, and James J. Wright, *Propagation and stability of waves of electrical activity in the cerebral cortex*, *Physical Review E* **56** (1997), no. 1, 826.
- [179] James Ross, Michelle Margetts, Ingo Bojak, Rachel Nicks, Daniele Avitabile, and Stephen Coombes, *Brain-wave equation incorporating axodendritic connectivity*, *Physical Review E* **101** (2020), no. 2, 022411.
- [180] Dipanjan Roy, Anandamohan Ghosh, and Viktor K. Jirsa, *Phase description of spiking neuron networks with global electric and synaptic coupling*, *Physical Review E* **83** (2011), no. 5, 051909.
- [181] Maria Luisa Saggio, Dakota Crisp, Jared M Scott, Philippa J. Karoly, Levin Kuhlmann, Mitsuyoshi Nakatani, Tomohiko Murai, Matthias Dümpelmann, Andreas Schulze-Bonhage, Akio Ikeda, Mark Cook, Stephen V Gliske, Jack Lin, Christophe Bernard, Viktor K. Jirsa, and William C. Stacey, *A taxonomy of seizure dynamotypes*, *eLife* **9** (2020), e55632.
- [182] Maria Luisa Saggio, Andreas Spiegler, Christophe Bernard, and Viktor K. Jirsa, *Fast-Slow Bursters in the Unfolding of a High Codimension Singularity and the Ultra-slow Transitions of Classes*, *The Journal of Mathematical Neuroscience* **7** (2017), no. 1, 7.
- [183] Helmut Schmidt, George Petkov, Mark P. Richardson, and John R. Terry, *Dynamics on Networks: The Role of Local Dynamics and Global Networks on the Emergence of Hyper-synchronous Neural Activity*, *PLoS Computational Biology* **10** (2014), no. 11, e1003947.
- [184] Helmut Schmidt, Wessel Woldman, Marc Goodfellow, Fahmida A. Chowdhury, Michalis Koutroumanidis, Sharon Jewell, Mark P. Richardson, and John R. Terry, *A computational biomarker of idiopathic generalized epilepsy from resting state EEG*, *Epilepsia* **57** (2016), no. 10, e200–e204.
- [185] Marco Segneri, Hongjie Bi, Simona Olmi, and Alessandro Torcini, *Theta-Nested Gamma Oscillations in Next Generation Neural Mass Models*, *Frontiers in Computational Neuroscience* **14** (2020), 47.
- [186] Donald A. Sholl, *The measurable parameters of the cerebral cortex and their significance in its organization*, *Progress in Neurobiology* **2** (1956), 324–333.
- [187] Dee U. Silverthorn, Bruce R. Johnson, William C. Ober, Claire W. Garrison, and Andrew C. Silverthorn, *Human physiology: An integrated approach*, 6th ed ed., Pearson Education, (2013).
- [188] Anna Simon, Roger D. Traub, Nikita Vladimirov, Alistair Jenkins, Claire Nicholson, Roger G. Whittaker, Ian Schofield, Gavin J. Clowry, Mark O. Cunningham, and Miles A. Whittington, *Gap junction networks can generate both ripple-like and fast ripple-like oscillations*, *European Journal of Neuroscience* **39** (2014), no. 1, 46–60.

- [189] Douglas R. Smith and Charles H. Davidson, *Maintained Activity in Neural Nets*, Journal of the ACM **9** (1962), no. 2, 268–279.
- [190] Hal Smith, *Distributed Delay Equations and the Linear Chain Trick*, An Introduction to Delay Differential Equations with Applications to the Life Sciences (Hal Smith, ed.), Texts in Applied Mathematics, Springer, New York, NY, (2011), pp. 119–130.
- [191] Shelagh J. M. Smith, *EEG in the diagnosis, classification, and management of patients with epilepsy*, Journal of Neurology, Neurosurgery & Psychiatry **76** (2005), no. suppl 2, ii2–ii7.
- [192] Haim Sompolinsky, Andrea Crisanti, and Hans J. Sommers, *Chaos in Random Neural Networks*, Physical Review Letters **61** (1988), no. 3, 259–262.
- [193] Erik K. St. Louis, Lauren C. Frey, Jeffrey W. Britton, J. L. Hopp, P. Korb, M. Z. Koubeissi, W. E. Lievens, and E. M. Pestana-Knight, *Electroencephalography (EEG): An introductory text and atlas of normal and abnormal findings in adults, children, and infants*, American Epilepsy Society, Chicago, (2016).
- [194] Merav Stern, Haim Sompolinsky, and Laurence F. Abbott, *Dynamics of random neural networks with bistable units*, Physical Review E **90** (2014), no. 6, 062710.
- [195] Moira L. Steyn-Ross, D. A. Steyn-Ross, J. W. Sleigh, and D. T. J. Liley, *Theoretical electroencephalogram stationary spectrum for a white-noise-driven cortex: Evidence for a general anesthetic-induced phase transition*, Physical Review E **60** (1999), no. 6, 7299–7311.
- [196] Michael Stone and Paul Goldbart, *Mathematics for Physics: A Guided Tour for Graduate Students*, Cambridge University Press, July (2009).
- [197] Halgurd Taher, Alessandro Torcini, and Simona Olmi, *Exact neural mass model for synaptic-based working memory*, PLOS Computational Biology **16** (2020), no. 12, e1008533.
- [198] Terence Tao, Van Vu, and Manjunath Krishnapur, *Random matrices: Universality of ESDs and the circular law*, The Annals of Probability **38** (2010), no. 5, 2023–2065.
- [199] William O. Tatum, *Handbook of EEG Interpretation*, Springer Publishing Company, May (2021).
- [200] Roger D. Traub, R. Miles, and R. K. Wong, *Model of the origin of rhythmic population oscillations in the hippocampal slice*, Science **243** (1989), no. 4896, 1319–1325.
- [201] Roger D. Traub, D. Schmitz, John G. R Jefferys, and A. Draguhn, *High-frequency population oscillations are predicted to occur in hippocampal pyramidal neuronal networks interconnected by axoaxonal gap junctions*, Neuroscience **92** (1999), no. 2, 407–426.
- [202] Roger D. Traub and R. K. Wong, *Cellular mechanism of neuronal synchronization in epilepsy*, Science **216** (1982), no. 4547, 745–747.
- [203] Roger D. Traub, R. K. Wong, R. Miles, and H. Michelson, *A model of a CA3 hippocampal pyramidal neuron incorporating voltage-clamp data on intrinsic conductances*, Journal of Neurophysiology **66** (1991), no. 2, 635–650.
- [204] Roger D. Traub, *Neocortical pyramidal cells: A model with dendritic calcium conductance reproduces repetitive firing and epileptic behavior*, Brain Research **173** (1979), no. 2, 243–257.
- [205] Roger D. Traub, Diego Contreras, and Miles A. Whittington, *Combined Experimental/Simulation Studies of Cellular and Network Mechanisms of Epileptogenesis In Vitro and In Vivo*, Journal of Clinical Neurophysiology **22** (2005), no. 5, 330.
- [206] Mauro Ursino and Giuseppe-Emiliano La Cara, *Travelling waves and EEG patterns during epileptic seizure: Analysis with an integrate-and-fire neural network*, Journal of Theoretical Biology **242** (2006), no. 1, 171–187.
- [207] Albert M. Uttley, *The probability of neural connexions*, Proceedings of the Royal Society of London. Series B - Biological Sciences **144** (1955), no. 915, 229–240.
- [208] David C. Van Essen, Stephen M. Smith, Deanna M. Barch, Timothy E.J. Behrens, Essa Yacoub, and Kamil Ugurbil, *The WU-Minn Human Connectome Project: An Overview*, NeuroImage **80** (2013), 62–79.
- [209] Ab van Rotterdam, Fernando H. Lopes da Silva, J. van den Ende, Max A. Viergever, and Aad J. Hermans, *A model of the spatial-temporal characteristics of the alpha rhythm*, Bulletin of Mathematical Biology **44** (1982), no. 2, 283–305.

- [210] Dieter Vollhardt, *Dynamical mean-field theory for correlated electrons*, *Annalen der Physik* **524** (2012), no. 1, 1–19.
- [211] Christopher S. von Bartheld, Jami Bahney, and Suzana Herculano-Houzel, *The search for true numbers of neurons and glial cells in the human brain: A review of 150 years of cell counting*, *Journal of Comparative Neurology* **524** (2016), no. 18, 3865–3895.
- [212] Gilles Wainrib and Jonathan Touboul, *Topological and Dynamical Complexity of Random Neural Networks*, *Physical Review Letters* **110** (2013), no. 11, 118101.
- [213] Arne Weigenand, Michael Schellenberger Costa, Hong-Viet Victor Ngo, Jens Christian Claussen, and Thomas Martinetz, *Characterization of K-Complexes and Slow Wave Activity in a Neural Mass Model*, *PLOS Computational Biology* **10** (2014), no. 11, e1003923.
- [214] Fabrice Wendling, Fabrice Bartolomei, Jean J. Bellanger, and Patrick Chauvel, *Epileptic fast activity can be explained by a model of impaired GABAergic dendritic inhibition*, *European Journal of Neuroscience* **15** (2002), no. 9, 1499–1508.
- [215] John A. White, Matthew I. Banks, Robert A. Pearce, and Nancy J. Kopell, *Networks of interneurons with fast and slow γ -aminobutyric acid type A (GABAA) kinetics provide substrate for mixed gamma-theta rhythm*, *Proceedings of the National Academy of Sciences* **97** (2000), no. 14, 8128–8133.
- [216] Miles A. Whittington, Roger D. Traub, Nancy Kopell, G. Bard Ermentrout, and E. H Buhl, *Inhibition-based rhythms: Experimental and mathematical observations on network dynamics*, *International Journal of Psychophysiology* **38** (2000), no. 3, 315–336.
- [217] Hugh R. Wilson and Jack D. Cowan, *Excitatory and inhibitory interactions in localized populations of model neurons*, *Biophysical journal* **12** (1972), no. 1, 1–24.
- [218] Hugh R. Wilson and Jack D. Cowan, *A mathematical theory of the functional dynamics of cortical and thalamic nervous tissue*, *Kybernetik* **13** (1973), no. 2, 55–80.
- [219] Wessel Woldman, Mark J. Cook, and John R. Terry, *Evolving dynamic networks: An underlying mechanism of drug resistance in epilepsy?*, *Epilepsy & Behavior* **94** (2019), 264–268.
- [220] Wessel Woldman, Helmut Schmidt, Eugenio Abela, Fahmida A. Chowdhury, Adam D. Pawley, Sharon Jewell, Mark P. Richardson, and John R. Terry, *Dynamic network properties of the interictal brain determine whether seizures appear focal or generalised*, *Scientific Reports* **10** (2020), no. 1, 7043.
- [221] James J. Wright, A. A. Sergejew, and David T. J. Liley, *Computer simulation of electrocortical activity at millimetric scale*, *Electroencephalography and clinical Neurophysiology* **90** (1994), no. 5, 365–375.
- [222] James J. Wright and David T. J. Liley, *Simulation of electrocortical waves*, *Biological cybernetics* **72** (1995), no. 4, 347–356.
- [223] Semir Zeki, *A vision of the brain*, *A Vision of the Brain*, Blackwell Scientific Publications, (1993).
- [224] Lars H. Zetterberg, Lars. Kristiansson, and Kåre Mossberg, *Performance of a model for a local neuron population*, *Biological Cybernetics* **31** (1978), no. 1, 15–26.
- [225] Lars H. Zetterberg, *Stochastic Activity in Population of Neurons: A Systems Analysis Approach*, (1973).
- [226] Jokūbas Žiburkus, John R. Cressman, and Steven J. Schiff, *Seizures as imbalanced up states: Excitatory and inhibitory conductances during seizure-like events*, *Journal of Neurophysiology* **109** (2012), no. 5, 1296–1306.

Acknowledgments. Andre D.H. Peterson acknowledges financial support in the form a fellowship from the Graeme Clark Institute. Blake J. Cook acknowledges the financial support of the EPSRC through a DTP studentship award to the University of Birmingham. Wessel Woldman acknowledges the financial support of Epilepsy Research UK through an Emerging Leader Fellowship award F2002, and the NIHR through grant AI01644. John R. Terry acknowledges the financial support of the EPSRC through grants EP/N014391/2 and EP/T027703/1, and the NIHR through grant AI01646. Andre D. H. Peterson and John R. Terry acknowledge the financial support of the Royal Society through International

Neural Field Models: A mathematical overview and unifying framework

Exchange grant IE170112. All authors gratefully acknowledge the comments of Stephen Coombes on an early draft of the manuscript.